NEW APPROACHES TO WOOD QUALITY ASSESSMENT

A thesis submitted in partial fulfilment of the requirements for the

Degree

of Doctor of Philosophy in Forestry Science

in the University of Canterbury

by

Monika Sharma

University of Canterbury

2013

Table of contents

TABLE OF CONTENTS ..... **I**

LIST OF FIGURES ..... **IV**

LIST OF TABLES ..... **X**

ACKNOWLEGEMENTS ..... **XIII**

ABSTRACT ..... **XIV**

ABBREVIATIONS ..... **XVI**

CHAPTER 1. GENERAL INTRODUCTION **1**

1.1 Corewood 4

1.2 Defining corewood 5

1.3 Characteristic features of corewood 6

1.4 Compression wood 8

1.5 Variation in wood properties among trees 11

1.6 Factors affecting stiffness and stability 11

1.7 Hardwood - eucalyptus 12

1.8 Tools to characterize wood properties 13

1.9 Selection age 15

1.10 Thesis aims and thesis structure 17

CHAPTER 2. AMBERLEY TRIALS **17**

2.1 Introduction 17

2.1.1 Variation in stiffness 17

2.1.2 Variation in shrinkage 19

2.2 Acoustic methods to sort wood 21

2.2.1 The resonance method 22

2.2.2 The time of flight method 23

2.2.3 Acoustics in wood 24

2.3 Material and methodology 26

2.3.1 Material 26

2.3.2 Sample preparation 28
2.3.3 Acoustic velocity measurement 29
2.3.4 Density and volume measurements 29
2.3.5 Longitudinal shrinkage measurement 31
2.3.6 Statistical analysis 32
2.4 Results and discussion 33
2.4.1 Comparison between compression wood and opposite wood 33
2.4.2 Relationship between wood quality traits 38
2.4.3 Ranking of families 47
2.5 Conclusions 59

CHAPTER 3. X-RAY DIFFRACTION IN COREWOOD 61

3.1 Introduction 61
3.1.1 Cell wall structure 62
3.1.2 Measuring MFA 65
3.2 X-ray Diffraction 66
3.2.1 X-ray diffraction in wood 67
3.2.2 Optical analogue 69
3.3 Material and methodology 72
3.3.1 Statistical analysis 76
3.4 Results and discussion 77
3.4.1 Comparative study of wood types 79
3.4.2 Ranking of families 86
3.5 Conclusions 94

CHAPTER 4. DYNAMIC MECHANICAL ANALYSIS IN COREWOOD 95

4.1 Introduction 95
4.2 Stress-strain curves and viscoelasticity 95
4.3 Dynamic mechanical analysis 96
4.4 Wood structure a digression – as it affects DMA analysis 102
4.5 Material and methodology 106
4.5.1 Statistical analysis 107
4.6 Results and discussion 108
4.7 Conclusions 115

CHAPTER 5. EARLY SCREENING OF HARDWOOD 117

5.1 Introduction 117

5.1.1 Growth stresses 117

5.1.2 Growth stresses and defects 120

5.1.3 Growth stress measurements 121

5.1.4 Tension wood 123

5.1.5 Variation in growth stresses 124

5.2 Material and methodology 124

5.2.1 Statistical analysis 126

5.3 Results and discussion 127

5.3.1 Comparison of opposite wood and tension wood properties 128

5.3.2 Relationship between calculated and measured growth strain 131

5.3.3 Interrelationship between wood properties 132

5.4 Conclusions 139

CHAPTER 6. SUMMARY 141

REFERENCES 146

List of figures

Figure 1.1 (a) Softwood (*Dacrycarpus dacrydioides*) showing axial tracheids (T) and uniseriate rays (R) and (b) hardwood (*Eucalyptus delagatensis*) showing vessels (V), fibres (F) and uniseriate rays (R) (Barnett and Jeronimidis, 2003) 3

Figure 1.2 Schematic section of a typical *Pinus radiata* stem showing different wood zones (Burdon et al., 2004) 6

Figure 1.3 Schematic representation of the microfibrillar structure within the cell wall of a softwood tracheid (Côté, 1967) 8

Figure 1.4 Schematic representation of the gradual improvement in properties with age (Bendtsen, 1978) 8

Figure 1.5 (a) Transverse section of delignified compression wood tracheid in *Larix laricina*. (b) Schematic model of a double cell wall in a compression wood tracheid, where black symbolizes the high lignin content in middle lamella and primary wall (M+P) and in S2(L) (Timell, 1986) 10

Figure 1.6 Cross-section of wood in tilted and straight trees (a) Straight tree with arcs of compression wood (dark) distributed at random, (b) leaning tree with compression wood confined to the lower side 16

Figure 2.1 Radial and vertical variation in stiffness in radiata pine showing the steep drop off in stiffness in the inner wood close to the groundline (Xu and Walker, 2004). P1 are the boards containing pith, P2 are the boards adjacent to the P1 boards, while P4 and (where present) P5 boards are adjacent to the bark. 18

Figure 2.2 Stiffness variation among butt logs of radiata pine trees (Xu, 2000), where numbers (1-5) represent five different stiffness classes 19

Figure 2.3 Variation of oven-dry shrinkage for radiata pine wood discs from the base of the tree (Wang et al., 2009) 19

Figure 2.4 Response of the end of a viscoelastic bar in response to a propagating stress wave, Δt is the lapse time between two wave peaks. 21

Figure 2.5 Resonance patterns for the first three harmonics 23

Figure 2.6 Schematic illustration of acoustic velocity measurement using time of flight method with two stop probes 23

Figure 2.7 Time determination using threshold value needs a system that takes account of the initial slope of the arriving signal. 24

Figure 2.8 Plantation layout of Amberley trial showing four sections-I, II, III, and IV. There are 12 replicates in each section (1-48) with 7x7 trees in each replicate with trees at 2.5m spacings, i.e. there were 2352 trees in total with 588 trees per section. 27
Figure 2.9 Leaning trees at Amberley. Note the pruned stemwood at the base 28
Figure 2.10 (a) Longitudinal section of wood with distinct wood types, lighter shade (opposite wood) and darker shade (compression wood) (b) prepared opposite (top) and compression wood samples (bottom).....29
Figure 2.11 Jig for length measurement with a sample inserted in two tubular ends that locate the map pins 32
Figure 2.12 Box plots for green moisture content, green velocity squared, green density and dry density (~5% moisture content) in *Pinus radiata* for opposite wood (OW) and compression wood (CW) and at tree age (24 and 34 months). OW.24 (n=492), CW.24 (n=490), OW.34 (n=1241) and OW.34 (n=1044).....36
Figure 2.13 Box plot for dynamic modulus (MOE) normalised for basic density (MOE/basic density) in compression wood and opposite wood of young *Pinus radiata* trees 44
Figure 2.14 Box plot for longitudinal shrinkage normalised for basic density in compression wood and opposite wood of young *Pinus radiata* trees.....45
Figure 2.15 Box plots for dynamic modulus and longitudinal shrinkage for opposite wood of 34 months old 50 *Pinus radiata* families.....51
Figure 2.16 Variation within best and worst family for longitudinal shrinkage and dry dynamic modulus of elasticity in opposite wood *Pinus radiata* trees at age 34 months.52
Figure 2.17 Plot representing deviation in dynamic modulus from overall mean (intercept) along with 95% confidence limit of families in opposite wood of 34 months old *Pinus radiata*. The intercept was 2.98GPa 53
Figure 2.18 Plot representing deviation in longitudinal shrinkage from overall mean (intercept) along with 95% confidence limit of families in opposite wood of 34 months old *Pinus radiata*. The intercept was 0.99%.....54
Figure 2.19 Plot between longitudinal shrinkage and dry dynamic modulus. All points irrespective of style represent mean values of opposite wood of 50 families of young *Pinus radiata*. Solid squares represent the values for 12 families selected for detail studies 55
Figure 2.20 Box plots for dynamic modulus and longitudinal shrinkage for compression wood of 34 months old 50 *Pinus radiata* families.....56

Figure 2.21 Plot representing deviation in longitudinal shrinkage from overall mean (intercept) along with 95% confidence limit of families in compression wood of 34 months old *Pinus radiata*. The intercept was 3.23% 59
Figure 3.1 Variation in MFA with tree height (Donaldson, 1992) 63
Figure 3.2 (a) Bragg's law, all the reflected beams are in phase (b) Reflected beams lie on the surface of a cone of semi-angle 2θ (Askeland et al., 2011) 66
Figure 3.3 (a) Monoclinic unit cell. (b) Major cellulose crystal planes contributing to the diffraction pattern from wood. The fiber axis is vertical and is perpendicular to the X-ray beam (Evans, 1999). 68
Figure 3.4 (a) Single cell; white walls representing walls perpendicular to X-rays and black walls representing walls parallel to X-rays. (b) Optical analogue for a single fiber; solid circles reflecting spots for walls perpendicular to X-rays and triangles reflections from walls parallel to X-rays (c) Diffraction pattern of wood, which shows extended arcs instead of individual spots 70
Figure 3.5 Four hypothetical independent peaks for two sets of walls, solid lines representing walls perpendicular to X-rays and dotted lines representing walls parallel to X-rays. Below is the actual integration profile for the (002) plane 71
Figure 3.6 Properties of the Gaussian distribution (Cave and Robinson, 1998) 72
Figure 3.7 Photograph showing sampling scheme. Sample A was used for chemical analysis, sample B was used for DMA work and sample C was used for X-ray diffraction 73
Figure 3.8 Excel sheet of Ian Cave's program showing different parameters used to fit curves to analyse data obtained from X-ray diffraction 75
Figure 3.9 X-ray diffraction pattern in opposite wood and compression wood, where white line represent model and black lines represent actual data. In opposite wood, peaks are asymmetric thus only the left hand peak is fitted in this diagram 80
Figure 3.10 Box plot of T values (MFA+2σ) for compression wood and opposite wood in young *Pinus radiata* 81
Figure 3.11 Box plot of microfibril angle (MFA) and standard deviation (σ) for compression wood and opposite wood of young *Pinus radiata* 81
Figure 3.12 Correlation between dynamic modulus and MFA in compression wood (triangular labels) and opposite wood (circular labels) in young *Pinus radiata* 82
Figure 3.13 Predicted versus measured dynamic modulus in opposite and compression wood of young *Pinus radiata* 83

Figure 3.14 Correlation between longitudinal shrinkage and MFA in compression wood (triangular labels) and opposite wood (circular labels) in young *Pinus radiata*.....84
Figure 3.15 Predicted versus measured longitudinal shrinkage in opposite and compression wood of young *Pinus radiata* 85
Figure 3.16 Correlation between dry velocity squared and MFA in compression wood (triangular labels) and opposite wood (circular labels) in young *Pinus radiata*.....85
Figure 3.17 Correlation between MFA in compression wood and MFA in opposite wood in young *Pinus radiata*.....86
Figure 3.18 Box plots for MFA values in opposite wood for families in young *Pinus radiata* 88
Figure 3.19 Variation in T (MFA+2σ) and dry velocity squared in opposite wood within the best and the worst family of young *Pinus radiata*.....88
Figure 3.20 Plot representing deviation in MFA from intercept along with 95% confidence limit of families in opposite wood of young *Pinus radiata*. The intercept was 39.03°...89
Figure 3.21 Box plots for MFA values in compression wood for families in young *Pinus radiata*.....92
Figure 3.22 Plot representing deviation in MFA from overall mean (intercept) along with 95% confidence limit of families in compression wood of young *Pinus radiata*. The intercept was 44.33°.....93
Figure 4.1 Stress-strain relationship in different materials.....96
Figure 4.2 Stress-strain behaviour in elastic, viscous and viscoelastic materials.....97
Figure 4.3 a) Force displacement curve in a viscoelastic material b) the Stress (σ_0) can be resolved into two components, in-phase (σ') and out-phase (σ'').....99
Figure 4.4 Relationship between complex, storage, and loss modulus in viscoelastic materials 100
Figure 4.5 Change in storage modulus with temperature for thermo plastic materials (Menard, 2008).....101
Figure 4.6 Schematic illustration of cell wall structure of S2 layer in spruce wood (Fahlén and Salmén, 2005).....103
Figure 4.7 Force displacement curve for small wood specimen of *Picea sitchensis* (Navi et al., 1995) 104

Figure 4.8Comparison of stress strain curves of an early wood (grey line) and a compression wood fibre (black line) of *Picea abies* tested in axial tension in wet condition along with schematic drawing of cell shape and cellulose MFA (Goswami et al., 2008b).....104
Figure 4.9 Variation in storage modulus and tanδ with temperature and frequency in young *Pinus radiata* opposite wood at 9% moisture content 108
Figure 4.10 Box plot for storage modulus normalised for the density for compression wood and opposite wood of young *Pinus radiata* 111
Figure 4.11 Box plot for tanδ for compression wood and opposite wood in young *Pinus radiata*.....112
Figure 4.12 Relationship between storage modulus and dynamic modulus in compression wood and opposite wood of young *Pinus radiata* 113
Figure 4.13 Correlation between predicted and measured storage modulus in opposite wood of young *Pinus radiata* 114
Figure 4.14 Correlation between predicted and measured storage modulus in compression wood of young *Pinus radiata* 114
Figure 4.15 Relationship between tanδ and longitudinal shrinkage in compression wood and opposite wood of young *Pinus radiata*.....115
Figure 5.1 Stress distribution in small and large diameter trees (Kubler, 1987) 119
Figure 5.2 Diagram representing the different parameters used to measure strain in a spilt log 126
Figure 5.3 Box plots for longitudinal shrinkage, volumetric shrinkage, basic density, green acoustic velocity squared, measured growth strain, and green dynamic modulus of opposite wood and tension wood in young *Eucalyptus regnans* 130
Figure 5.4 Calculated versus measured growth strain in young *Eucalyptus regnans* 131
Figure 5.5 Typical cartography of tension wood sectors along a trunk 3 months after tilting. Bark and pith appear in black, tension wood sectors are in grey. The notch in the bark marks the original upper face of the trunk after the tilting. Locations of the cross sections along the stems are given on each subfigure, where number corresponds to distance from the base (S) in centimetres (Coutand et al., 2007) 135
Figure 5.6 Correlation between longitudinal shrinkage and MFA in opposite wood of young *Eucalyptus regnans*.....136
Figure 5.7 Correlation between green acoustic velocity squared and MFA in opposite wood of young *Eucalyptus regnans*.....136

Figure 5.8 Relationship between longitudinal shrinkage and green acoustic velocity squared in young *Eucalyptus regnans*.....138
Figure 5.9 Relationship between volumetric shrinkage and basic density in young *Eucalyptus regnans*.....139

List of tables

Table 2.1 Summary statistics of wood properties in normal wood (vertical stems) in 34 months old *Pinus radiata* (number of samples=132) 34

Table 2.2 Comparison of wood properties in opposite wood and compression wood at three different tree ages for young *Pinus radiata* trees.....35

Table 2.3 Estimated means and 95% confidence intervals of wood properties in opposite wood and compression wood at different tree ages after controlling the effect of replicate and family in young *Pinus radiata* trees 38

Table 2.4 Pearson correlation matrix (with *p*-values in parentheses) for wood properties in opposite wood at three different tree ages in young *Pinus radiata* 40

Table 2.5 Pearson correlation matrix (with *p*-values in parentheses) for wood properties in compression wood at three different tree ages in young *Pinus radiata*.....42

Table 2.6 Pearson correlation coefficients (with *p*-values in parentheses) for wood properties between opposite and compression wood for young *Pinus radiata* trees at two tree ages 46

Table 2.7 Mean values of dynamic modulus and longitudinal shrinkage of opposite wood along with the ranking of families in 24 and 34 months old *Pinus radiata* trees. 48

Table 2.8 Spearman ranking correlation for different wood properties in opposite wood for 24 months and 34 months old *Pinus radiata* 50

Table 3.1 Summary statistics of selected samples along with coefficient of variation of wood properties in young *Pinus radiata* trees 77

Table 3.2 Estimated means and 95% confidence intervals of physical properties and microfibril orientation in opposite wood and compression wood in young *Pinus radiata* after controlling for the effect of replicate and family.....78

Table 3.3 Pearson Correlation matrix (with *p*-values in parentheses) for wood properties in opposite wood of young *Pinus radiata* 79

Table 3.4 Pearson Correlation matrix (with *p*-values in parentheses) for wood properties in compression wood of young *Pinus radiata* 79

Table 3.5 Regression equations for opposite and compression wood, where DM stands for dynamic modulus, BD for basic density and MFA for microfibril angle. 83

Table 3.6 Regression equations for opposite and compression wood where LS stands for longitudinal shrinkage, BD for basic density and MFA for microfibril angle.....84
Table 3.7 Mean values of wood properties and coefficients of variation in opposite wood for 12 *Pinus radiata* families.....87
Table 3.8 Mean values of dry acoustic velocity squared and MFA along with ranking of opposite wood for 12 families in young *Pinus radiata*.....90
Table 3.9 Mean values of wood properties and coefficients of variation in compression wood of 12 *Pinus radiata* families 91
Table 4.1 Estimated means and 95% confidence interval of wood properties in opposite wood and compression wood after controlling for the effect of replicate and family in young *Pinus radiata.* Storage modulus and tanδ were measured at 25°C, 1Hz and 9% moisture content as was the wood density.....109
Table 4.2 Pearson correlation matrix (with *p*-values in parentheses) for wood properties in opposite wood of young *Pinus radiata*.....110
Table 4.3 Pearson Correlation matrix (with *p*-values in parentheses) for wood properties in compression wood of young *Pinus radiata* 110
Table 4.4 Regression equations for opposite and compression wood, where SM stands for storage modulus, D for density at 9% moisture content and MFA stands for microfibril angle.....114
Table 5.1 Summary statistics of whole stem characteristics for 2-year-old *Eucalyptus regnans* (number of trees=87) 128
Table 5.2 Wood properties of opposite and tension wood in young *Eucalyptus regnans* (number of samples of each wood type=87).....129
Table 5.3 Pearson correlation coefficients (with *p*-values in parentheses) for estimated growth strain with stem properties in young *Eucalyptus regnans* (number of stems=48).....131
Table 5.4 Pearson correlation coefficients (with *p*-values in parentheses) for measured growth strain with wood properties independently in two wood types in young *Eucalyptus regnans* (48 number of samples with two gauges on either side of the stem).....132
Table 5.5 Pearson correlation coefficients (with *p*-values in parentheses) for wood properties in opposite wood of young *Eucalyptus regnans* (number of samples=87).....132
Table 5.6 Pearson correlation coefficients (with *p*-values in parentheses) for wood properties in tension wood of young *Eucalyptus regnans* (number of samples=87).....133

Table 5.7 Pearson correlation coefficients (with *p*-values in parentheses) for wood properties between opposite and tension wood in young *Eucalyptus regnans* (number of samples of each wood type =87). 133

Acknowlegements

I would like to express my gratitude to my supervisors Dr. Luis Apiolaza and Dr. Jan Wikaira for their unflinching support and stimulating suggestions during this research and thesis writing.

I gratefully acknowledge the financial support provided by the University of Canterbury in the form of 'Compromised Wood Quality' PhD Scholarship.

A number of experts have offered their advice and constructive criticism throughout the course of this thesis. I sincerely acknowledge Prof. John walker, Dr. Clemens Altaner (University of Canterbury), Prof. Kenneth Entwistle (University of Manchester), and Dr. Shakti Chauhan (Forest Research Institute India) for their intellectual inputs and continuous encouragements.

Technical and administrative staff has provided their unconditional support and help in completion of this thesis. I sincerely appreciate Nigel Pink, Lachlan Kirk and Vicki Wilton for their assistance in laboratory work and David Clark for taking care of computer related matters. I am grateful to Jeanette Allen, postgraduate coordinator in School of Forestry, for sorting out administrative work without any hassle.

I am also grateful to all staff and postgraduate students of School of Forestry for maintaining a pleasant and friendly working environment.

At last I thank my family and friends for their personal support and encouragement.

Abstract

This study approaches wood quality in young trees by very early screening – and consequent selection for propagation – on the basis of physical and mechanical properties.

In chapter 1 corewood properties are reviewed and the importance and problems associated with early screening are discussed. Due to randomly distributed reaction wood in young trees it is advantageous to lean trees to avoid intermixing of the two wood types and minimise any uncertainty in the results.

In chapter 2 physical and mechanical properties are described for opposite and compression wood in a population of *Pinus radiata* comprising of 50 families, at a young (<3 years) age. The dynamic stiffness was determined using the resonance acoustic technique. Density was measured using water displacement method, and longitudinal and volumetric shrinkage were measured from green to ~5% moisture content. The compression wood and opposite wood differ significantly in all the measured properties. Compression wood was characterised by high density and high longitudinal shrinkage. The mean stiffness of opposite wood was 3.0 GPa with a mean standard deviation of 0.39, and the mean longitudinal shrinkage of opposite wood was 0.99% with mean standard deviation of 0.31 across the samples examined. This variation in stiffness and longitudinal shrinkage in opposite wood can be exploited to screen for wood quality. The variation in stiffness and longitudinal shrinkage within a family was comparable to variation among families. In spite of large within site variability it was possible to distinguish between the worst and the best families in opposite wood at young age.

In chapter 3 ranking of selected families of *Pinus radiata* was done based on microfibril angle, which is considered as the main factor influencing both stiffness and longitudinal shrinkage. The ranking was compared with ranking done using acoustic velocity which is more practical and fast method of screening trees. The mean MFA in opposite wood was 39° with a mean standard deviation of 3.7 and in compression wood the mean MFA was 44° with a mean standard deviation of 2.9. The variation in MFA in opposite wood offers opportunities to breed for trees with low MFA. A strong negative correlation (R=-0.68) between acoustic velocity squared and MFA in opposite wood suggested that the resonance technique can be used effectively to screen very young wood rather than using MFA.

At high MFA, the cell wall matrix also plays an important role in determining the mechanical and physical properties of the wood. At present the chemical composition of wood samples is determined by wet chemical analysis, which is time consuming and laborious. Therefore, it is impractical to characterise large numbers of samples. Mechanical properties, particularly tanδ (dissipation of energy), which changes with temperature and frequency as the structure of the material changes at the molecular level, was studied using dynamic mechanical analysis (DMA). The idea was to assess if it can be used as a quality trait for tree screening instead of wet chemical analysis. Compression wood and opposite wood were characterised for storage modulus and tanδ at constant moisture content. In practice the instrument used, TA instrument Q800, was unable to provide the desired range of temperature and humidity so no glass transition at 9% moisture content in the temperature range of 10°C to 85°C at 1 and 10 Hz frequency was observed that might be attributed to the hemicelluloses (or lignin). In spite of the huge difference in chemical composition of opposite and compression wood, the difference in their mean tanδ at 25°C and 1 Hz values was just 7%. The positive correlation between MFA and tanδ in opposite wood suggested that MFA also plays a role in the dissipation of energy. The strong relationship between storage modulus and dynamic modulus (R=0.74) again justifies the reliability of resonance technique to screen young wood for stiffness.

Concurrently eighty seven, two-year-old leant *Eucalyptus regnans* were studied for growth strains along with other physical and mechanical properties, independently in tension and opposite wood. The leant trees in *Eucalyptus regnans* vary in their average growth strain. Strong correlation between measured and calculated strain (R=0.93) suggests that the quick split method can be used to screen large populations for growth stresses. Tension wood was characterised by high density and was three times stiffer than opposite wood and twice as high in volumetric shrinkage. The high longitudinal shrinkage in opposite wood could be due to comparatively high MFAs in opposite wood of the young trees. There was no correlation between growth strain values and other measured properties in opposite wood. It is possible to screen for growth strain at age two, without any adverse effect on stiffness and shrinkage properties.

Abbreviations

BD	Basic density
CV	Coefficient of variation
CW	Compression wood
DAI	Diameter asymmetry index
DMA	Dynamic mechanical analysis
E_L	Modulus of elasticity along longitudinal direction
E_R	Modulus of elasticity along radial direction
E_T	Modulus of elasticity along tangential direction
FSP	Fibre saturation point
GPa	Gigapascal
LGS	Longitudinal growth strain
LS	Longitudinal shrinkage
MC	Moisture content
MFA	Microfibril angle
MOE	Modulus of elasticity
MOR	Modulus of rupture
NW	Normal wood
OW	Opposite wood
PEI	Pith eccentric index
R	Correlation coefficient
R^2	Coefficient of determination
RS	Radial shrinkage
S1, S2 and S3	Sub layers of secondary cell wall of a tracheid
SM	Storage modulus (elastic component)

tanδ	Dissipation of energy
TOF	Time of flight
TS	Transverse shrinkage
TW	Tension wood
V^2	Acoustic velocity squared
VS	Volumetric shrinkage
με	Micro strain

Chapter 1. General Introduction

This thesis is concerned with the wood characteristics and properties of very young trees (<3 years), both a hardwood (*Eucalyptus regnans*) and a softwood (*Pinus radiata*). This is reflected in the introduction where the review refers primarily to young wood.

Around the world, the forest industry is increasingly drawing its raw material from short rotation crops in order to fulfil the ever growing demand for wood (Bendtsen, 1978; Zobel, 1980). As a consequence, disproportionately more corewood (wood formed in the first 10-15 growth rings) of poor intrinsic quality is coming in the market, and cannot be utilised for structural purposes.

Stiffness has a significant effect on the structural timber outturn (Gaunt, 1998; Moore, 2012). Based on an industrial survey (Ivković et al., 2006) stiffness is recommended as the main breeding objective trait for radiata pine in Australia. A large amount of wood, mainly comprising of corewood is downgraded to industrial use (pulp, paper and low quality packaging etc.) because of its poor stiffness below 7GPa (Sorensson et al., 1997) or 8GPa (Moore, 2012). The wood below this stiffness is also dimensionally unstable (Megraw et al., 1998). Success of any industry is driven by its economic gains. It is anticipated that improving industrial grade wood (corewood) can lead to higher economic gains than improving already acceptable wood (outerwood) (Gaunt, 1998).Thus with the main emphasis on improving corewood, this thesis investigate the structure property relationship in corewood, so that the factors influencing wood quality, particularly longitudinal stiffness and stability in corewood can be identified and used for further breeding.

Wood quality of solid wood products mainly revolves around stiffness (for structural products) and dimensional stability (for both structural and high value boards). Stiffness or modulus of elasticity (MOE) relates to linear deformation produced by a stress (below the elastic limit) which is completely recoverable after the applied load is removed. Where the applied stress exceeds the elastic limit there is some permanent, irrecoverable deformation, which in this thesis is examined by DMA (dynamic mechanical analysis). Wood is an anisotropic material; it has three moduli of elasticity in mutually perpendicular axes; E_L along the longitudinal axis (parallel to the stem), E_R along the radial axis (perpendicular to the stem but normal to the growth rings) and E_T along the tangential axis (perpendicular to the stem but tangent to the growth rings). Among E_R, E_T and E_L, the value of E_L is far larger and this

direction is the principal axis for solid wood products. Thus the E_L (the longitudinal stiffness is often simple termed “stiffness”) has been recognized as a key quality standard of wood and timber.

The changes in dimensions as wood products are exposed to varying relative humidity conditions cause practical problems. The extent of change in dimensions can be related to dimensional stability of the wood and is regarded as another important quality parameter in solid wood products. When freshly-felled wood dries, it shrinks. This shrinkage is attributed to the loss of adsorbed water located within the swollen cell walls of the green timber. Wood shrinkage is anisotropic, it shrinks about twice as much tangentially (TS) as radially (RS) and shrinkage is generally very low in the longitudinal direction (LS) (Walker, 2006). The TS, RS, and LS together approximates to total volumetric shrinkage (VS). Both stiffness and stability are dependent upon the cellular structure and composition of the wood.

Softwood and hardwood are quite different in their cellular structure, with the former being simpler and more uniform (Figure 1.1). In softwood, both conduction of water and structural support are performed by long pointed fibrous cells called tracheids. Whereas in hardwood there are specialized cells performing specific function. Conduction is mainly performed by cells called vessel elements and the support system is made up of fibres. The molecular architecture of the wood cell wall follows the same principle in both wood types—cellulose microfibrils are arranged in an amorphous matrix of hemicelluloses and lignin. The cellulose fibrils run fairly parallel to each other and form a helix around the cell axis. The angle between the cellulose fibril and longitudinal axis of the cell, termed the microfibril angle (MFA), is an important factor determining the mechanical properties of the wood. The MFA in softwood species is generally higher than in hardwood species. For example, in *Pinus sylvestris* (a softwood) the MFA decreases from a maximum of 45° near the pith to 15° at a distance of ~85mm and further decreases to ~0° at 160mm from the pith. Whereas in *Quercus robur* (a hardwood) the angle near the pith is 20° and decreases gradually to ~0° at 40mm and stay there in the rest of the stem (Lichtenegger et al., 1999).

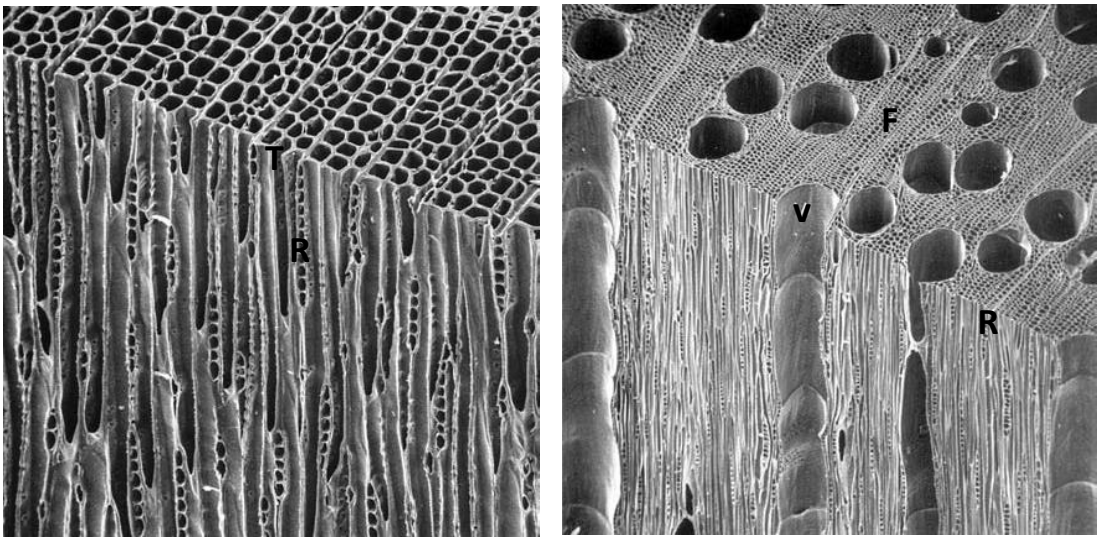

Figure 1.1 (a) Softwood (*Dacrycarpus dacrydioides*) showing axial tracheids (T) and uniseriate rays (R) and (b) hardwood (*Eucalyptus delagatensis*) showing vessels (V), fibres (F) and uniseriate rays (R) (Barnett and Jeronimidis, 2003)

Another factor that influence the wood quality is reaction wood. There is a natural tendency for leaning trees to reorient themselves to the vertical position wherever the stem leans in response to snow, wind or phototropism. While reorienting trees tend to form reaction wood which develops in response to stress; gravity being the most common cause of this stress. The physiological response to the effect of gravity on the leaning stem is to induce an asymmetric distribution of growth regulators around the circumference of the shoot, which causes reaction wood formation and stimulates eccentric growth (Wilson and Archer, 1977). In softwood, the reaction wood is termed compression wood (CW) as it often appears in localized zones of the trees held in compression; i.e. the underside of the leaning stem. Whereas in hardwood, reaction wood is called tension wood (TW) as it tends to form in the region held in tension, i.e. upper side of the leaning stem. The wood diametrically opposed to reaction wood is known as opposite wood (OW) and wood on sides not completely delineated is termed as normal wood (NW) or sometime as sidewood (Timell, 1986). The reaction wood is in abundance in very young trees. The structure and composition of reaction wood is different from normal wood and need to be considered while screening trees for wood quality at young age. In next sections the structure of corewood and reaction wood in softwoods is reviewed in detail as this thesis is primarily focused on wood quality of very young radiata pine in a series of trials. Hardwoods are discussed more briefly as my work in this area was

exploratory using mixed seed of unknown genetic origin. Hardwoods are discussed further in chapter five.

1.1 Corewood

Slow-grown narrow-ringed wood of conifers is superior in quality to that of rapidly-grown wide-ringed wood (Pearson and Gilmore, 1980). Subsequently, it was recognized that fast growth in trees *per se* did not result in poor wood quality, rather the abundance of corewood arising from the shorter harvesting cycle was the main reason (Kennedy, 1995). Moody (1970) at the US Forest Products Laboratory demonstrated that lumber containing pith-associated wood (corewood) is of low strength. Again, Bendtsen (1978); Kretschmann and Bendtsen (1992) observed that corewood is inferior in its mechanical properties to mature wood, and that the strength and stiffness of logs decrease with increasing amounts of corewood.

Corewood can account for 50% of the stemwood of 25 year-old well-thinned, fast grown radiata pine (Cown, 1992). It will be somewhat less under the current circumstances where the mean rotation age for New Zealand radiata pine is 27-30 years (Sutton, 1999). However, Sorensson et al. (1997) have suggested that it might fall to 20 years in coming decades which implies an increased proportion of low quality corewood in the market.

The change from corewood to outerwood is neither sharp nor the same for all intra-ring properties. Walker and Nakada (1999) argued that defining precise corewood limit is pointless because different properties observe different maturation ages e.g. in *Pinus radiata* longitudinal shrinkage is problem mainly up to age three years, in contrast, density increases up to age 30 years. For Douglas fir (*Pseudotsuga menziesii*) the shortest juvenile period is shown by latewood density (first 14 years) and the longest by latewood proportion and earlywood density (37 years) (Abdel-Gadir and Krahmer, 1993). For *Pinus taeda* the corewood-outerwood demarcation point for mechanical properties and specific gravity is between 12-13 years and for cell length it is 18 years (Bendtsen and Senft, 1986).

The percentage volume of corewood at a particular age also varies between species; for *Pinus taeda* (loblolly pine) the estimated percentage of corewood in 20 year old trees is around 60% whereas for *Populus deltoides* (cottonwood) it is 80% (Bendtsen and Senft, 1986). In a 25-year-old *Pinus radiata* tree, corewood constitutes around 50% of the total merchantable volume (Cown, 1992).

1.2 Defining corewood

Juvenile wood, a term which predates its synonym corewood, is formed by a young vascular cambium near the stem centre (Zobel and van Buijtenen, 1989). But according to Larson (2001) the term juvenile wood is a misnomer. He states that "*juvenile wood is produced in first 1-3 years of growth. Thereafter, similar but not identical wood is produced in the central core of wood at all height levels of the stem. The more appropriate word is corewood or crown formed wood because it is produced either within the living crown or in proximity to physiological processes emanating from the living crown*". Amarasekara and Denne (2002) distinguished between three types of wood: (i) juvenile wood found in the region around the pith where properties are associated with cambial age independent of crown influence; (ii) crown-formed wood which describes variations in wood properties associated with crown size (differences in crown size from suppressed to dominant trees lead to a substantial increase in average ring width and a decrease in mean percentage latewood, modulus of rupture (MOR) and modulus of elasticity (MOE)); (iii) corewood which is a general term that refers to the core region (the centre of the tree) where most wood properties tend to vary outwards from the pith. Burdon et al. (2004) characterized wood variations two dimensionally (i) from the pith outwards (radial) and (ii) from the ground upwards (vertical). They applied the juvenile versus maturity concept for the vertical progression, and corewood versus outerwood for the radial progression (Figure 1.2).

In New Zealand radiata pine, wood representing the first ten growth rings is defined arbitrarily as corewood (Cown, 1992), although strictly it can either be juvenile or mature depending upon the height of the stem (Burdon et al., 2004).

This thesis is concerned with very young wood at the base of the tree and such material will be simply described as corewood.

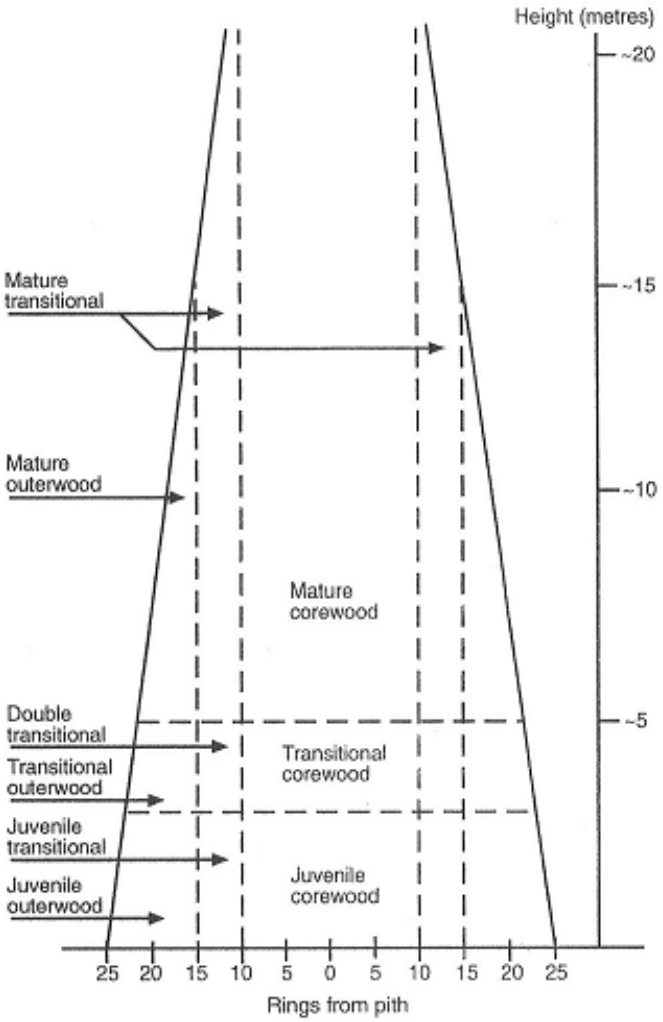

Figure 1.2 Schematic section of a typical *Pinus radiata* stem showing different wood zones (Burdon et al., 2004)

1.3 Characteristic features of corewood

Softwood timber mainly consists of tracheids which are required to perform two distinct functions. The principal role of earlywood (also called spring wood) tracheids with their wide lumens and thin cell walls is to transport nutrients and water, whereas with latewood tracheids (sometimes called summer wood) with small lumens and thick cell walls the principal role is to provide strength. In young trees, because of the strong influence of the crown, earlywood type cells are produced mostly throughout the growing season (Larson et al., 2001). In some trees the juvenile zone appears to consist mainly of earlywood (Hiller, 1954). Tracheids also vary in length and are shorter near the pith (Cown, 1975). Thus corewood is characterized by short tracheids with large lumen and thin cell walls.

The cell wall of a tracheid (Figure 1.3) has a primary wall that is laid down during growth, while the secondary wall is formed subsequently and has three distinct sub-layers; S1, S2 and S3. Cell walls are composed of ordered cellulose molecules aggregated into microfibrils which are embedded in the matrix of amorphous hemicelluloses and lignin. The orientation of microfibrils differs in the sub-layers. In the S1 and S3 layers microfibrils are oriented at an angle of between 50° and 90° to the cell axis. Whereas in the S2 layer the microfibrils are oriented at an angle of only 10° to 40° from the tracheid axis (Donaldson and Xu, 2005). The S2 layer of the secondary wall constitutes approximately 80% of the wall, and the angle of orientation of microfibrils in it is considered as the MFA (Cave, 1968; 1969; Preston, 1974). The MFA is critical to the mechanical balance of the tree. When a tree is young the MFA is quite high and the cell wall has a low longitudinal elastic modulus (Cave, 1969), but increased strain to fracture (Fratzl et al., 2004) allowing the stem to sway in the wind and reorient. A high microfibril angle and lignin content is needed to resist gravity and wind loads for young trees (Lichtenegger et al., 1999; Reiterer et al., 1999). As high microfibril angle incorporates extensibility (Burgert, 2006) needed during wind loading and increased lignin adds stiffness resistance to compression forces (Hepworth and Vincent, 1998). With increasing cambial age (in subsequently formed tracheid cells) the MFA decreases to provide stiffness for keeping the trunk upright (Barnett and Bonham, 2004). The MFA is about 30-40^{o} at the pith but decreases to 10-15° at the age of 10-11 years in *Pinus radiat*a (Wu et al., 2007) and in *Picea abies* the angle near the pith is ~35° and deceases to 2°-8° in 15 to 35 years (Gorisek et al., 1999). There is not much variation in the orientation of microfibrils in the S1 and S3 layers related to age or height within a tree (Donaldson and Xu, 2005). Lignin concentration is lower (Donaldson, 1987) and microfibrils are more closely packed in the S2 layer than in the S1 or S3. The juvenile tracheids particularly at the base of the stem are characterised by thick S3 layer (Donaldson and Xu, 2005). The low density of corewood is associated with thin cell walls and large lumen and a comparatively narrow S2 wall layer. Thus corewood has high lignin and low cellulose content, due to the larger contribution of the primary, S1 and S3 layers.

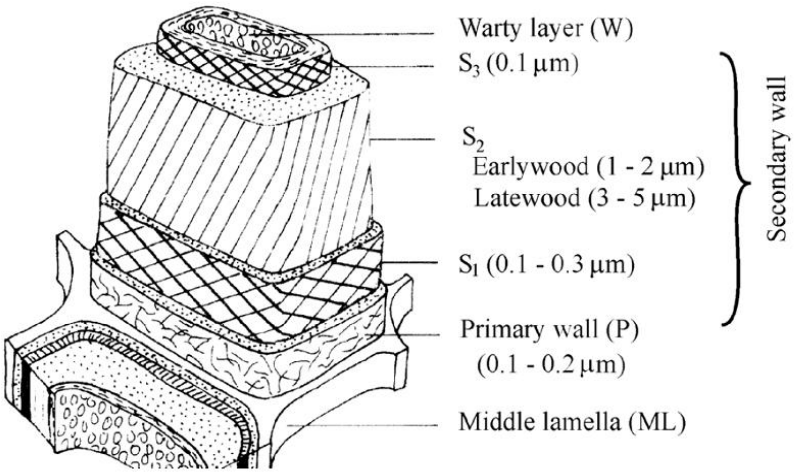

Figure 1.3 Schematic representation of the microfibrillar structure within the cell wall of a softwood tracheid (Côté, 1967).

Corewood properties are quite different from outerwood and it is characterized by low basic density, short tracheids with thin walls, low transverse shrinkage, high longitudinal shrinkage, high MFA and green moisture content (Figure 1.4) (Bao et al., 2001; Bendtsen, 1978).

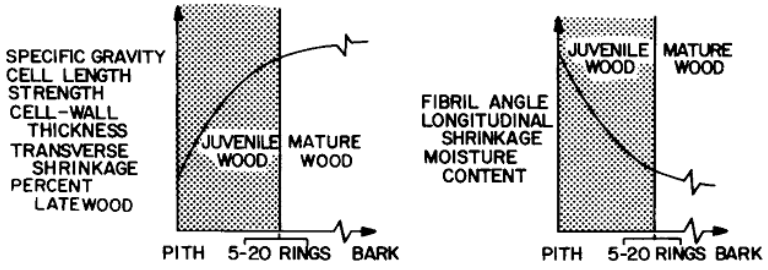

Figure 1.4 Schematic representation of the gradual improvement in properties with age (Bendtsen, 1978)

1.4 Compression wood

Compression wood (CW) is formed to counteract and correct the lean of the stem due to snow, wind or phototropism, The developing CW tracheids tend to extend along the grain, thus exerting an axial pressure that slowly bends the stem back to its vertical orientation (Timell, 1986). Compression wood is very prevalent in corewood due to crown asymmetries and stem malformation found in seedlings and young trees (Apiolaza et al., 2008). Nursery seedlings are grotesquely malformed compared to mature trees in plantations. Seedlings when

planted in the forest are invariably planted at an angle; and 1-2 year-old trees are very susceptible to all the elements that displace the stem. Subsequently vertical stems can have significant amounts of CW that have resulted from corrections to a previous leaning or from small less-obvious asymmetric loadings within the stem, although severity and amount of CW is higher in obviously leaning trees (Donaldson et al., 2004). In contrast, Lachenbruch et al. (2010) argue that there is no significant difference in the amount (but not severity) of CW in straight and crooked trees.

This thesis is interested in ranking young trees according to the physical and mechanical properties of normal or opposite wood. The presence of compression wood with its distinctive and highly variable physical and mechanical properties has the potential to obscure or invalidate that ranking. For this reason, a plan to tilt the trees was implemented. This implied that the properties of compression wood could also be characterized but it was found in the Amberley trial that the angle of lean was variable so that the assessment of compression wood was of varying intensity.

The severity of CW ranges from only slightly modified normal wood to the fully developed type. Different authors used different criteria for classifying CW severity. Burdon (1975) examined CW under transmitted light and classified it into six grades from 0 to 5 (normal wood to severe CW). Harris (1977) graded wood visually on the basis of its darker colour into four grades depending on the width of the dark coloured patch from 0-3 (normal to severe). Yumoto et al. (1983) graded CW at microscopic level and considered spiral grooves and extent of the secondary layer lignification as the main determinant of the severity of CW. First, he classified wood on the basis of the degree of development of spiral grooves into three classes, which were further subdivided on the basis of the extent of lignification and cell wall thickness.

Severe CW is dull reddish in colour and has very different properties than opposite wood. The tracheids are shorter in length and also have smaller mean tracheid widths (Yeh et al., 2005). CW tracheids are characterized by their round shape with thick cell walls; and severe CW also has large intercellular spaces. The secondary wall lacks the S3 layer and the S1 and S2 layers are thicker than in normal wood (Figure 1.5). In S1 the cellulose microfibrils run transversely, while in S2 they run at an angle of 30-45° to the longitudinal axis of the cell. The S2 layer is divisible in to two layers, an inner S2 and an outer S2. The outer S2 layer is characterized by a high lignin and galactan content, low cellulose content and no helical cavities. Due to its high lignin content the outer S2 layer is designated as S2(L) by (Côté et

al., 1968) and is considered to be the anatomical feature most characteristic of CW (Yumoto et al., 1983).

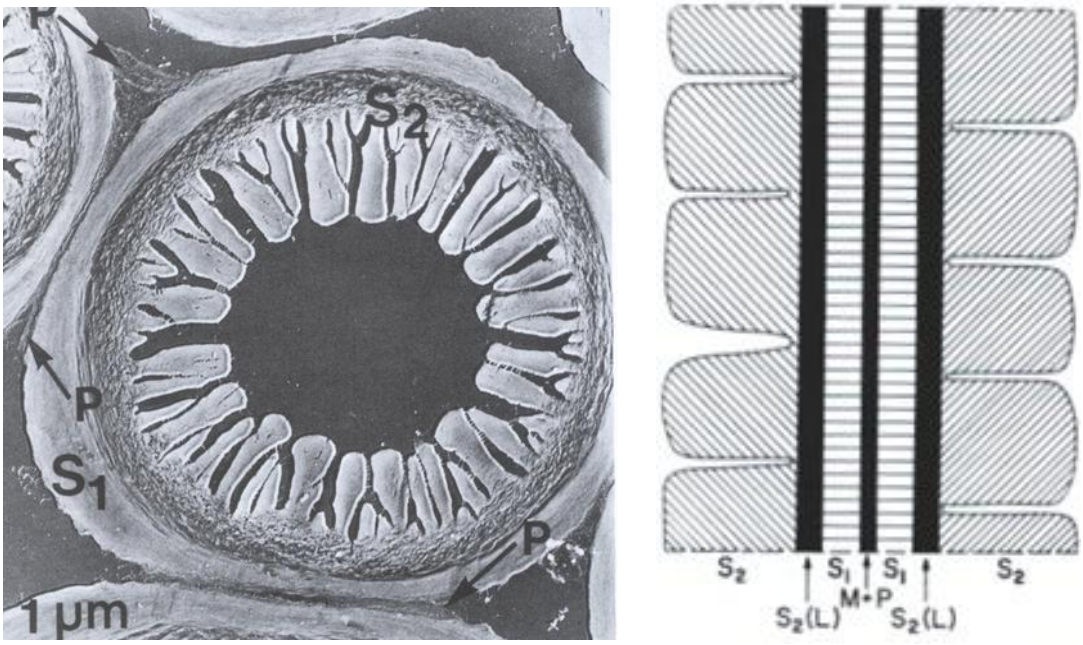

(a) **(b)**

Figure 1.5 (a) Transverse section of delignified compression wood tracheid in *Larix laricina*. (b) Schematic model of a double cell wall in a compression wood tracheid, where black symbolizes the high lignin content in middle lamella and primary wall (M+P) and in S2(L) (Timell, 1986)

CW has a high lignin and galactose content but is low in glucose and mannose (Kibblewhite et al., 2009). The CW lignin is more crosslinked than the lignin in NW due to its higher content of p-hydroxyphenyl propane unit (Brennan et al., 2012; Westermark, 1985). The other chemical characteristic of CW is 1,4 β galactan in the S2(L) layer, which is either absent or present in the primary wall in small amounts in OW (Altaner et al., 2010; Timell, 1986). CW is also characterized by a high basic density. Timell (1982) determined the specific gravity of normal and severe CW from nine conifer species and concluded that the average specific density of CW is 85% higher than that of NW. The CW is also characterized by exceptionally high LS. Harris (1977) reported 4.5% longitudinal shrinkage in severe CW in *Pinus radiata*.

The average MFA is higher in CW than in OW, but in the juvenile corewood at the base of the tree both have similar microfibril angles (Donaldson et al., 2004). Wooten et al. (1967) measured the longitudinal shrinkage and MFA in CW, NW and OW from 2 years old

seedlings of *Pinus taeda* and reported unusually high LS in CW samples compared to NW and OW. The MFA was comparable in all the three types; it was even higher in certain OW samples. The high basic density and differences in chemical composition and cell wall anatomy contribute to the high longitudinal shrinkage of CW particularly in corewood.

1.5 Variation in wood properties among trees

In addition to corewood being poor in terms of stiffness and dimensional stability, there are large variations among individual trees of the same species, which are observed especially in softwood (Walker et al., 1993). Harris (1981) suggested that a large part of tree variability is under genetic control and hence improvements can be made in corewood properties by selective tree breeding. Thus Cown et al. (2002) reported that the corewood density of radiata pine differs markedly between individual trees and clonal selection could be an effective way of modifying corewood properties. Apiolaza (2011) analyzed basic density in 23,330 stem cores from 18 trials in New Zealand and suggested that, although the heritability for basic density ranges between moderate to high (mean, 0.6), the phenotypic coefficient of variation is very low (<8%), thus limiting the opportunities to improve basic density through breeding. Tsehaye et al. (2000a) studied wood variation in *Pinus radiata* and reported that stiffness is a better parameter for screening than density and the stiffest trees are 80-85% stiffer than the least stiff trees. They suggested that selecting seedlings on the basis of such criteria at the time of planting would improve the timber by at least one machine stress grade. Similarly, Lindström et al. (2004) through their studies on 3-year old clones of radiata pine, suggested that there is a two-fold difference in MOE between stiffest and least stiff trees and there is potential for MOE genetic improvement of corewood.

1.6 Factors affecting stiffness and stability

Genetic turnover and so delivery of improved wood properties can be achieved more quickly if mass screening is performed at an early age. For that, specific traits need to be chosen that best distinguish between trees. To specify the appropriate parameters, it is necessary to quantify wood quality characteristics i.e. density, percentage of CW, chemical composition, tracheid dimensions and MFA, so that the fundamental parameter or combination of parameters most influencing stiffness and dimensional stability can be identified and considered for genetic improvement.

Stiffness and stability are influenced by the combination of all the above mentioned parameters. MFA has proved to be a better predictor of stiffness than density, at least in young trees (Cave and Walker, 1994; Tsehaye et al., 1998). In corewood, a higher correlation was found between MFA and stiffness (-0.92) than between density and stiffness (0.43) (Baltunis et al., 2007). The same study suggested that all the three properties are heritable and maximum heritability is for density. Density is a major factor influencing MOE in outerwood (Cown et al., 1999) but only because the rapid change in MFA, so noticeable in young trees, is largely complete by ring 15. In contrast, in young trees, acoustic velocity (a surrogate measure of MFA) has proved to be a better predictor than density for screening purposes in terms of stiffness (Chauhan and Walker, 2006). The genetic correlation between corewood and outerwood density is higher than between corewood and outerwood MOE (Burdon and Young, 1991; Kumar and Lee, 2002). Also the genetic correlation between MOE and density is low in corewood (growth rings 6-7) (Kumar et al., 2006). Thus the weightage given to density and MFA will very much depend upon the relative importance attached to improving MOE in corewood or in outerwood.

In corewood, where MFA is large, the effect of the cell wall matrix on stiffness and stability is more pronounced. Where MFA is greater than 40^{o}, the stiffness of wood also depends upon the shear properties of the non-crystalline matrix of hemicelluloses and lignin (Barber and Meylan, 1964; Cowdrey and Preston, 1966; Yamamoto and Kojima, 2002). Recently Xu et al. (2011) reported that at high MFA (>35°) the longitudinal stiffness was low and poorly correlated to the variation of MFA in S2 layer. This suggested a reduced contribution of the cellulose microfibrils and increased contribution by the amorphous matrix to longitudinal mechanical properties at high angles (Via et al., 2009). High dimensional instability is also related to specific hemicelluloses e.g. galactan (Floyd, 2005).

In summary, for screening purposes, in addition to the MFA and density, the chemical composition, particularly the effect of the amorphous matrix also needed to be considered in corewood of softwood where the MFA is quite high.

1.7 Hardwood - eucalyptus

As discussed above, softwood properties in short rotation crops are affected by corewood properties. In particular, a high MFA found in the corewood of most softwood results in low stiffness. In contrast the MFA is quite low in hardwoods and poor wood quality in young

hardwoods is due to issues that differ from those for softwoods, e.g. brittleheart, collapse, growth stresses and tension wood.

More generally and broadening the discussion to include outerwood, the MFA in the S2 layer in hardwood fibres (such as eucalyptus) ranges from about 5° to 20° (Evans et al., 2000), whereas the comparable range for softwood is from about 10° to 30° (Boyd, 1980). There is also less variation in MFA within a tree; e.g. it decreases from 19° at age 3 to 14° at age 15 in *Eucalyptus nitens* (Evans et al., 2000). Despite these advantages, eucalyptus display high growth stresses (Kubler, 1987) which greatly impact their stability and the economics of sawing them. High level of growth stresses in eucalyptus is the most serious growth phenomenon affecting wood quality, product yield, and product dimensions. The details are discussed in chapter five.

Warp in lumber is fundamentally driven by gradient in growth and/or by drying stresses (Simpson, 1983). The main reasons for dimensional instability in eucalyptus are a steep gradient in longitudinal growth stress in the radial direction and abnormally high longitudinal shrinkage in tension wood. Large growth stresses are also related to tension wood in seven hardwood species (Okuyama et al., 1994).

There is a large variation in wood properties among trees growing within a uniform site. A large variation was reported by Evans et al. (2000) among trees both in terms of *Eucalyptus nitens* MFA and density. Density and MFA accounted for 96% of variation in longitudinal MOE (Schimleck et al., 2001). Malan and Gerischer (1987) reported a large variation in the level of growth stresses among trees in *Eucalyptus grandis*. They suggested selecting trees with a reduced level of growth stresses, apart from a reduction in splitting, also results in reduced within tree variability in wood quality. Murphy et al. (2005) also reported large variation in stress measurements in *Eucalyptus dunnii* and suggested that it exhibits sufficient heritability to make tree breeding helpful in reducing the incidence of growth stresses in eucalyptus. Thus when screening *Eucalyptus species*, in addition to basic measurements like basic density, MOE, and LS; growth stresses need to be considered.

1.8 Tools to characterize wood properties

For mass screening of trees, rapid, effective and cheap tools and techniques are required. Acoustic methods predict stiffness by measuring the velocity of a sound wave propagating through wood. In forestry it has been proved to be one of the best assessment tools and is

widely used (Huang et al., 2003). It can effectively be used for mass screening of fast grown radiata pine clones at an early stage (Lindström et al., 2002). A high correlation has been found between static MOE (measured in a standard bending test) and dynamic MOE (measured by acoustics) (Lindström et al., 2004).

The cell wall matrix comprised of lignin and hemicelluloses, also influences wood properties of solid wood at high MFA, most notably the shrinkage (Cave, 1972). Accurate characterization of lignin and hemicelluloses relies on wet chemistry, which is both expensive and slow. Practical alternatives that are rigorous, robust, and rapid are needed to either correlate or measure directly those chemical entities that are being targeted. In related work at the University of Auckland, researchers are focused on wet chemistry and infrared microscopy to assess the chemical composition of wood. To complement that work, this thesis examines the application of dynamic mechanical analysis (DMA) that may respond to the presence of key chemical constituents, such as specific hemicelluloses and lignins.

DMA, which relates mechanical properties to changes at molecular level in viscoelastic materials, can be used to explore changes in wood properties that might be attributed to the matrix materials of the cell wall. In DMA, a sinusoidal stress is applied and the changes in mechanical properties (storage modulus and loss modulus) are studied as a function of temperature and/or frequency. The storage modulus is related to the elastic component, whereas the loss modulus is related to the viscous component of the material.

Wood is a viscoelastic material composed of elastic cellulose fibrils embedded in a viscous matrix of lignin and hemicelluloses. The nanostructure of wood consists of cellulose microfibrils associated with hemicelluloses, particularly glucomannan agglomerating to form macrofibrils which in turn are surrounded by lignin, xylans, and the rest of the glucomannans (Åkerholm and Salmén, 2001). It is assumed that hemicelluloses act as a coupling agent between cellulose and lignin. Chemically isolated fibres are weaker in strength and stiffness than mechanically isolated fibres and the proposed explanation for this is that chemical treatments alter the structure of hemicelluloses attached to cellulose fibrils (Burgert et al., 2005). Hemicelluloses are the most sensitive constituents of wood to temperature, humidity, and stress because they are non-crystalline (like lignin), hygroscopic (unlike lignin), have low molecular weight and accessible to water (unlike crystalline cellulose). Tensile testing on CW tissue and mechanically isolated single fibres demonstrated that hemicelluloses play a key role in mechanical properties (Burgert et al., 2002). Molecular mechanisms have also been proposed for this (Altaner and Jarvis, 2008; Keckes et al., 2003). Water, that is absorbed

within the cell wall, plays a crucial role (Burgert and Fratzl, 2005). It has been shown by *in situ* tensile deformation experiments that the major part of the deformation takes place in the soft matrix between the stiff fibres (Burgert et al., 2003).

In DMA when a sinusoidal stress is applied, the mechanical vibrational energy losses within the wood are related to its water content (moisture content) and arise due to stress-induced modifications of the hydrogen bonding structure, particularly in hemicelluloses. Such energy loss measurements can be used to make some deductions regarding the amounts of the specific hemicelluloses in the sample (Entwistle, 2005).

In this thesis it is hypothesized that, at constant moisture content, the changes in energy loss are directly related to changes in hemicelluloses and that dynamic mechanical analysis could be used as another predictor of the influence of hemicelluloses on wood properties.

Finally, growth stresses can be assessed by measuring longitudinal growth strain using strain gauges. Chauhan and Entwistle (2010) working with *Eucalyptus nitens* reported a good correlation between measured strain using strain gauges, and predicted stress values using log dimensions and measurement of outward bending of the two half-rounds on sawing along the pith. They showed that simple measurement of the opening of a log on sawing together with log dimensions provide a quick and reliable approach in assessing growth stresses in trees.

1.9 Selection age

Even today, most of the studies on wood quality improvement through tree breeding work with trees aged 7-8 years or older. While this may be a valid approach where one is seeking to maximize the amount of wood at the end of the rotation (Jayawickrama and Carson, 2000), others have questioned this strategy with regard to wood quality characteristics and properties (Apiolaza, 2009). Apiolaza (2009) justified the importance of very early screening over long-term evaluation by focusing on wood quality thresholds, below which the sawn timber would have little value. In turn, this relates to the highly variable, low quality wood in the corewood zone. According to Apiolaza (2009), shorter breeding cycles should outweigh the lower accuracy due to early selection. However, when Lindström et al. (2004) examined wood property variations in three-year old clones of radiata pine, they found that CW reduces stiffness and inflates wood density. Furthermore, there was no correlation between CW percentage and MOE. CW is very prevalent in corewood, partly due to the high growth rates in this region of the stem (Harris, 1977). Burdon (1975) examined 12-year-old *Pinus radiata*

growing on four sites in New Zealand and estimated that 30% to 45% of the stem volume was mild to severe CW. The comingling of CW with OW and NW introduced uncertainties in the analysis and made the prediction of 'true' NW properties problematic. The contrast in properties between CW and OW means that, where the two wood types occur together in the same piece of wood, the results of any analysis are confounded. Thus the main problem of characterizing wood in very young stems is the random distribution of reaction wood: random in the sense that looking at the external characteristics of the stem it is not possible to deduce where the compression wood arcs are likely to be located, except in the outermost wood of a leaning stem.

Deliberately tilting trees at an angle produces distinct sectors of opposite and severe CW. Severe CW is associated with the underside of the leaning trees whereas mild CW is not limited to the underside of a leaning stem or one side of a vertical stem (Donaldson et al., 2004; Harris, 1977; Xu et al., 2009). Figure 1.6 shows the cross-section of wood in tilted and non tilted (straight) trees. It can be seen that in the leaning tree the two wood types OW (light coloured) and CW (dark coloured) are well separated, whereas in the straight tree there is an intermixing of the two wood types. Thus for screening purposes in a leaning stem the two wood types can be evaluated independently. Apiolaza et al. (2011) reported large differences in density and stiffness within OW, and these differences would be useful for screening purposes in clones, particularly when using leaning trees to reduce unwanted variation. In this thesis, trees were leant to separate two wood types for characterization purpose.

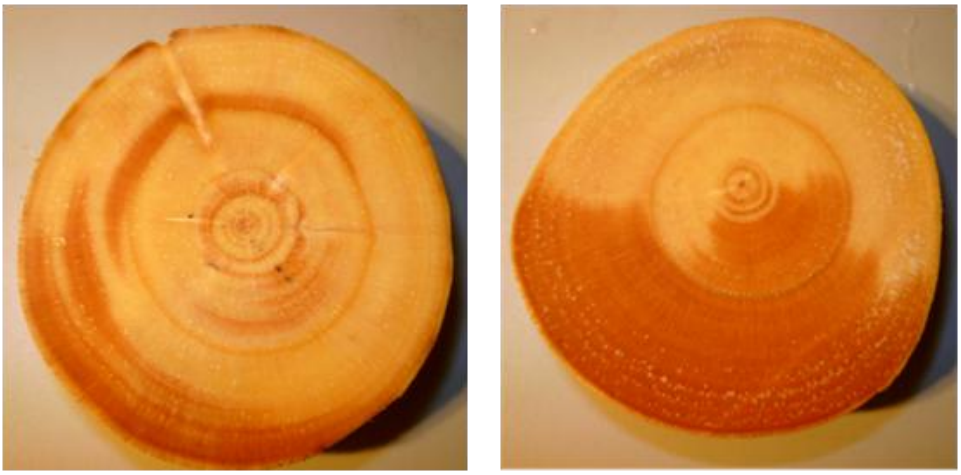

(a) **(b)**

Figure 1.6 Cross-section of wood in tilted and straight trees (a) Straight tree with arcs of compression wood (dark) distributed at random, (b) leaning tree with compression wood confined to the lower side

1.10 Thesis aims and thesis structure

This study evaluates different methods for early screening of young trees (< 3 yrs). The aim was to investigate the structure property correlations in corewood by studying its physical, mechanical and structural properties with the focus on normal wood. This thesis has three themes.

1. Measurement of physical and mechanical properties of 2-3 year-old *Pinus radiata* (basic density; acoustic velocity and hence longitudinal stiffness; axial and volumetric shrinkage; and warp) in both CW and OW. Also, similar measurements on *Eucalyptus regnans* along with assessments of growth stress.
2. Measurement of microfibril angles using X-ray diffraction in two wood types, in *Pinus radiata*.
3. Determination of energy loss and damping by dynamic mechanical analysis in *Pinus radiata*.

Data from these measurements was used to evaluate various selection procedures that could be adopted by tree breeders.

Chapter 2 deals with the basic assessment of <3 years old leant trees. Basic assessment includes measurement of acoustic velocity, density, LS and VS. The wood types are compared for wood properties. In addition to phenotypic correlation between measured properties, phenotypic variation among and within families is also presented.

Chapter 3 deals with the study of MFA in two wood types and the variations among families are also presented.

Chapter 4 sought to characterizes stress relaxation processes using DMA with the primarily purpose of providing data that can be used in Auckland in matching studies of wood chemistry. For my purposes, the aim was to look for any glass-transition in the temperature range 10-80^{o}C and look for any correlation with the physical and mechanical properties measured in Chapter 2. Two wood types (CW and OW) are characterized at constant moisture content. The tanδ—a measure of energy dissipation—is compared for wood types and its correlation with above-mentioned wood properties is presented.

Chapter 5 focuses on growth stresses in leant trees of *Eucalyptus regnans* along with a basic assessment of other wood properties.

Results along with scope of future work emanating from this thesis are discussed in chapter 6.

Chapter 2. Amberley Trials

2.1 Introduction

The New Zealand forest industry is based on plantation forests, which cover 1.8 million hectares, around 6.6 percent of New Zealand's land area. *Pinus radiata* accounts for approximately 90 percent of the total planted area. This species grows quickly under local conditions and the average time from plantation to harvest is around 28-30 years whereas even in the 1980s there were still stands aged over 40 being felled (Sutton, 1999). The shorter rotation means that increased proportion of corewood in harvested logs is causing many difficulties in wood utilization for structural and appearance purposes owing to its poor stiffness and dimensional instability. The properties of corewood can be improved by breeding. Screening trees for their corewood properties at a very young age should result in better quality of timber from the whole tree, taking advantage of the large natural variation in the unimproved population. In this chapter the variation in stiffness and shrinkage in radiata pine is reviewed. The principles of sorting by acoustics are discussed. OW and CW are characterized and compared for density, dynamic modulus, and longitudinal shrinkage (LS) and volumetric shrinkage (VS) in young *Pinus radiata*. The variation in wood properties is examined for two wood types, in 50 radiata pine families.

2.1.1 Variation in stiffness

There is large variation in stiffness not just between trees but also within trees in *Pinus radiata*. Tsehaye et al. (2000a) examined the stiffness variation in a 25 year old stand of *Pinus radiata*. Wood boards were classified according to log type (butt, middle, top position) and distance from the pith (position 1 to 4). They found that the stiffness increased from pith to cambium and the steepest gradient in stiffness occurred near the pith. On moving from position 1 to 2, 2 to 3, and 3 to 4 stiffness increased by 34%, 27%, and 11%, respectively. The study also reported that for any position (1 to 4) the mean value for MOE changed little in going from the butt logs to the top logs.

A more detailed study of 60 trees from a single 27 year old stand of *Pinus radiata* by Xu and Walker (2004) again reported that radial stiffness increased from pith to cambium (P1 to P5 as shown in Figure 2.1). Of particulate interest in this research is that the wood in the lowest 2-3 metres of the stem (butt logs) was less stiff than wood further up the stem.

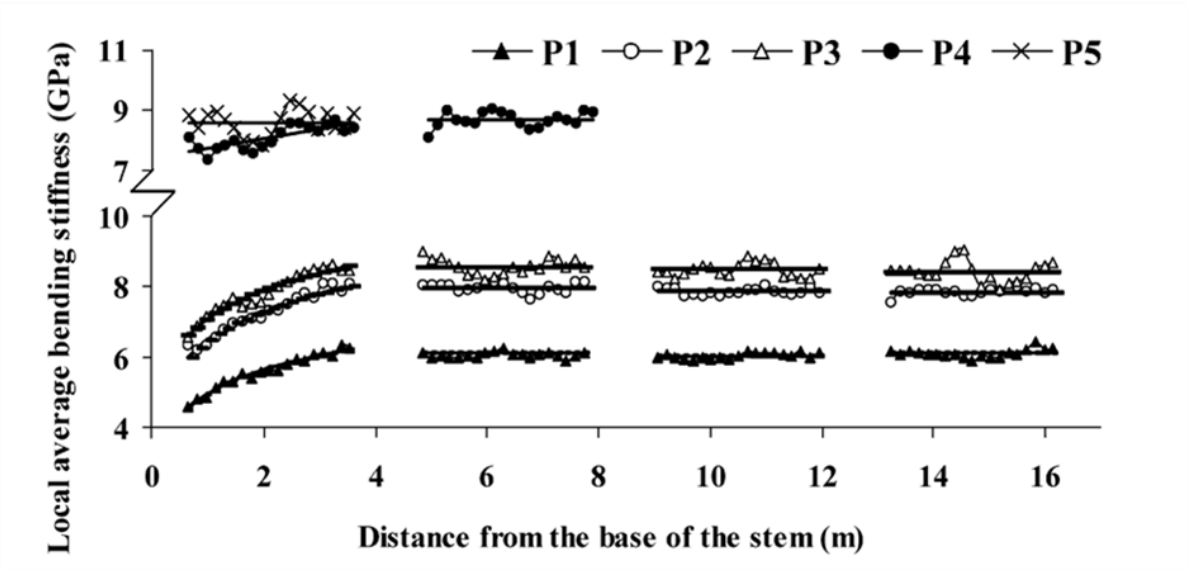

Figure 2.1 Radial and vertical variation in stiffness in radiata pine showing the steep drop off in stiffness in the inner wood close to the groundline (Xu and Walker, 2004). P1 are the boards containing pith, P2 are the boards adjacent to the P1 boards, while P4 and (where present) P5 boards are adjacent to the bark.

To reveal the variation among trees the logs types were grouped into five different stiffness classes. The variation amongst the butt logs of these trees is shown in Figure 2.2 by grouping them into quintiles of increasing stiffness (1-5 as marked in Figure 2.2). There was a huge difference in stiffness between the bottom 20% and top 20% of butt logs which suggests a significant potential for improving stem stiffness through tree breeding.

Breeders seeking to make very early selection could exploit the between-tree variation observed near the groundline (in trees aged 2 to 3 as reported in this thesis) where wood is the least stiff (~3GPa).

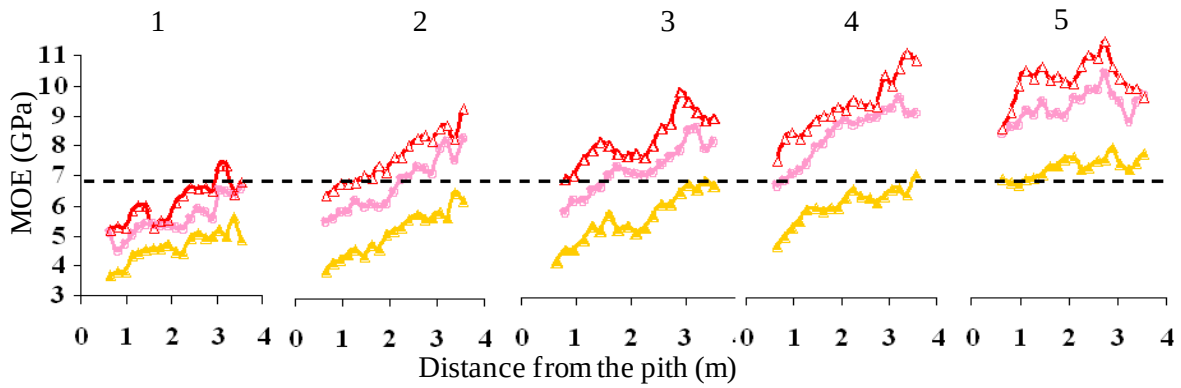

Figure 2.2 Stiffness variation among butt logs of radiata pine trees (Xu, 2000), where numbers (1-5) represent five different stiffness classes

2.1.2 Variation in shrinkage

The variation in shrinkage within a tree is directional. TS and RS increased from pith to cambium whereas LS decreased (Figure 2.3) (Wang et al., 2009). .

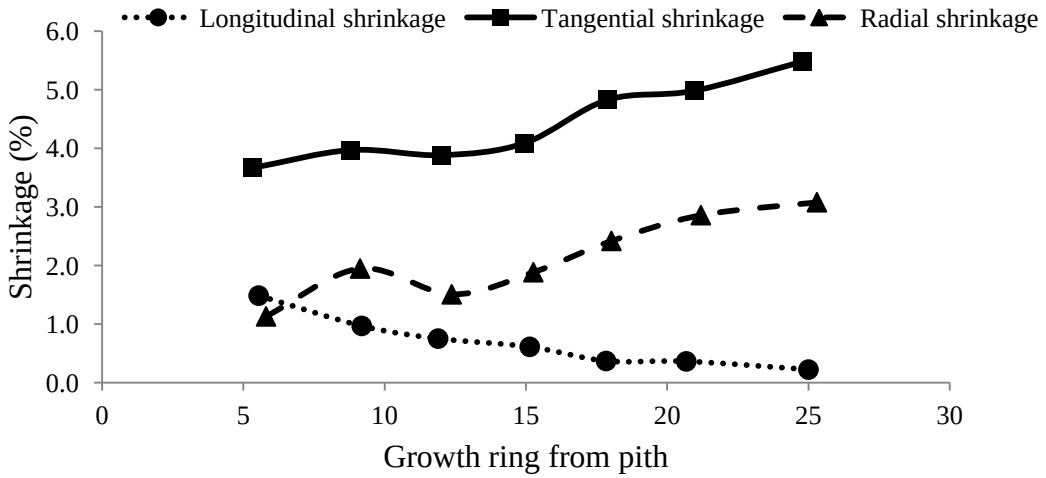

Figure 2.3 Variation of oven-dry shrinkage for radiata pine wood discs from the base of the tree (Wang et al., 2009)

Generally the LS is less than 0.5%, except for the corewood. For RS and TS in outer rings (3-6) the shrinkages were 30-50% greater that for the inner rings (1-2), whereas LS was much greater (>200%) in the inner two rings than that observed in the outer rings (Ivković et al., 2009).

The anisotropy in shrinkage – the directional response to loss of cell wall water – depends upon a number of factors. The magnitude of volumetric shrinkage of the cell wall is directly related to the number of water molecules adsorbed within the cell wall. That in turn is related to the number of accessible hydroxyls on the surface of the cellulose microfibrils, the non-crystalline hemicelluloses, and lignin, and the quantity of cell wall material, i.e. the basic density of the wood (Stamm, 1964). Water cannot penetrate in to the crystalline microfibrils and therefore they do not change in length or cross-section. The non-crystalline hemicelluloses can bond water causing the cell wall to shrink or swell (Olsson & Salmén, 2004; Walker, 2006 Table 3.5). The microfibrils in the cell wall restrain the matrix from shrinking in the direction in which they are aligned, which is broadly parallel to cell axis in outer wood. Thus wood shrinks excessively in transverse direction in outerwood as summarised by Walker (2006). Anisotropy in radial and tangential direction is affected by factors such as the presence of rays (restraining radial shrinkage) (Skaar, 1988), earlywood-latewood proportion (Pentoney, 1953), and higher MFA in radial cell walls (Barber and Meylan, 1964).

Radial variation in shrinkage depends mainly upon the MFA. LS increases with increase in MFA, whereas TS decreases (Meylan, 1968). Variation in LS in corewood and CW where the MFAs are comparable can be attributed to the difference in cell wall anatomy, chemical composition and basic density. CW is characterized by an outer S2(L) layer, rich in lignin (Côté et al., 1968) and β-1-4- galactan (Altaner et al., 2007). High LS has been reported in samples with high galactan content (Floyd, 2005).

The high MFA in corewood at the base of the tree means that this wood has the highest tendency to shrink in longitudinal direction. Excessive spring and bow in timber is reported where the corewood proportion is high and relates to the steep MFA and LS gradient across the stem (Wang et al., 2009). The same study reported significant variation between trees. Gapare et al. (2008) also reported significant genetic variation among trees in *Pinus radiata* for LS in inner first two rings and a decreasing heritability for LS from pith to cambium.

LS in the corewood of radiata pine is of economic importance and can be improved by genetics.

2.2 Acoustic methods to sort wood

In recent years acoustics have been adopted by the industry to characterise logs and lumber. It is a viable alternative to traditional visual and machine stress grading of timber (Sandoz, 1989). There are a number of commercial systems that incorporate acoustics for grading in sawmill, e.g. by Calibre-equipment (http://calibre-equipment.com/) and MiCROTEC (http://www.microtec.eu/en). The published literature regarding the use of acoustic tools for predicting stiffness is extensive (Chauhan and Walker, 2006; Grabianowski et al., 2006; Huang et al., 2003; Ivkovic et al., 2009; Lindström et al., 2002; Tsehaye et al., 2000b). Acoustics was used in this work to determine the longitudinal wood stiffness in small wood specimens (~100mm long).

According to the one dimensional wave theory when a viscoelastic homogeneous solid is hit (e.g. by a hammer) at one end, a compressive wave is generated that travels through the medium at a speed *V*. In the case of a rod or bar when the wave reaches the far end it is reflected and travels back down the bar. Monitoring the movement of a cross-section in such a bar in response to a propagating stress wave results in waveforms that consist of a series of equally spaced pulses whose magnitude decreases exponentially with time (Ross and Pellerin, 1994) (Figure 2.4).

The propagation speed *V* of such a wave can be determined by coupling the measurements of the time between the pulses Δt and the length of the bar *l* by

$$V = \frac{2l}{\Delta t} \qquad 2\text{-}1$$

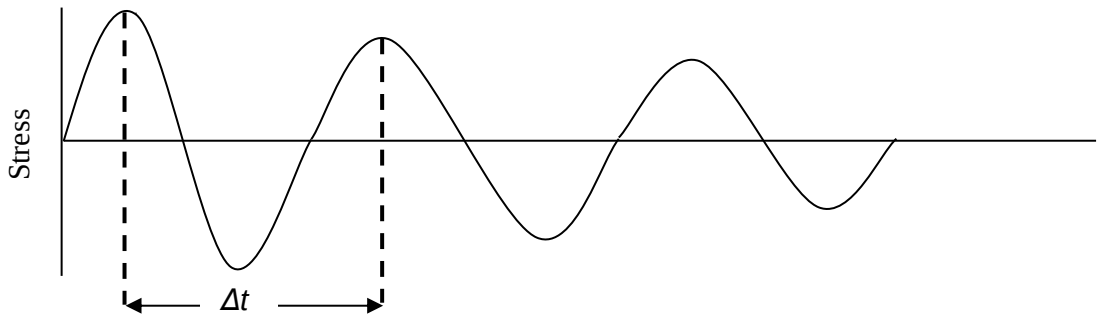

Figure 2.4 Response of the end of a viscoelastic bar in response to a propagating stress wave, Δt is the lapse time between two wave peaks.

Two types of elastic waves are propagated in the material- dilatational and shear waves. Dilatational waves are longitudinal waves, where the particle motion is in the direction of wave propagation. Shear waves are transverse waves where particle motion is in perpendicular direction to the wave propagation. When the lateral dimensions of the rod are small compared to the length, multiple reflections and subsequent interference of these two reflected waves results in a plane wave. For the plane acoustic wave, the speed of propagation in a rod of diameter much less than the acoustic wavelength, depends upon the modulus and the density of the material and is given by the following equation

$$V = \sqrt{\frac{E}{\rho}} \qquad 2\text{-}2$$

Where V is the wave velocity, E is Young's modulus and ρ is density.

In practice, acoustic measurements follow broadly one of two approaches, the resonance method and the time of flight (TOF) method.

The principle of the resonance method is to determine the resonance frequency of a system by applying an oscillating force of varying frequency or by impact excitation and analyzing the vibration spectra. The frequency at which the material resonates depends on the size of the sample and the way it is hinged, i.e. the boundary conditions. For longitudinal vibrations with free-free boundary conditions, the frequencies of the allowed modes of vibration in a bar are given by

$$f_n = \frac{V}{\lambda} = \frac{nV}{2l} \qquad 2\text{-}3$$

where f_n is the frequency of the vibration of nth mode, n (1,2,3….) are the vibrational modes, V is the velocity of the propagating wave and λ is the wavelength of the wave. For the first overtone, i.e. the fundamental frequency, λ is equal to $2l$; where l is the length of the sample, for the second overtone λ is l and so on (Figure 2.5).

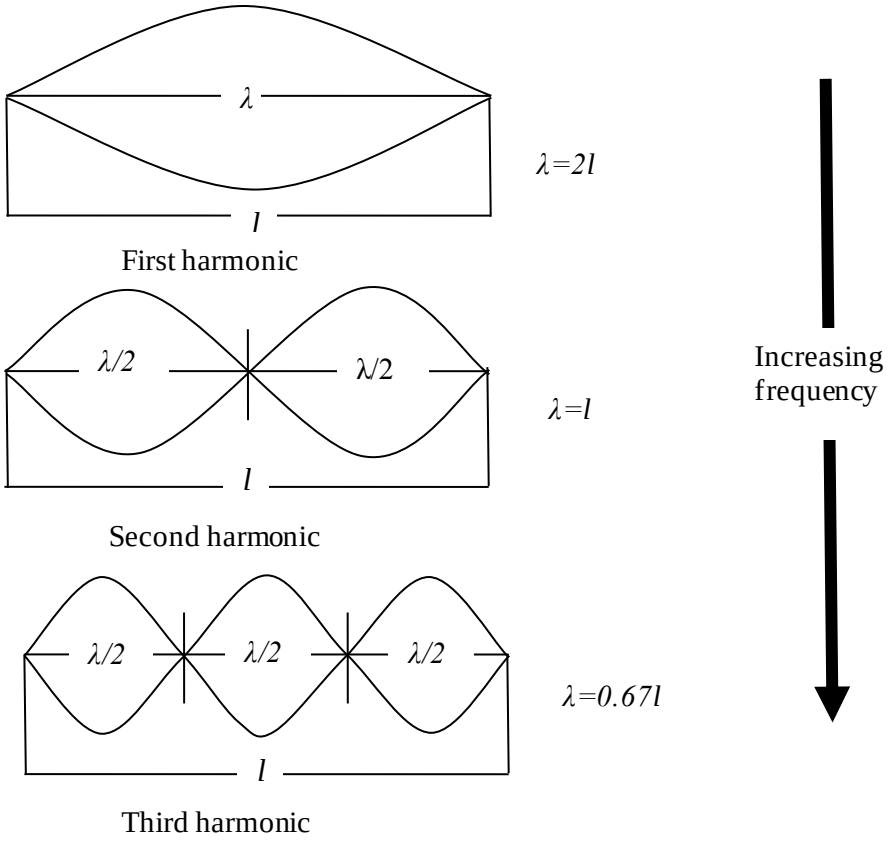

Figure 2.5 Resonance patterns for the first three harmonics

Ideally, the time of flight (TOF) method involves measuring the transit time of the wave as it moves past two sensors that are driven into the sample (Figure 2.6). A stress wave is introduced by mechanical impact at the "start" transducer. The produced signal/wave passes through the sample and is received by the two "stop" transducers.

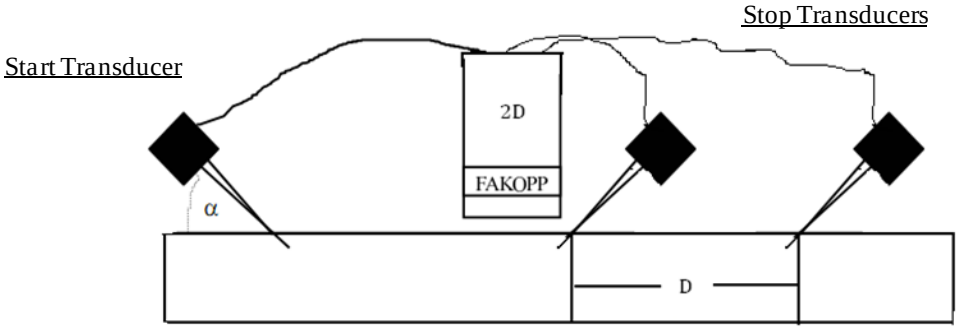

Figure 2.6 Schematic illustration of acoustic velocity measurement using time of flight method with two stop probes

Wave velocities are determined by picking up the time of a certain feature of a propagating pulse, such as the amplitude maximum or trigger threshold, as the wave passes each of the two sensors (Figure 2.7). The use of two detector sensors provides a direct measurement of the lapse time, with a single stop sensor the estimated lapse time is sensitive to corrections due to time travel in both the start and stop probes.

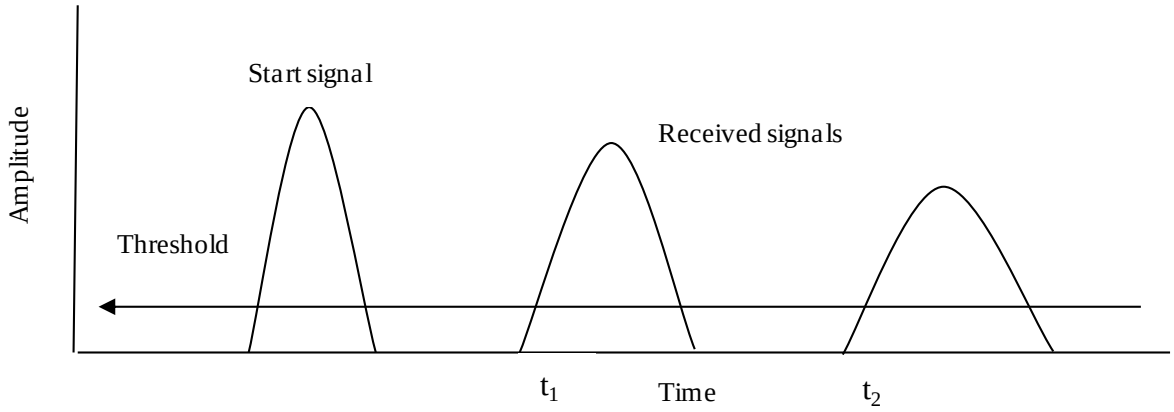

Figure 2.7 Time determination using threshold value needs a system that takes account of the initial slope of the arriving signal.

2.2.3 Acoustics in wood

Measurements of sound velocity are the most practical predictors of wood quality, useful not only in identifying low stiffness but also distortion-prone wood (Ilic, 2004). The principle of using stress waves was hypothesized by Jayne as far back as 1959. He proposed that the resonance frequency and the dissipation of energy are controlled by the same mechanisms that determine the static behaviour of the material (Jayne, 1959). In words of Ross and Pellerin (1994) "*at the microscopic structure level the strength and static elasticity of the wood depend upon the orientation and structural composition of the cells. Such properties are observable through the frequency of oscillation in vibration or speed of sound transmission*". The stress wave transmission time is shortest along the fiber and longest across the grain (perpendicular to fiber). For southern pines stress wave transmission velocity along the fiber are typically about 5km/s whereas perpendicular to fiber, velocity ranges from 1 to 1.17 km/s (Ross et al., 1999). Acoustic velocity is a surrogate measure of stiffness and also reflects properties like tracheid length or MFA (Andrews, 2000). A wood sample with high velocity corresponds to a low MFA and thus high stiffness at constant density.

Although wood is inhomogeneous and anisotropic material, several researchers (Bertholf, 1965; Ross, 1985) found that the one dimensional theory of wave propagation could be used to predict accurately the dynamic strain patterns in wood and wood based composites. Bertholf (1965) verified the predicted stress wave behaviour with the actual strain wave measurements and also the dependence of the propagation velocity on the MOE of clear wood. The dynamic MOE calculated using stress wave velocity was well correlated with the static MOE measured by static bending tests (Ross et al., 2000).

Both TOF and resonance methods can be used to determine stress wave velocity but the latter method has a limitation. It is a destructive method and can only be used for cut logs, not for standing trees as it needs reflective ends. TOF method measures the fastest flight path between two probes in the outerwood of trees, whereas the resonance method assesses the area-weighted cross-sectional average (including both corewood and bark) for logs (Grabianowski et al., 2006). The average acoustic velocity measured by TOF method (Fakopp-2D)[1] in pine logs was significantly higher than that measured by resonance method (WoodSpec) (Chauhan and Walker, 2006; Wang et al., 2005).

The proposed explanation for this is that TOF tool responds to energy other than the main wave front. This weak signal, called incremental speed, travels the shortest distance between the two ends mainly in the stiff outerwood whereas the resonance method is negligibly affected by this energy (Andrews, 2004) and is the outcome of the cross-sectional or volume-weighted contributions of the entire log (bark, stiff outerwood and low stiffness corewood).

In New Zealand, pine trees and logs are successfully evaluated using longitudinal stress wave techniques. Acoustics not only distinguishes between logs up a single stem but also between boards from the same log, whether all butt, 2nd, or 3rd etc (Tsehaye et al., 2000b). Today, resonance method is preferred for assessing cut stems and logs (Lindström et al., 2002) whereas young standing trees have to be assessed by TOF method (Matheson et al., 2008) .

With very small specimens (as used in this thesis) the resonance method has advantage over TOF. TOF measurements are susceptible to (1) errors/uncertainties due to poor/variable contact between probes and the wood, (2) lapse times within the probes themselves are comparable to the transit times in short 100mm specimens, and (3) measurements vary with different observers. In contrast, resonance values using WoodSpec are highly reproducible

[1] Fakopp-2D and WoodSpec are two commercial acoustic tools that work on TOF and resonance principles, respectively

and can be cross-checked by operation in various modes such as the resonance generated by a piezoelectric crystal, by tapping, or by microphone. Further, WoodSpec is designed to record undistorted signals at the high resonance frequencies that are generated in short specimens of 100mm length.

Acoustic velocity is affected by changes in moisture content and temperature. As a rough approximation, the propagation speed of stress waves decreases by 1% when the moisture content increases by 1%; the propagation speed drops by 0.05% at 12% moisture content with a rise in temperature by 1^{o} Fahrenheit (between 0 to 200^{o} Fahrenheit) (Gerhards, 1982). Below fiber saturation point (FSP) acoustic velocity decreased rapidly and linearly with increasing moisture, whereas above FSP changes in velocity were gradual and curvilinear (Moreno Chan et al., 2010). Thus for comparative purposes, moisture content needs to be specified.

In this thesis specimens are evaluated at room temperature (15-20°C) and the effect of temperature is ignored.

The first objective in this chapter is to analyze and compare the wood quality of OW and CW in young *Pinus radiata* and explore the association between various wood quality variables independently in OW and CW. The second objective is to study variation within and among 50 families of young *Pinus radiata* in OW and CW.

2.3 Material and methodology

2.3.1 Material

A progeny trial comprising 50 radiata pine control-pollinated families was established at Amberley, Canterbury, New Zealand in September 2007. The mating design involved 45 parents with between 1 and 13 crosses each (mean=2.1) following an opportunistic approach (i.e. no formal mating design).

The trial followed a randomized complete block design with single tree plots and 48 replicates of 7x7 trees (2352 trees) at 2.5m spacing. Replicates were grouped into 4 sections (Figure 2.8), with only one of the 12 replicates in each section kept straight/vertical. In the other 11 replicates the trees were tilted to approximately 35° from their vertical axis in after 1 year of plantation by pushing the trees over and staking (Figure 2.9). The first section (marked I in Figure 2.8) was destructively assessed for wood properties in September 2009 (at age 24

months), the second section (II) was assessed in April 2010 (at age 31 months), and finally the last two sections were assessed in July 2010 (at age 34 months).

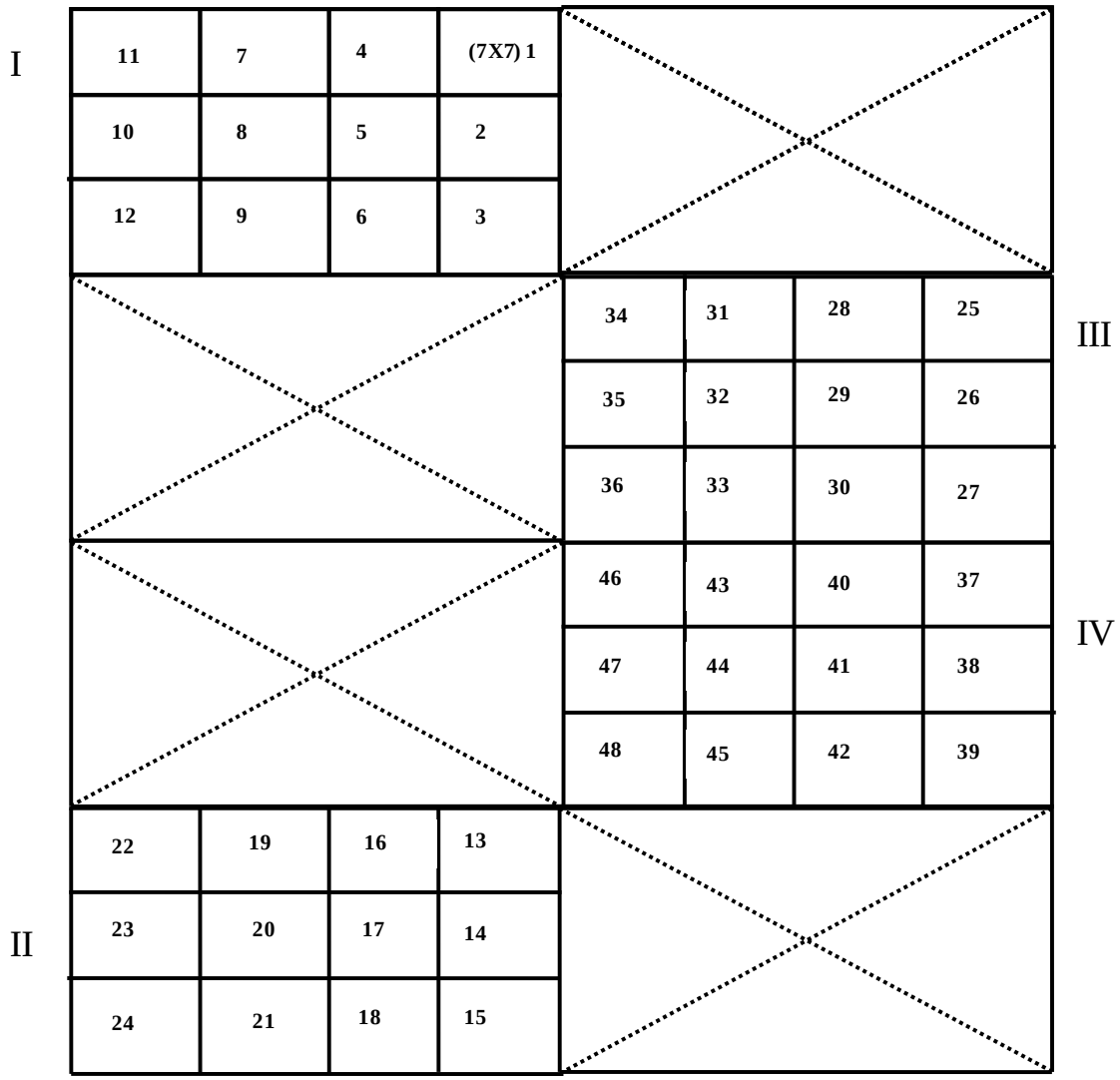

Figure 2.8 Plantation layout of Amberley trial showing four sections-I, II, III, and IV. There are 12 replicates in each section (1-48) with 7x7 trees in each replicate with trees at 2.5m spacings, i.e. there were 2352 trees in total with 588 trees per section.

Figure 2.9 Leaning trees at Amberley. Note the pruned stemwood at the base

The notionally flat and uniform site proved to display noticeably greater within-site variability than anticipated. Localized water-logging during the first winter resulted in some mortality and variable growth of trees. Dead and small diameter trees were eliminated from the analysis.

2.3.2 Sample preparation

All surviving stems from these sections were harvested and the short stem bolt free of branches was taken from the base of each tree for wood quality assessment. The stem bolts were debarked and the diameters across and along the lean were measured. With the straight trees (in total nominally 4sections x 1replication x 49 trees in each rep.) the pruned bolt/stem cross-section was sawn to produce a single standard 100mm long rectangular sample of normal wood (NW) that subjectively sought to avoid material that might be compression wood. With the leant trees (nominally 4x11x49) each bolt was split into two halves to get two 100 mm samples of segregated OW and CW (Figure 2.10). CW material could not be extracted in very small diameter trees (where their growth was possibly suppressed due to winter water-logging) and in trees where the lean was not extreme enough.

After measuring diameter, volume, axial length, and acoustic velocity in the green condition, the samples were dried in an oven at 35°C until a constant weight was achieved. The dried

samples corresponded to ~5% moisture content. This drying regime was dictated by the need to supply material to the University of Auckland for chemical analysis. Conventional oven-drying above 100°C might have resulted in some unquantifiable thermal degradation of hemicelluloses.

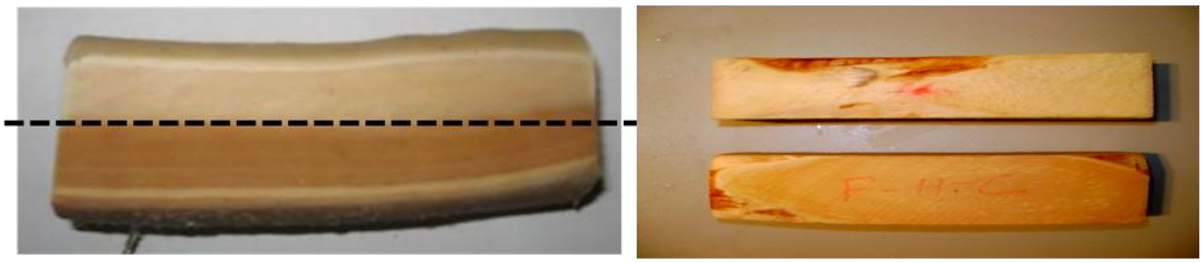

(a) **(b)**

Figure 2.10 (a) Longitudinal section of wood with distinct wood types, lighter shade (opposite wood) and darker shade (compression wood) (b) prepared opposite (top) and compression wood samples (bottom)

2.3.3 Acoustic velocity measurement

Acoustic velocity was measured using WoodSpec, a resonance-based acoustic tool, developed by Paul Harris of Industrial Research Limited. In the sweep mode a piezo-speaker was used to generate sound waves with frequency ranging from 10 to 20 kHz and the resonance frequencies were displayed on the screen. In the trigger mode a tap at one end using a small weight (<1 g) on the end of a plastic arm/tie was used to generate a sound wave. A microphone at the opposite end of the specimen captured the vibrations. In both instances, a fast Fourier transformation (performed by the software) extracted the fundamental and higher frequencies of the longitudinal vibration. The acoustic velocity was determined using the following formula

$$V = 2lf \qquad 2\text{-}4$$

Where V is the velocity, l is length of the sample and f is the fundamental frequency.

The software analysed the probability of a valid reliable reading and in a limited number of instances the procedure needed to be repeated until this condition was satisfied.

2.3.4 Density and volume measurements

The mass of each sample was measured using a digital balance with a precision of 0.01 g.

The water displacement method (Archimedes principle) was used to measure the volume of the samples. A container filled with water with enough head-space for the sample was placed on the digital balance. The balance was then tared and the sample was submerged in the water with the help of a thin needle. The sample must be completely underwater and should not be in contact with the sides or bottom of the container. The recorded weight on dipping equals the mass of the displaced water. The volume of displaced water – and so the volume of the wood sample – was determined assuming that the density of water is 1000kg/m^3 or 1g/ml.

$$Sample\ volume\ (m^3) = \frac{Mass\ of\ water\ displaced\ (kg)}{Density\ of\ water\ (kg/m^3)} \quad 2\text{-}5$$

$$Green\ density\ (kg/m^3) = \frac{Green\ mass\ (kg)}{Green\ volume\ (m^3)} \quad 2\text{-}6$$

$$Dry\ density\ (kg/m^3) = \frac{Dry\ mass\ (kg)}{Dry\ volume\ (m^3)} \quad 2\text{-}7$$

Dry mass (taken at ~5% moisture content) and green volume was used to approximate the conventional definition of basic density, rather than tendentiously describing a new term of basic density at 5% moisture content.

$$Basic\ density\ (kg/m^3) = \frac{Dry\ mass\ (kg)}{Green\ volume\ (m^3)} \quad 2\text{-}8$$

In addition to density the following characteristics were calculated from the mass and volume measurements

$$Volumetric\ shrinkage\ (\%) = \frac{Green\ volume - Dry\ volume}{Green\ volume} \quad 2\text{-}9$$

$$Moisture\ content_{(greenwood)} = \frac{Green\ mass - Dry\ mass}{Dry\ mass} \quad 2\text{-}10$$

2.3.5 Longitudinal shrinkage measurement

The longitudinal dimension was measured using a specially designed jig (Figure 2.11). The jig consists of two tubular ends separated by a distance of 100.6 mm. One end is attached to the adjustable movement of a micrometer dial gauge while the other one is fixed. For length measurement two spherical-headed map pins were inserted in line on the opposite end faces of each specimen. The pin heads provided fixed, determinate reference points for length measurements. The spherical heads of the pin were inserted into the tubular ends of the jig and the displacement of the micrometer dial gauge was recorded. The elegance of this system is that it measures the change in length, δl, (before and after drying) with precision which is more critical than measuring the original length of the sample, *l*, with precision. The total length of the specimen was also determined using the jig, but for this measurement a lower accuracy is sufficient (±0.05mm).

After oven-drying at 35°C (to ~5% moisture content) the specimen was placed in to the jig and the difference between the original recorded dial gauge reading and the new reading was equivalent to the LS of the specimen.

Dry dimensions can be corrected for bow. For bow measurements a dot (pen mark) at the approximately centre of the outer face of the specimen was taken as the reference point and this dot/mark was pressed against the adjustable end attached to the micrometer. Measurements were taken both in green ($Outer_{green}$) and dry ($Outer_{dry}$) condition. Bow was calculated as follows

$$Bow = Outer_{green} - Outer_{dry} \quad \text{2-11}$$

Dry dimensions were corrected as follows

$$Corrected\ length = \sqrt{(Dry\ length)^2 + (Bow)^2} \quad \text{2-12}$$

Longitudinal shrinkage was calculated as follows

$$Longitudinal\ shrinkage\ (\%) = \frac{Green\ length - Corrected\ length}{Green\ length} \quad \text{2-13}$$

This device permitted rapid, repeatable measurements of specimen length and bow. This approach is a considerable improvement on the repeated use of a vernier calliper on the cross-

cut ends of the same samples. First the specimen ends are never cut precisely parallel so the recorded axial length would vary according to the location where the vernier calliper reading is taken, as it is impossible to return to remeasure at exactly the same point after drying. Through inserted pins, it is possible to make use of the same location before and after drying the samples. With the dial gauge jig the change in length, δl, is measured with great precision and quicker than with a vernier calliper. It is more precise as two cross-cut ends of samples are never perfectly parallel to one another so with calipers the error arising from two measurements of length (in the green and dry condition) is comparable to the shrinkage that occurs during drying.

Figure 2.11 Jig for length measurement with a sample inserted in two tubular ends that locate the map pins

2.3.6 Statistical analysis

For analysis the trees harvested in April 2010 and July 2010 were considered together as one group as 34 months old trees. The software R (R Development Core Team, 2011) was used to analyse the data. Brief analysis of all the measured variables was done in terms of mean, coefficient of variation along with minimum and maximum. To study the effect of wood type and tree age on wood properties; (green moisture content, green density, density (~5% moisture content), green velocity squared, dry velocity squared, basic density, dynamic modulus, longitudinal shrinkage and volumetric shrinkage) the following linear mixed model was used

$$Response = \mu + WT + TA + WT{:}TA + R + FC + TID + e \qquad 2\text{-}14$$

where μ, *WT*, *TA* and *WT:TA* are the fixed effects of the overall mean (μ), wood type (WT), tree age (TA) and interaction of wood type and tree age (WT:TA). *R*, *FC*, *TID*, and *e* represent the random effects of replicate, family, tree identity and residuals. The expectation of the response is $E[response] = \mu + WT + TA + WT:TA$ and random effects have zero mean and variances σ_R^2, σ_{FC}^2, σ_{TID}^2 and σ_e^2.

The five variables, dry velocity squared, basic density, dynamic modulus, longitudinal shrinkage and volumetric shrinkage were analysed in more details. Pearson correlation was also determined independently for two wood types between the five main variables after subtracting the residuals (random effect and error) using the above model equation. The significance level used was p=0.01.

Variation attributed to family effect was analysed in dynamic modulus and longitudinal shrinkage in 34 months old trees using following model independently in wood types

$$Response = \mu + R + FC + e \qquad 2\text{-}15$$

where μ is the fixed effects of the overall mean. *R*, *FC*, and *e* represent the random effects of replicate, family, and residuals. The expectation of the response is $E[response] = \mu$ and random effects have zero mean and variances σ_R^2, σ_{FC}^2, σ_{TID}^2 and σ_e^2. Family was considered as a random effect as the individuals representing a family were a random sample of all possible progeny; also the main aim is to study the variance in wood properties attributable to family effect, i.e. attributable to the genetic makeup of the families. Families were ranked based on the best linear unbiased predictions obtained from the above mentioned model (2-15). Families in OW were ranked separately in order of their stiffness and in order of longitudinal shrinkage. Among families with comparable high stiffness the family with low shrinkage was considered as best family and similarly among families with comparable low stiffness the family with high longitudinal shrinkage was considered as the worst family. Comparison of ranking in OW at different age was done using Spearman ranking correlation test.

2.4 Results and discussion

2.4.1 Comparison between compression wood and opposite wood

There were comparatively few straight trees in this study so they were not considered in any detail. Further some specimens were contaminated by variable amounts of generally mild

compression wood. Table 2.1 summarizes the data for normal wood (NW) harvested after 34 months of plantation. NW properties were reasonably similar to OW properties so it might be argued that with hindsight there was no need to tilt the trees in the first place. Equally it implies OW would be a satisfactory proxy for NW. Since the NW sample size is small and subsequent work with pine at Harewood (not reported in this thesis) was with leaning stems only a comparison between CW and OW was done in greater details. The summary statistics of the measured variables for OW and CW at different tree ages are given in Table 2.2.

Table 2.1 Summary statistics of wood properties in normal wood (vertical stems) in 34 months old *Pinus radiata* (number of samples=132)

Variables	Mean	CV %	Min	Max
Moisture content (%)	196	9.8	210	248
(Green velocity)^2 (km/s)^2	1.68	17.6	0.86	2.34
(Dry velocity)^2 (km/s)^2	7.95	11.7	5.48	11.16
Green density (kg/m^3)	1094	1.9	1010	1161
Dry density (kg/m^3)	428	5.8	370	491
Basic density (kg/m^3)	370	6.6	311	432
Longitudinal shrinkage (%)	0.90	35.6	0.28	1.84
Volumetric shrinkage (%)	13.5	24.1	6.69	23.6
Dynamic green modulus (GPa)	1.84	17.4	0.97	2.57
Dynamic dry modulus (GPa)	3.41	14.1	2.32	5.4

Table 2.2 Comparison of wood properties in opposite wood and compression wood at three different tree ages for young *Pinus radiata* trees

Tree age (months)		24		34	
No. of samples		480		1240	
Variables	Wood type	Mean	CV %	Mean	CV %
Moisture content (%)	CW	194	16.2	111	18
	OW	256	12.2	199	10.6
(Green velocity)^2 (km/s)	CW	1.53	7.3	1.92	5.8
	OW	1.11	19.8	1.45	18.4
Dry velocity (km/s)	CW	4.72	9	5.85	9
	OW	4.56	13.7	7.09	11
Green density (kg/m^3)	CW	1106	1.3	1130	2.7
	OW	1080	1.1	1081	2.6
Dry density (kg/m^3)	CW	459	10.6	590	11.2
	OW	404	6.3	421	7
Basic density (kg/m^3)	CW	380	11.6	540	10.7
	OW	305	9.2	364	7.3
Longitudinal shrinkage (%)	CW	2.13	17.7	3.24	20.8
	OW	1.57	27.5	1	30.8
Volumetric shrinkage (%)	CW	13.28	20.0	8.4	18.6
	OW	20.67	24.1	13.72	20.5
Dynamic green modulus (GPa)	CW	1.69	15.3	2.18	12.9
	OW	1.20	19.9	1.57	18.4
Dynamic dry modulus (GPa)	CW	2.17	13.3	3.44	11.5
	OW	1.84	15.3	2.98	13.1

The result suggests that there is significant effect of tree age and wood type on wood properties. Given in Figure 2.12 are the box plots for wood properties for opposite wood and compression wood at two tree ages. Within an age group the difference between mean values of wood types was more pronounced at age 34 months. This reflects the fact that at age 24 months the samples have more intermixing of OW and CW as trees were leant after one year of plantation.

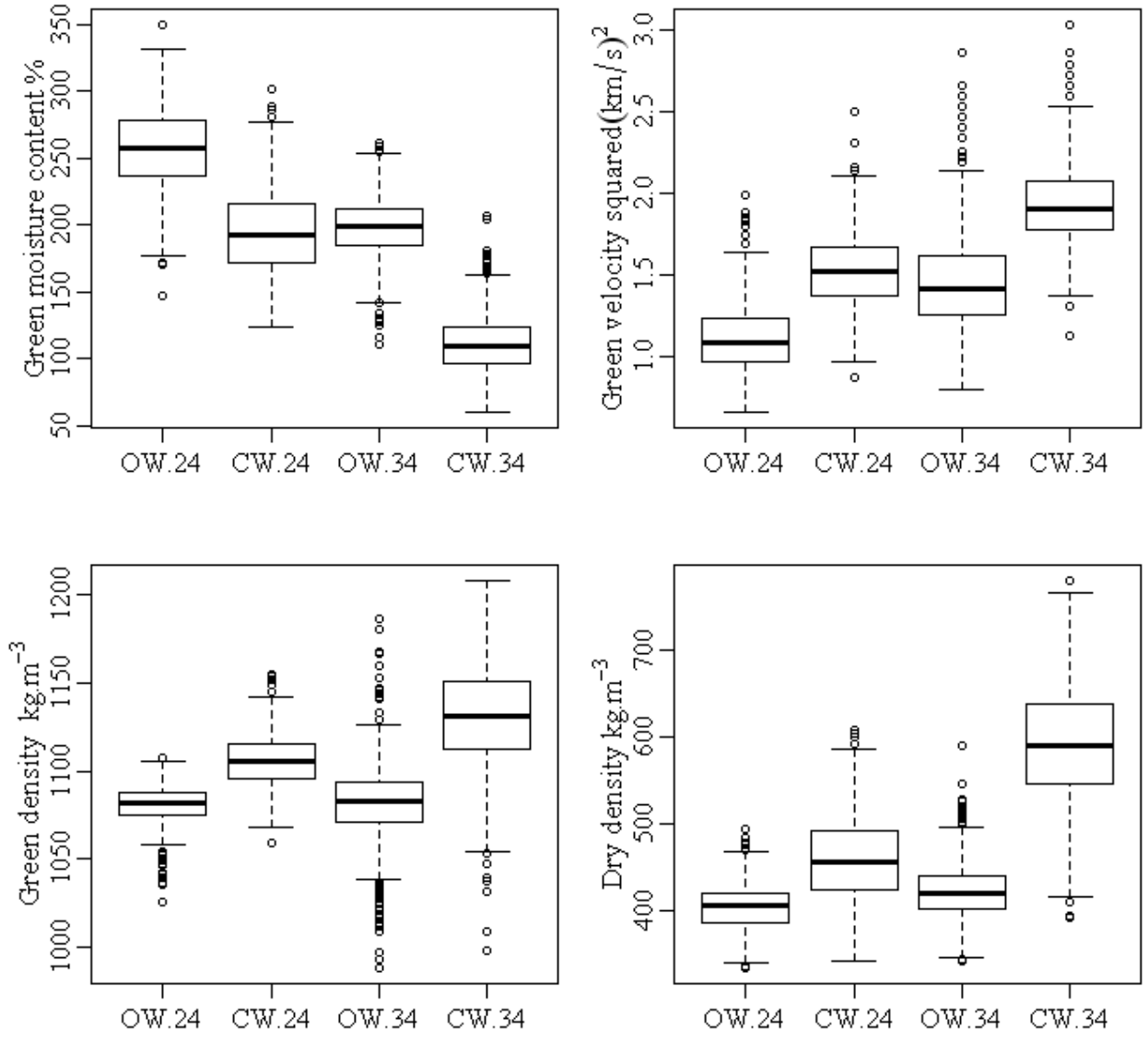

Figure 2.12 Box plots for green moisture content, green velocity squared, green density and dry density (~5% moisture content) in *Pinus radiata* for opposite wood (OW) and compression wood (CW) and at tree age (24 and 34 months). OW.24 (n=492), CW.24 (n=490), OW.34 (n=1241) and OW.34 (n=1044)

The primary interest was centred on dry velocity squared, dry MOE, basic density, LS and VS. Other properties were examined more cursorily.

- The moisture content in green conditions in CW was lower than in OW. In both instances the lumen space was calculated to be approximately 95% saturated. The moisture content in CW was higher in samples harvested at age 24 month compared to samples harvested at age 34 month due to their lower basic density.
- The green acoustic velocity was consistently higher in CW compared to OW for two harvest ages. This was attributed to the lower green moisture content in CW.
- The dry density was higher in CW. But the difference between the two wood types at a particular tree age was less pronounced at age 24 months.
- Both green and dry MOEs were higher in CW than in OW (Table 2.2) . This highlights the danger in selecting young trees for stiffness on the basis of MOE in straight/vertical stems as that would select for CW.

The estimated mean values and 95% confidence intervals of basic density, dry velocity squared, dynamic modulus, longitudinal shrinkage and volumetric shrinkage obtained using model (Equation 2-14) for wood type and tree age are given in Table 2.3.

Table 2.3 Estimated means and 95% confidence intervals of wood properties in opposite wood and compression wood at different tree ages after controlling the effect of replicate and family in young *Pinus radiata* trees

Wood type		Opposite wood			Compression wood		
Variables	Tree age (months)	Mean	Lower	Upper	Mean	Lower	Upper
Basic density (kg/m^3)	24	306	299	313	381	373	388
	34	364	359	369	541	535	546
Dry velocity^2 $(km/s)^2$	24	4.56	4.44	4.66	4.73	4.63	4.83
	34	7.08	7.01	7.16	5.86	5.78	5.92
Dynamic modulus (GPa)	24	1.84	1.78	1.91	2.17	2.10	2.23
	34	2.98	2.94	3.03	3.45	3.4	3.49
Longitudinal shrinkage (%)	24	1.57	1.50	1.65	2.13	2.05	2.20
	34	0.99	0.95	1.05	3.23	3.18	3.28
Volumetric shrinkage (%)	24	20.64	19.89	21.31	13.23	12.49	13.92
	34	13.72	13.2	14.12	8.38	7.97	8.85

2.4.2 Relationship between wood quality traits

2.4.2.1 Opposite wood

Table 2.4 shows the correlation coefficients between different wood quality variables along with their corresponding significance level.

There are two variables, basic density and acoustic velocity squared that one would not expect to be correlated. Basic density is a measure of the quantity of matter; acoustic velocity is a measure of the quality of matter. Basic density is looking at the amount of dry wood tissue in a given volume. Acoustic velocity is measuring the properties of the cell wall tissue irrespective of density. This distinction between quantity and quality of matter is a useful approximation but different proportions of the S2 layer (for example) as a consequence of changes in cell wall thickness due to changes in basic density are likely to affect acoustic velocity. The dry dynamic modulus (in the longitudinal direction) is the product of two independent variables: the quantity of wood (basic density) and its intrinsic quality (measured

as velocity squared, V^2). At a fundamental level the intrinsic quality of the cell wall tissue of a piece of wood as assessed by acoustics (V^2) is believed to be primarily determined by the microfibril angle (for example (Huang et al., 2003)). This is examined in the next chapter.

The correlations between measured variables were consistent broadly across the two harvest times.

Longitudinal shrinkage (LS) was negatively correlated with acoustic velocity squared. Thus samples with high acoustic velocity not only were stiff but also dimensionally stable.

Acoustic velocity squared is the obvious candidate if a single property of OW were to be used to select for superior wood performance of corewood as it correlates well with both the longitudinal dynamic modulus and longitudinal shrinkage

Volumetric shrinkage (VS) was negatively, but weakly, correlated to basic density. The very high shrinkage, especially at age 24 months, is far greater than that would be predicted by Stamm (1964). Where high shrinkage was recorded, the centres of the faces and edges were pulled indicative of internal collapse and this phenomenon was more noticeable in low density samples. Thus the high VS most probably arose from the collapse of cell walls in samples with very low basic density. It could be possible that a threshold value of density is must to avoid collapse in opposite wood as the correlation between basic density and volumetric shrinkage decreases from -0.67 at age 24 months to -0.27 at age 34 months as the mean basic density increases from 306kg/m^3 at age 24 months to 364 kg/m^3 at age 34 months.

Table 2.4 Pearson correlation matrix (with *p*-values in parentheses) for wood properties in opposite wood at three different tree ages in young *Pinus radiata*

Variables	Tree age (months)	Dry acoustic velocity^2 $(km/s)^2$	Dynamic modulus (GPa)	Longitudinal shrinkage (%)	Volumetric shrinkage (%)
Basic density (kg/m^3)	24	0.20 (<0.01)	0.50 (<0.01)	-0.30 (<0.01)	-0.67 (<0.01)
	34	0.10 (<0.01)	0.52 (<0.01)	-0.20 (<0.01)	-0.27 (<0.01)
Dry acoustic velocity^2 $(km/s)^2$	24		0.90 (<0.01)	-0.64 (<0.01)	-0.32 (<0.01)
	34		0.83 (<0.01)	-0.69 (<0.01)	-0.17 (<0.01)
Dynamic modulus (GPa)	24			-0.53 (<0.01)	-0.28 (<0.01)
	34			-0.62 (<0.01)	-0.07 (0.02)
Longitudinal shrinkage (%)	24				0.53 (<0.01)
	34				0.21 (<0.01)

2.4.2.2 Compression wood

While data are reported and analysed concerning compression wood, it is important to emphasise that the practical focus in this PhD is on characterizing the properties of opposite wood.

Table 2.5 shows the correlation coefficients between different wood quality variables along with their corresponding significance level.

When considering the CW data it is important to take account of the fact that the trees were not tilted until year 1, and the angle of the lean was variable. When the trees were felled at age 2 some did not provide much CW, so despite leaning the stem some of the CW samples were contaminated by the presence of some OW. This is likely to be the reason why the average basic density of CW in 2 year old trees was only about 381 kg/m^3 whereas in the ~3 year old trees it was about 541 kg/m^3 (Table 2.3).

Unexpectedly, and in contrast to OW, CW basic density and dry acoustic velocity squared, were weakly negatively correlated at least in the 34 months old trees. This implies that in CW cells changes in wall thickness and changes in cell wall structure occur concurrently. Denser CW cells are associated with a lower acoustic velocity, and by implication a larger MFA.

Again in contrast to OW, basic density was positively correlated to longitudinal shrinkage in CW, so high density CW was dimensionally very unstable. Acoustic velocity squared was negatively correlated to LS. Thus selection on the basis of basic density results in trees with unstable high density stiff CW, whereas selection on the basis of acoustic velocity squared results in stable but comparatively less stiff CW.

The correlation between basic density and VS was different for different tree ages; it was positive at age 34 months but negative for 24 months old trees. The difference can be attributed to the fact that as the trees were leant after 1 year, the intermixing of OW and CW would be more pronounced in CW samples taken from small diameter trees (younger in age). The CW samples harvested at age 24 months were comparatively low in basic density and LS and high moisture content (Table 2.2) than CW samples at age 34 months.

Also the negative correlation between LS and VS in CW at age 24 months could be explained by the fact that samples with low LS have more intermixed OW present, which has more VS.

Table 2.5 Pearson correlation matrix (with *p*-values in parentheses) for wood properties in compression wood at three different tree ages in young *Pinus radiata*

Variables	Tree age (months)	Dry acoustic velocity^2 $(km/s)^2$	Dynamic modulus (GPa)	Longitudinal shrinkage (%)	Volumetric shrinkage (%)
Basic density (kg/m^3)	24	-0.09 (0.06)	0.70 (<0.01)	0.67 (<0.01)	-0.44 (<0.01)
	34	-0.45 (<0.01)	0.65 (<0.01)	0.71 (<0.01)	0.27 (<0.01)
Dry acoustic velocity^2 $(km/s)^2$	24		0.61 (<0.01)	-0.48 (<0.01)	-0.01 (0.79)
	34		0.37 (<0.01)	-0.61 (<0.01)	-0.06 (0.04)
Dynamic modulus GPa	24			0.21 (<0.01)	-0.15 (<0.01)
	34			0.24 (<0.01)	0.36 (<0.01)
Longitudinal shrinkage (%)	24				-0.18 (<0.01)
	34				0.26 (<0.01)

The results are in accordance with previously reported results. Donaldson et al. (2004) reported a mean density 572kg/m^3 in CW and 477kg/m^3 in OW in leaning 18-year old *Pinus radiata* trees. The CW was 22% denser than the OW. Dadswell and Wardrop (1949) in their review paper on reaction wood mentioned that severe CW is 33% denser than corresponding NW wood. In the present case the mean basic density at ~5% moisture content for trees at age 34 months was ~540kg/m^3 for CW and 362kg/m^3 for OW. The low density of OW in present study can be attributed to juvenile nature of samples and the absence of latewood: thus the CW was 50% denser than OW. At age 24 months the difference between wood types was only 25%, which can be attributed to the intermixing of two wood types in the first year prior to leaning the stem.

In the OW of very young trees the low basic density can be attributed to the absence or low percentage of latewood (clear visible) (Larson et al., 2001), thin tracheid cell walls and large lumen diameters (the latter were not measured in this study). For example, Ying et al. (1993) reported 85% earlywood in the first growth year and 79% in the second growth year for *Pinus taeda*. The high density in CW can be attributed to the very thick cell walls (Donaldson et al., 2004).

The thick cell walls and the small lumen in CW tracheids explain for the low green moisture content in CW (110%) compared to OW (200%). Above fibre saturation point (where the cell walls are fully swollen, but there is no free water in the lumens), the velocity of the stress wave decreases with increasing moisture content because material stiffness is constant. This phenomenon has been well reported by Moreno Chan (2007).The essential argument is that the free water adds mass to the sample, while not influencing the material properties of the cell wall. Therefore velocity increases more due to drying in OW than in CW

Huang et al. (2003) provided an early review that related acoustic velocity to microfibril angle. The high dry acoustic velocity in OW compared to CW at ~5% moisture content could be attributed to a lower microfibril angle in OW. The difference in their mean acoustic velocities was just 8% so only a small difference in MFAs is expected. The results of MFA measurements are discussed in chapter 3.

Stiffness (dynamic modulus) of any material is the product of acoustic velocity squared and the density at the time of measurement. With CW its higher stiffness was mainly due to high density. Thus when CW and OW are compared by first normalizing for density, the normalized OW dynamic modulus was higher (Figure 2.13) due to high acoustic velocity in

OW, which illustrates comparatively low MFA in OW. Alternative terminology is relative stiffness or specific stiffness (akin to the American use of the term specific gravity for basic density). This is a standard procedure in mechanical engineering (Ashby and Jones, 1994) that was adopted by (Huang et al., 2003) when discussing wood as similar to a porous fibrous composite. The fact that normalizing the stiffness, in this case by dividing by basic density, is equivalent to reverting to V^2 does not invalidate the procedure.

The higher specific or normalized stiffness of OW compared to that of CW means that the cell walls of OW are stiffer than those of CW, and by inference the expectation that the MFA will be lower in OW.

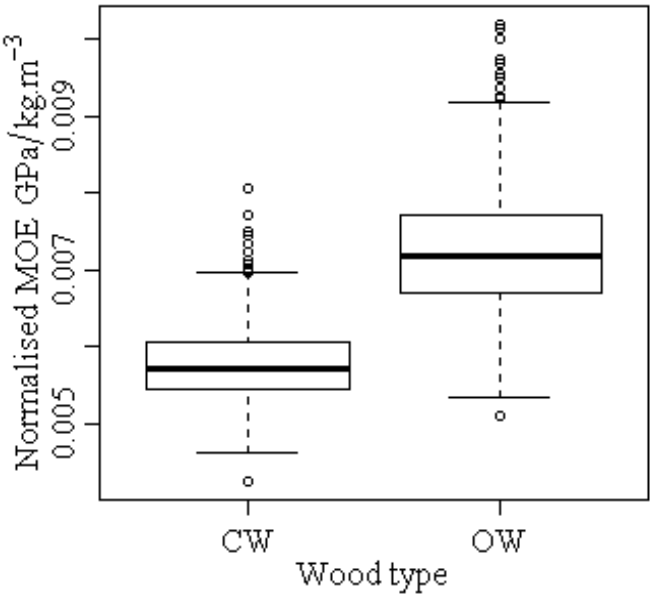

Figure 2.13 Box plot for dynamic modulus (MOE) normalised for basic density (MOE/basic density) in compression wood and opposite wood of young *Pinus radiata* trees

LS in OW and CW were comparable to previously reported results. Ying et al. (1993) reported 0.89% average LS in the first growth ring in *Pinus taeda*, and in CW the LS was 3-4% (Dadswell and Wardrop, 1949). LS was weakly negatively related to basic density in OW. Timell (1986) also mentioned that in NW, dense samples display a lower LS. In CW the relationship between basic density and LS was positive which is in accordance with the results reported by Harris (1977) in *Pinus radiata*: the denser the CW higher the LS. Density alone cannot explain high LS in CW as the specific LS (normalized for density) of CW was still greater than that for OW (Figure 2.14). Dadswell (1958) suggested that the comparatively

less lignified and thicker S1 layer with transverse orientation could influence LS in CW; whereas Timell (1986) suggested helical cavities and absence of a restraining S3 layer as the main contributors for high shrinkage in CW. Harris (1977) investigated the influence of MFA, density and other anatomical properties on the LS of different grades of CW, and reasoned that among anatomical properties such as cell wall thickness, intercellular spaces, helical cavities or presence of S3 layer, only tracheid wall thickness was correlated with longitudinal shrinkage. He concluded that both MFA and tracheid wall thickness are responsible for high LS in CW.

Galactose content has been correlated to high LS (Floyd, 2005). In CW the lignified secondary layer ($S2_{(L)}$) is characterised by a high level of (1-4)-β-galactan content (Altaner et al., 2010). Thus along with physical and structure factors the galactan content in CW might contribute to the high LS in CW.

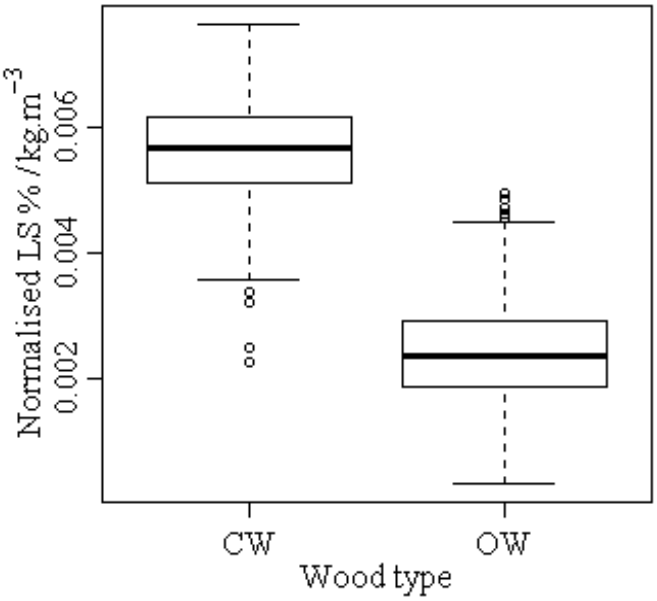

Figure 2.14 Box plot for longitudinal shrinkage normalised for basic density in compression wood and opposite wood of young *Pinus radiata* trees

VS was reported to be higher in OW in the literature. Verrall (1928) compared two wood types in different conifer species and reported high VS in OW e.g. for *Pinus palustris* the average VS was 9.9% for CW and 14% for NW. In the present study at age 34 months, the mean VS for CW was 8.4% and for OW it was 13.7%. Theoretically VS increases with

density; such a positive relationship was found in CW. In contrast, a negative relationship between density and VS in OW was found in this study. It could be attributed to the fact that the thin walls in OW have collapsed while drying. Collapse was noticed in samples with low density. In spite of the high density the comparatively low VS in CW can be explained by its anatomical structure. The absence of the S3 wall results in cell wall shrinkage only towards the primary cell wall i.e. increasing the size of the lumen without affecting the outer dimensions of the tracheid (Kelsey, 1963). Harris and Meylan (1965) also pointed out that on shrinkage in CW the change in cross-section of the cell wall material will not be translated into a decrease in the outer cell diameter, but rather in an opening of the helical cavities on the inside i.e. an increase in the cell lumen.

2.4.2.3 Correlation of wood properties in OW and CW wood within a tree

Table 2.6 shows the correlation coefficients for wood quality variables between OW and CW, (including their significance level) within trees at two tree ages. Correlations with the 3 yr old trees were either week or not significant at $p<0.01$. Therefore the ranking of families was done independently in two wood types. The correlations between OW and CW after only 24 months was comparatively stronger which could be attributed to significant intermixing of wood types, especially in the CW samples.

Fortunately, the intermixing of some OW in the CW samples, while making any ranking of families for CW properties problematic, is less of a practical issue. In practice, tree breeders are more concerned with OW wood properties and are likely to make selection on that basis.

Table 2.6 Pearson correlation coefficients (with *p*-values in parentheses) for wood properties between opposite and compression wood for young *Pinus radiata* trees at two tree ages

Tree age (months)	Basic density (kg/m^3)	Dry acoustic velocity^2 $(km/s)^2$	Dynamic modulus (GPa)	Longitudinal shrinkage (%)	Volumetric shrinkage (%)
24	0.39 (<0.01)	0.23 (<0.01)	0.36 (<0.01)	0.20 (<0.01)	0.12 (<0.01)
34	0.17 (<0.01)	0.25 (<0.01)	0.21 (<0.01)	0.16 (<0.01)	0.01 (0.74)

2.4.3 Ranking of families

2.4.3.1 Opposite wood

In making a selection, the tree breeder is likely to focus on only one or at most two wood quality traits. VS is likely to be of little interest as collapse and excessive VS are not major problems in the utilization of radiata pine. LS, and differential LS in a piece of timber will result in distortion on drying if the wood is not heavily restrained. Again this is a problem, but it can be mitigated. Also it is well known that LS is associated with wood having a high MFA (>35^{o}) and low longitudinal stiffness (<7GPa). In practice the choice of properties to select from are density, V^2 and longitudinal stiffness.

In this study dynamic modulus (product of acoustic velocity squared and density) and longitudinal shrinkage were used to rank opposite wood families. Mean values of families for dynamic modulus and longitudinal shrinkage obtained using model and their ranking at age 24 and 34 months are given in Table 2.7

Table 2.7 Mean values of dynamic modulus and longitudinal shrinkage of opposite wood along with the ranking of families in 24 and 34 months old *Pinus radiata* trees.

	24 months					34 months				
Family code	No. of samples	Dynamic modulus (GPa)	Dynamic modulus rank	Longitudinal shrinkage (%)	Longitudinal shrinkage rank	No. of samples	Dynamic modulus (GPa)	Dynamic modulus rank	Longitudinal shrinkage (%)	Longitudinal shrinkage rank
1	4	1.94	4	1.46	13	25	3.04	17	0.93	14
2	10	1.76	43	1.56	28	26	2.81	45	1.09	43
3	9	1.83	34	1.53	22	12	2.85	41	1.05	40
4	7	1.84	33	1.53	23	27	2.81	46	0.98	25
5	10	1.90	12	1.48	14	28	3.05	15	0.90	10
6	7	1.93	7	1.42	8	30	3.00	25	1.03	35
7	11	1.86	27	1.46	10	23	3.22	1	0.82	2
8	17	1.87	21	1.54	25	25	3.02	23	0.91	13
9	6	1.90	11	1.51	17	28	3.09	10	0.95	16
10	14	1.93	6	1.62	35	20	3.09	11	1.02	33
11	9	1.93	5	1.52	20	25	3.07	13	1.03	34
12	6	1.81	37	1.69	42	27	3.04	18	1.05	39
13	13	1.83	35	1.66	39	26	2.93	32	1.01	31
14	11	1.91	10	1.40	6	29	3.03	20	0.94	15
15	16	1.66	50	1.99	50	25	2.81	44	1.27	50
16	13	1.80	39	1.83	49	28	3.04	19	1.04	36
17	8	1.82	36	1.54	24	30	3.17	4	0.91	11
18	8	2.00	1	1.36	3	27	3.18	3	0.85	4
19	7	1.88	17	1.61	33	30	2.81	47	1.16	48
20	12	1.77	41	1.69	44	27	2.94	31	1.00	28
21	7	1.97	2	1.49	16	32	3.02	22	1.05	38
22	7	1.75	45	1.77	48	28	2.85	40	1.22	49
23	8	1.87	20	1.43	9	21	3.10	9	0.97	23
24	9	1.71	49	1.66	38	8	2.85	39	1.06	42
25	8	1.85	28	1.55	27	23	2.87	37	1.01	29

	24 months					34 months				
Family code	No. of samples	Dynamic modulus (GPa)	Dynamic modulus rank	Longitudinal shrinkage (%)	Longitudinal shrinkage rank	No. of samples	Dynamic modulus (GPa)	Dynamic modulus rank	Longitudinal shrinkage (%)	Longitudinal shrinkage rank
26	13	1.86	26	1.37	4	19	2.99	27	0.89	7
27	11	1.85	31	1.48	15	27	2.98	29	0.91	12
28	12	1.74	46	1.75	47	18	2.72	50	1.06	41
29	8	1.91	9	1.46	11	25	3.12	6	0.85	5
30	8	1.80	38	1.40	5	25	2.93	34	0.88	6
31	11	1.89	13	1.52	18	34	3.03	21	0.97	22
32	9	1.78	40	1.64	36	16	3.11	8	0.90	8
33	10	1.89	15	1.66	37	25	3.14	5	0.97	21
34	7	1.87	22	1.58	31	23	2.77	49	1.13	47
35	11	1.88	16	1.27	1	24	3.21	2	0.70	1
36	11	1.77	42	1.67	41	27	2.88	36	0.96	20
37	8	1.89	14	1.57	30	24	3.06	14	1.00	27
38	10	1.86	24	1.61	34	28	2.97	30	1.02	32
39	9	1.87	19	1.41	7	19	3.08	12	0.96	18
40	8	1.86	25	1.46	12	25	2.93	33	0.99	26
41	10	1.97	3	1.32	2	24	2.98	28	0.84	3
42	10	1.84	32	1.70	45	24	3.11	7	0.95	17
43	7	1.85	30	1.60	32	25	3.01	24	0.96	19
44	9	1.85	29	1.53	21	24	2.99	26	0.97	24
45	12	1.74	48	1.69	43	28	2.84	43	1.12	45
46	4	1.87	23	1.52	19	29	2.80	48	1.10	44
47	10	1.76	44	1.66	40	28	2.91	35	1.04	37
48	14	1.93	8	1.55	26	24	3.05	16	0.90	9
49	13	1.88	18	1.57	29	27	2.86	38	1.01	30
50	6	1.74	47	1.71	46	12	2.84	42	1.12	46

The main purpose of this study was to determine the earliest possible age for efficient screening. Spearman rank correlations were used to estimate the association between the ranking of families done at age 24 months and 34 months. Statistical results are presented in Table 2.8. All the measured variables are significantly correlated. There were large within-site variations. Sample sizes were also different with 492 trees tested at age 24 months and 1240 trees at age 34 months. Due to the small sample size of 24 months old trees, there were very few samples for some families. Also as trees were leant after one year of plantation there was significant intermixing of CW and OW in wood samples in the section harvested at age 24 months due to the small tree diameters, the delay in leaning the trees until the end of the first year (the decision to lean the trees was not foreseen when the trees were planted), and the uncertain/variable angle of the induced lean. In spite of these complexities, the best family at age 34 months with high stiffness and low longitudinal shrinkage was best in terms of longitudinal shrinkage at age 24 months and worst family (50^{th} rank) at age 34 months was ranked as 46^{th} in stiffness at age 24 months.

Thus it seems possible to rank families confidently at age 2 if one can control within site variation and lean trees within three months of plantation to avoid initial intermixing of two wood types, CW and OW.

Table 2.8 Spearman ranking correlation for different wood properties in opposite wood for 24 months and 34 months old *Pinus radiata*

Measured variables	Correlation coefficient	Significance level (p)
Basic density (kg/m^3)	0.56	<0.01
Dry acoustic velocity^2 $(km/s)^2$	0.50	<0.01
Dynamic modulus (GPa)	0.52	<0.01
Longitudinal shrinkage (%)	0.64	<0.01
Volumetric shrinkage (%)	0.60	<0.01

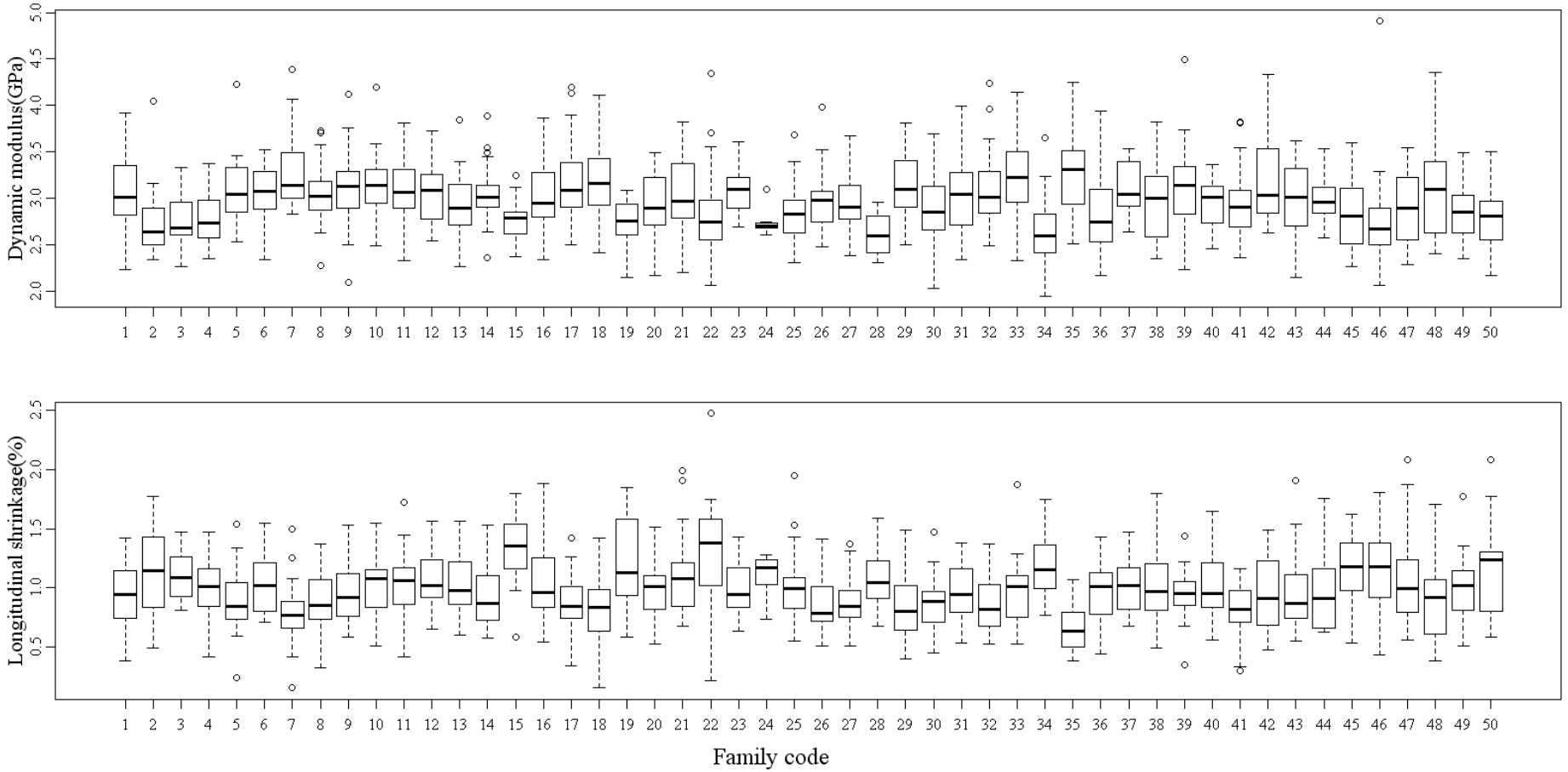

Figure 2.15 Box plots for dynamic modulus and longitudinal shrinkage for opposite wood of 34 months old 50 *Pinus radiata* families

The box plot for dynamic modulus and longitudinal shrinkage by families for 34 months old trees are given in Figure 2.15. At age 34 months the best family (35 in Figure 2.15) with high stiffness and low longitudinal shrinkage was 19% stiffer than the worst family and the LS was 51% less than in the worst family (15). This variation could be utilized to improve stiffness and longitudinal stability in corewood of *Pinus radiata* trees by breeding.

One of the drawbacks of family selection is that there are large within-family variations. The phenotypic values for individual tree for OW in the best and the worst family, selected on the basis of stiffness are shown in Figure 2.16. The range for MOE was 2.47-4.25GPa in the best family and 2.37-3.12GPa in the worst family. The best individuals in the worst family were as good as the worst individuals in the best family. The variation within a family is due to environmental (site variation) and genetic factors. Material for this trial was a mix of genotypes (45 parents) from the production population, which has some level of selection for basic density but no selection for wood stiffness. This type of mix (45 parents) is genetically more variable than a plantation stand which either consisted of clones or families with limited number of selected parents.

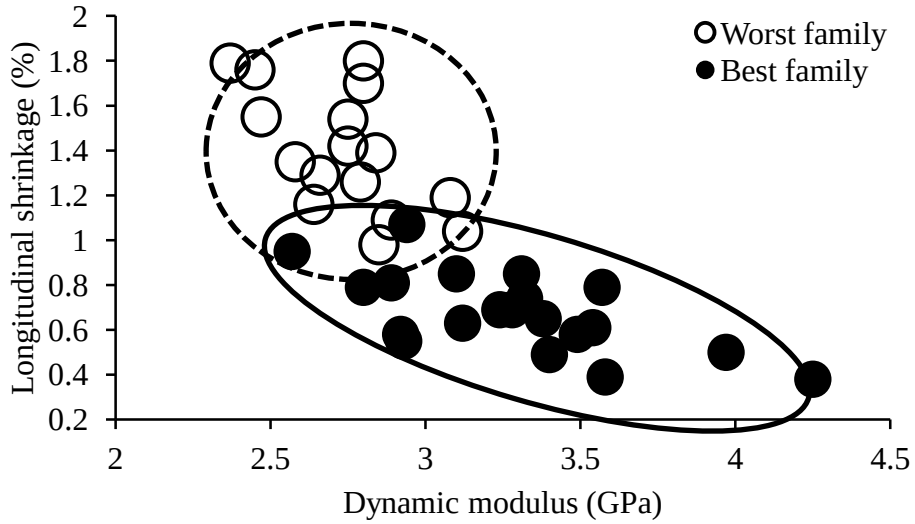

Figure 2.16 Variation within best and worst family for longitudinal shrinkage and dry dynamic modulus of elasticity in opposite wood *Pinus radiata* trees at age 34 months

Given in Figure 2.17 and Figure 2.18 are the plots representing deviation in dynamic modulus and longitudinal shrinkage from overall mean (intercept) along with 95% confidence limit of families in opposite wood of 34 months old *Pinus radiata* obtained using model Equation 2-15. For dynamic modulus the variance for residual error (σ^2=0.119), which is a measure of within families variation was higher than variance attributed to family (σ^2=0.020). Similarly

for longitudinal shrinkage the variance attributed to residual error was (σ^2=0.078) and the variance for family effect was (σ^2=0.0133).

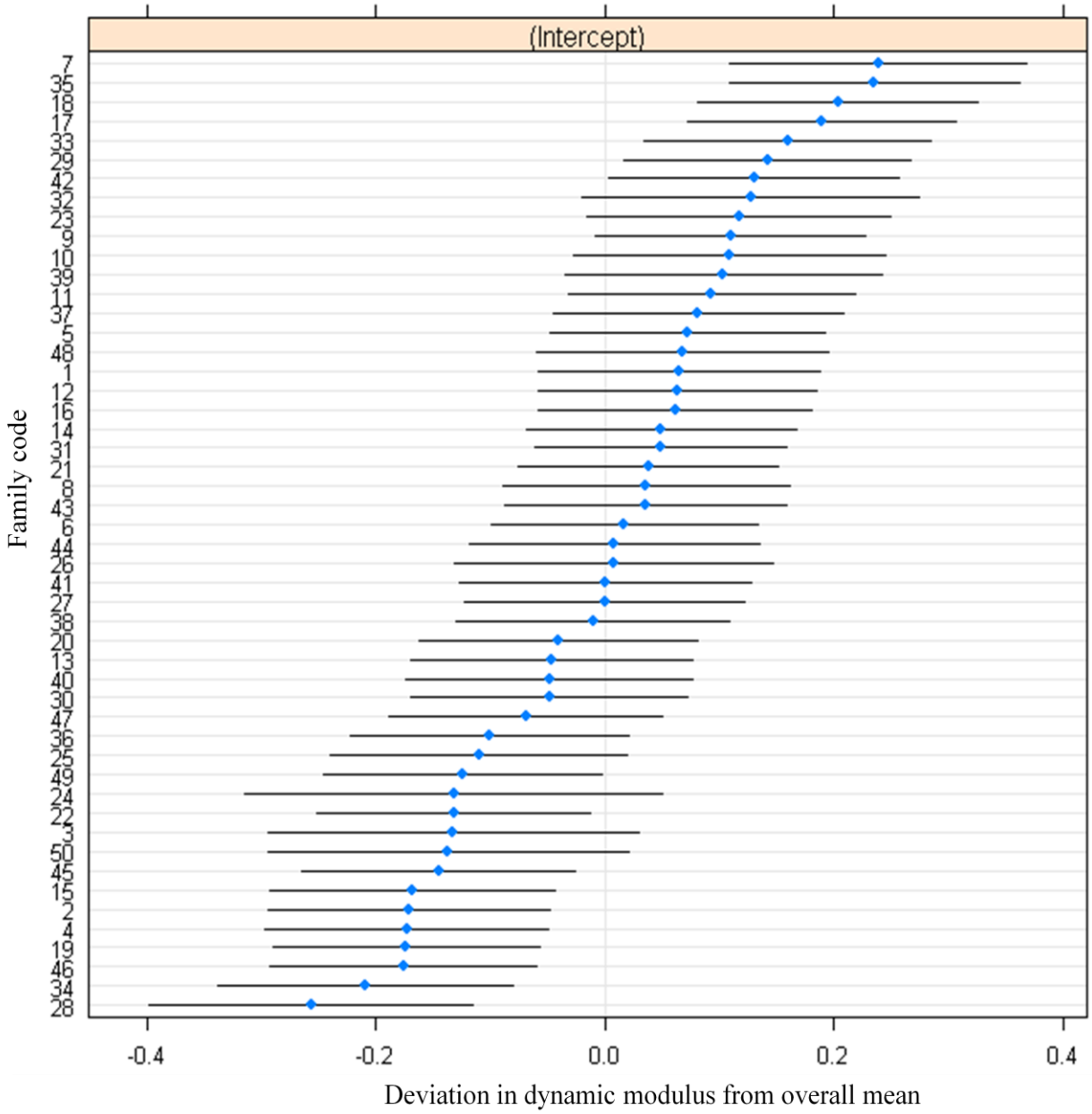

Figure 2.17 Plot representing deviation in dynamic modulus from overall mean (intercept) along with 95% confidence limit of families in opposite wood of 34 months old *Pinus radiata*. The intercept was 2.98GPa

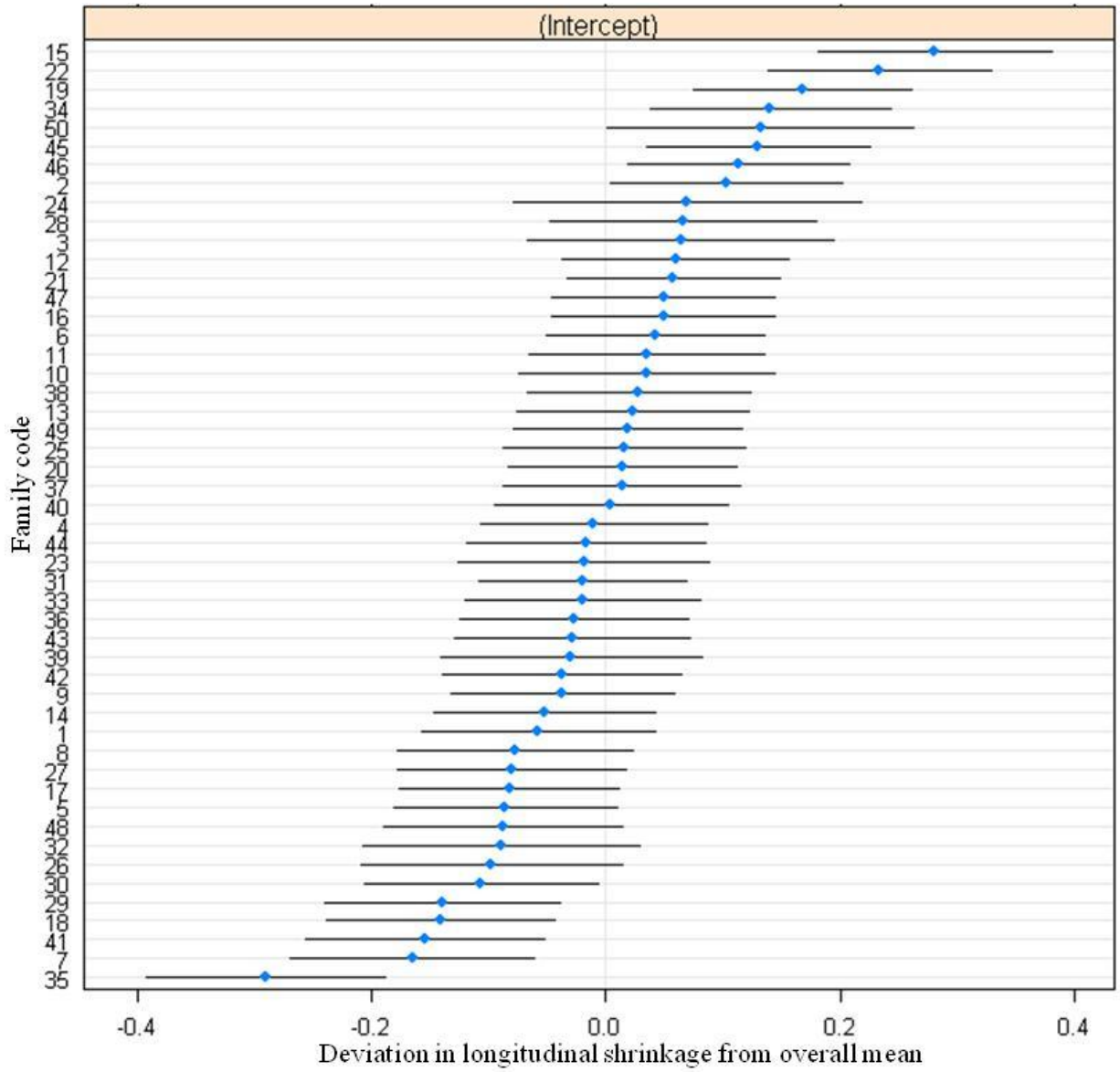

Figure 2.18 Plot representing deviation in longitudinal shrinkage from overall mean (intercept) along with 95% confidence limit of families in opposite wood of 34 months old *Pinus radiata*. The intercept was 0.99%

Figure 2.17 and Figure 2.18 clearly show that there is clear demarcation between best families and worst families in terms of dynamic modulus and longitudinal shrinkage and the stiffer families are also dimensionally stable. As there is large variation within a family, selecting individual best trees rather than selecting best families will result in more genetic gains.

Thus it is possible to rank 3 years old trees. The ranking will be more efficient if environmental variations can be controlled.

Twelve families shown in solid squares in Figure 2.19 were selected from the 50 families for further detailed studies. These families represent the whole range of LS and dry dynamic modulus of elasticity.

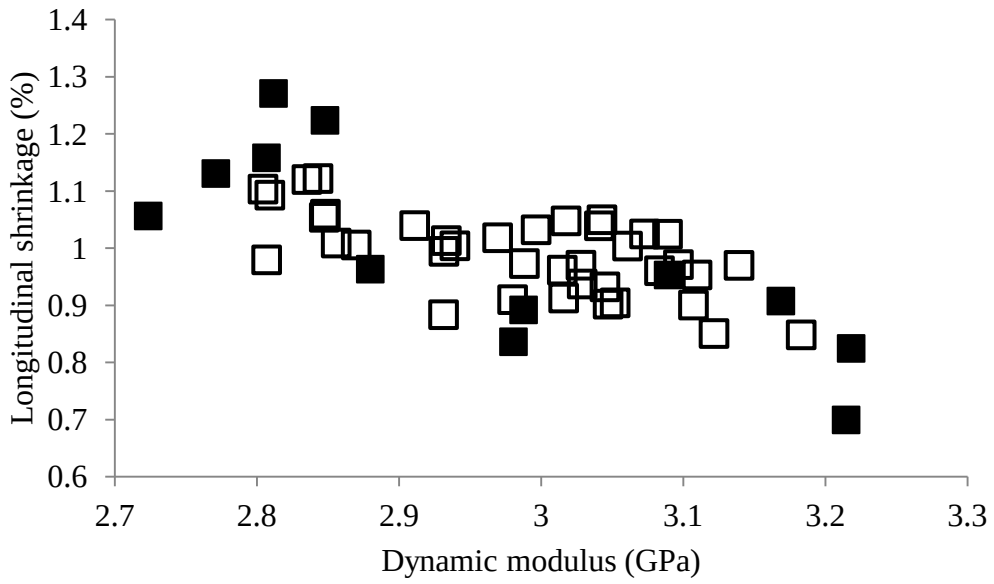

Figure 2.19 Plot between longitudinal shrinkage and dry dynamic modulus. All points irrespective of style represent mean values of opposite wood of 50 families of young *Pinus radiata*. Solid squares represent the values for 12 families selected for detail studies

2.4.3.2 Compression wood

The box plots for dynamic modulus of elasticity and longitudinal shrinkage in CW are given in Figure 2.20. As there was a positive correlation between stiffness and LS in CW it is not possible to rank CW for stiffness and stability simultaneously. CW is stiff than OW in these young trees due to its high basic density, but the high LS creates problems in its utilization. Thus ranking was done for LS. The most stable family (family 36 in Figure 2.20) with least LS is 35% lower in LS than the worst family (10). The mean stiffness was comparable (~3.5 GPa) for the best and the worst CW family. There was large variation within families, the range in LS in the best family was 1.20-4.43% and in the worst family 2.69-4.65%.

There were opposite trends in the ranking of CW and OW, the best family of CW has OW with a mean stiffness of 2.84GPa whereas the worst family with unstable CW has OW with a mean stiffness of 3.15GPa

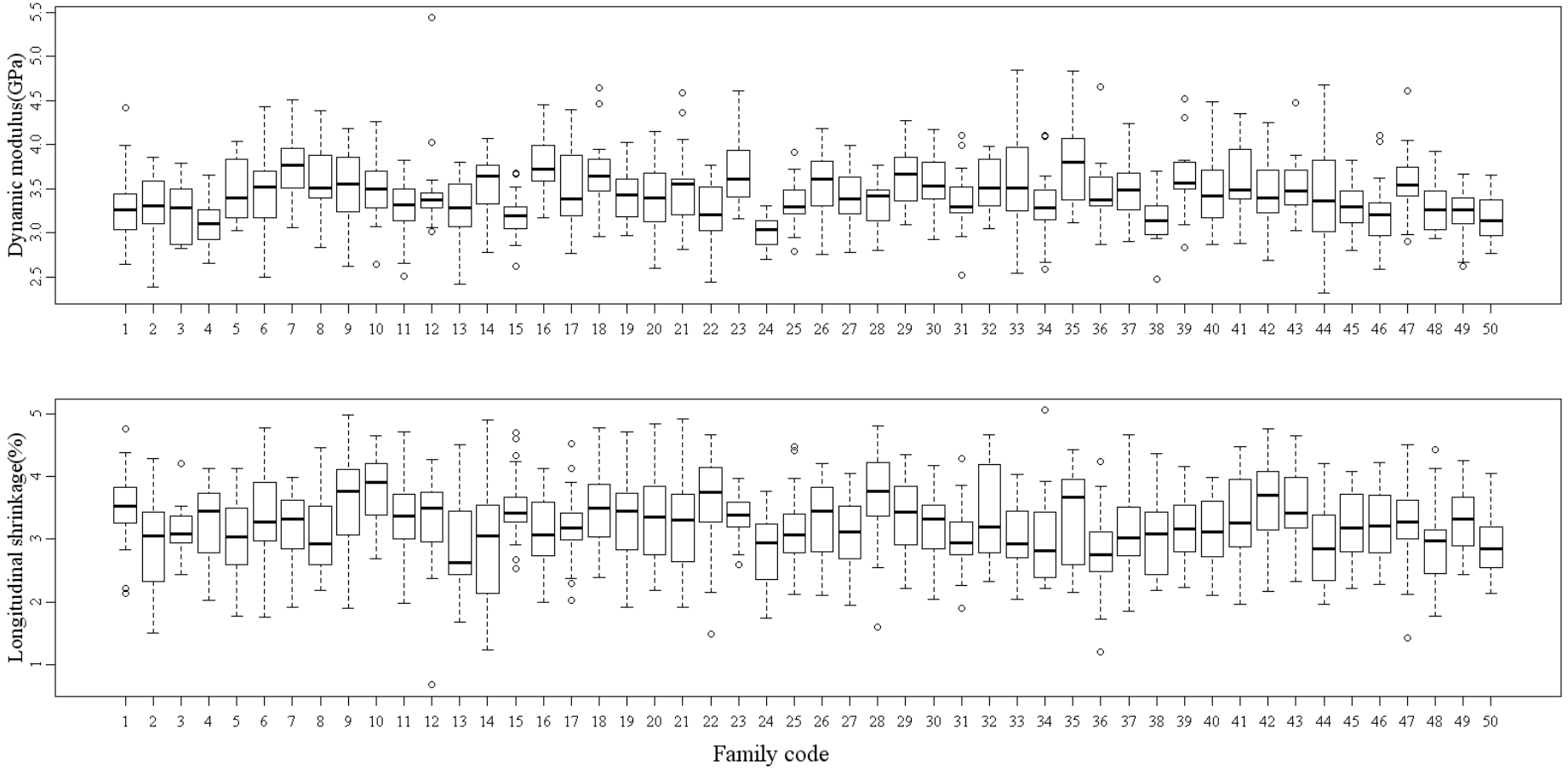

Figure 2.20 Box plots for dynamic modulus and longitudinal shrinkage for compression wood of 34 months old 50 *Pinus radiata* families

Given in Figure 2.21 is the plot representing deviation in longitudinal shrinkage from overall mean (intercept) along with 95% confidence limit of families in compression wood of 34 months old *Pinus radiata* obtained using model Equation 2-15. For longitudinal shrinkage the variance attributed to residual error was (σ^2=0.386) and the variance for family effect was (σ^2=0.034). There was large variation within families. The properties of CW depend upon its severity, which is related to the extent of leaning (leaning was not well controlled in the Amberley trial). NW bands were observed in some CW samples (so these trees were not leaning in a consistent direction). Furthermore, not every leaning tree provided CW material. Overall, in retrospect the Amberley trial conditions were not conducive to a well-structured study of CW.

The subsequent study at Harewood where the planter bags provided much better control over environmental conditions and the trees were leant within 3 months of plantation is expected to provide better experimental conditions, reflecting the evolution of the wood quality research programme. This work, which is not part of the thesis, reflects the iterative nature of research. What was learnt at Amberley was quickly incorporated in further studies.

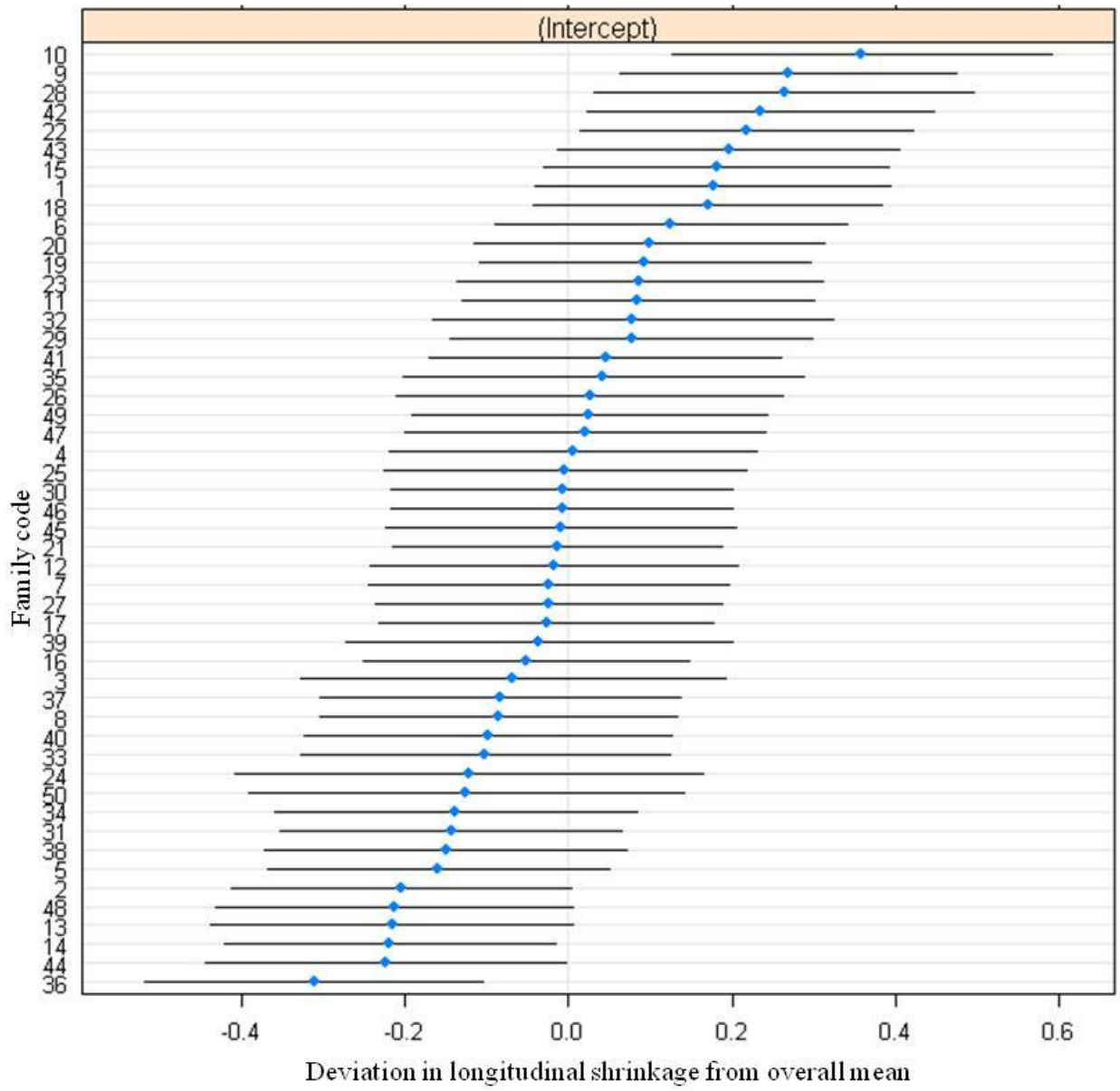

Figure 2.21 Plot representing deviation in longitudinal shrinkage from overall mean (intercept) along with 95% confidence limit of families in compression wood of 34 months old *Pinus radiata*. The intercept was 3.23%

2.5 Conclusions

- OW and CW of young *Pinus radiata* differ significantly in all the measured properties. CW was denser and shrinks more longitudinally than OW. The high VS was correlated to the low density in OW. Where high VS was measured, it was observed that the specimens had collapsed.

- There are merits in screening for dry acoustic velocity squared, as the range in values and the CV are greater than that for basic density. In practice dry acoustic velocity squared and basic density are likely to be used to screen trees for stiffness at a young age.
- LS was correlated to acoustic velocity in OW whereas density was the major factor influencing LS in CW.
- The good correlation between stiffness and LS in OW suggests that stiffer trees are also longitudinally stable.
- The variation within a family was comparable to variation among families.
- Controlled environment along with leaning within 3-5 months of plantation is recommended for tree screening at early age.

Chapter 3. X-ray Diffraction in Corewood

3.1 Introduction

In this thesis the case is proposed that stiffness and stability, and to a lesser degree density, are the key wood quality properties of radiata pine that need to be well determined in any breeding programme. Further, selection should be based on the direct measurement of properties of practical utility rather than indirectly on more fundamental characteristics such as microfibril angle (by X-ray diffraction) and energy loss (by dynamic mechanical analysis, DMA).

Screening for wood properties by X-ray diffraction within large populations is simply impractical: whether considering cost, the need for timeliness or the logistics of such an exercise. The Radiata Pine Breeding Company examined cores from 480 trees of radiata pine in New Zealand (Dungey et al., 2006) while the CRC (Cooperative Research Centres-Australia) for sustainable Production Forestry examined 188 trees of *Eucalyptus globules* (Apiolaza et al., 2005). My study at Amberley started with 2352 trees (somewhat less in practice when taking mortality into account). Unfortunately, past investment in such MFA work has resulted in a belief that MFA is the Gold Standard for defining wood quality, whereas its value may lie in providing a fundamental frame of reference for a more applied breeding programme – by analogy today the price of gold is quoted in US dollars (rather than thinking of US dollars in terms of the gold).

For such reasons, this chapter examines X-ray diffraction data from a number of individual trees (194) that I selected in order to cover the full range in stiffness values. The purpose is not to validate the research covered in Chapter 2, but to show that data, and the ranking of material, is broadly consistent with what may be argued is a more fundamental approach.

The properties of wood are closely related to the molecular structure of the cell wall. In particular the orientation of microfibrils in the secondary cell wall is a major factor influencing physical and mechanical properties of wood. The orientation of microfibrils in the thickest layer (S2) is considered as the microfibril angle (MFA). There is significant variation in MFA among trees (Donaldson, 1993; Ying et al., 1993). Youming et al. (1998) suggested that the MFA in loblolly pine is under moderate genetic control and decreases with age, thus stiffness can be improved by selecting young trees with low MFA. Roughly the

longitudinal stiffness can be improved by one grade with every 5° decrease in MFA (Walker and Butterfield, 1996). This chapter reviews the structure of the cell wall in terms of the orientation of the microfibrils in the cell wall. In this chapter X-ray diffraction is used to determine the variation in MFA among 3 year old radiata pine trees to screen them for stiffness and stability. To better understand the principle of X-ray diffraction in wood, an optical analogue of X-ray diffraction is also presented (Entwistle and Navaranjan, 2001). The optical analogue offers some advantages over software packages in this specific study as my work focuses on very young material with extremely high MFAs whereas standard packages cover a much wider range of MFA values 5-45^{o}. Also the optical analogy makes obvious, the location of the diffraction spots, and where in the chi-plot interference from other diffraction planes needs to be taken into account. Foresters have little or no understanding of X-ray diffraction and the optical analogue communicates the complexities better than fundamental justification (Cave, 1966; Verrill et al., 2011).

3.1.1 Cell wall structure

Wood in gymnosperms (softwoods) is primarily built up of axially elongated cells termed tracheids. The cell wall of tracheids is composed of a primary wall and a secondary wall. The secondary cell wall is a three layered structure (Bailey and Kerr, 1935) - S1, S2 and S3 named in order of their deposition. The primary wall is formed during the expansion of the cell. The expansion of tracheids ceases after the beginning of deposition of S1 layer (Abe et al., 1997). The cell wall is composed of nano-sized (~3.5nm in cross-section) string like cellulose aggregates, termed microfibrils, embedded in a matrix of hemicelluloses and lignin (Harris, 2006). The orientation of the microfibrils varies in different layers of the cell wall. In the primary cell wall the orientation of microfibrils is not well ordered and predominantly changes from longitudinal to transverse, relative to cell axis, from the outer to inner part of the primary wall (Wardrop and Harada, 1965). In the secondary layer the microfibrils are organised and lie broadly parallel to one another. However the three sub-layers differ in thickness and orientation of the cellulose fibrils.

The S1 layer is 0.1 to 0.3μm thick which is ~10% of the total cell wall thickness (Walker, 2006). Some authors (Harada and Côté Jr, 1985; Wardrop and Harada, 1965) suggested a crossed fibrillar texture in the S1 layer due to alternation between an S-helix (left handed) and a Z-helix (right handed) whereas others (Abe and Ohtani, 1991; Dunning, 1968) suggested the orientation shifts gradually from a S-helix to a Z-helix from the outer part towards the inner part in a clockwise direction. In *Pinus radiata* the microfibrils in the S1

layer are oriented in an S-helix with an average orientation of 95° varying from 79° to 117° between individual tracheids (Donaldson and Xu, 2005).

The S2 layer comprises around 80% of the total cell wall in latewood. The thickness of the layer increases with cambial age. In earlywood it is around 1-4μm whereas in latewood it is 3-8μm thick (Walker, 2006). In the S2 layer microfibrils are oriented in a steep Z-helix (Wardrop and Harada, 1965). The microfibrils are laid down in concentric lamellae, within these lamellae the microfibrils are parallel but between lamellae the angle oscillates (Kataoka et al., 1992; Wardrop and Harada, 1965). This switching through angles of around 10° in the S2 layer without changes from S-Z-S helices (Kataoka et al., 1992) gives rise to a steep layered trellis configuration (Harrington, 2002). In *Pinus radiata* the microfibril orientation is in Z-helix. The mean MFA consistently declines from pith to bark from 45° to 10° and also declines with height (Figure 3.1), the MFA is maximum in the corewood of butt logs (Donaldson, 1992). There is large variation among individual tracheids, with an average difference among adjacent cells of 10.9°, within the same growth ring (Donaldson, 1998).

Studies by Entwistle et al. (2007), amongst others (Peura et al., 2005), using an intense narrow beam of X-rays from a synchrotron explore changes in microfibril alignment both within-tracheid and between-tracheid, but from the practical point of view the stiffness of wood at the macrolevel takes account of some broad average of all these variations.

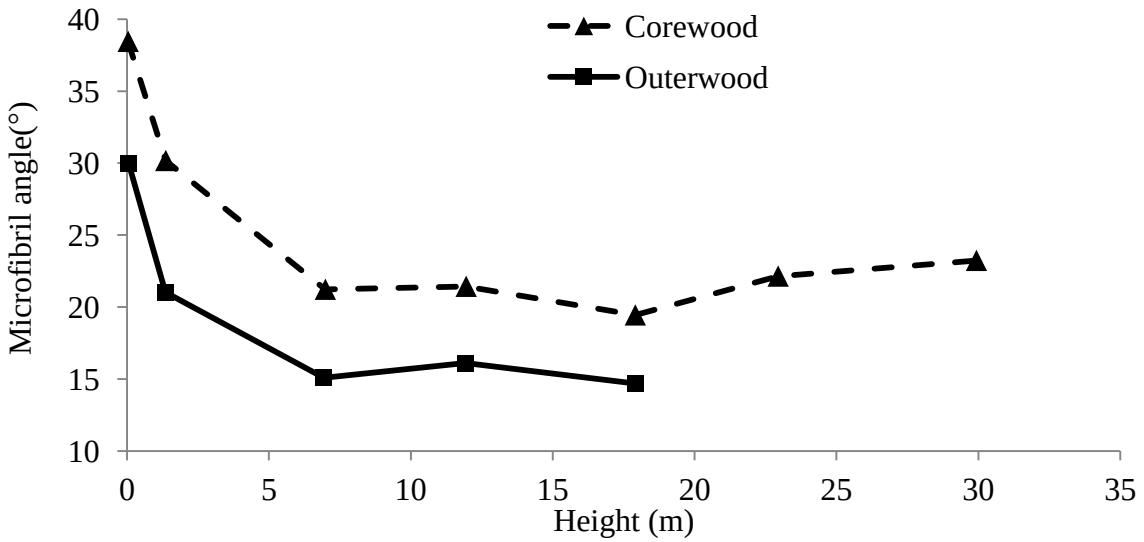

Figure 3.1 Variation in MFA with tree height (Donaldson, 1992)

The innermost layer (S3) represents approximately 4% of the cell wall and it is average 0.1μm thick. Its thickness varies considerably among adjacent cells ranging from 0.06μm to

0.3µm in *Pinus radiata* (Singh et al., 2002). Abe, in his review paper (2005), suggested that the development of the S3 layer is affected by factors like tree species, the season during which the tracheid develops, and the environment. Liese (1963) reported an S-helix in *Picea abies* but S and Z helices in equal frequencies for *Pinus sylvestris*. In *Pinus radiata* the S3 layer microfibrils are in a Z-helix and the orientation is in the range of 50° to 113°, varying continuously from the S2 to the lumen (Donaldson and Xu, 2005).

In the S1 and S3 layers the microfibrils display a crossed-fibrillar lattice with the microfibrils almost perpendicular to the cell axis, whereas they run in a single direction (S) broadly parallel to the cell axis in the middle S2 layer. The S2 allows the plant to adopt an erect growth habit. The thickness and orientation of microfibrils in the S1 and S3 layers are important parameters for the transverse properties of the cell wall. Particularly the S3 layer is more effective in stiffening the cell walls in the transverse plane, thus enabling the xylem cells to withstand the water capillary tensile forces (Booker and Sell, 1998). The thick S2 layer is considered to dominate the longitudinal properties of the cell wall. The orientation of microfibrils in S2 layer (which varies between 10°-45°in *Pinus radiata*) is considered to be the main determinant of the longitudinal elastic modulus (stiffness) (Cave, 1969). LS is a minimum around 25° and increases sharply once the MFA exceeds about 35° (Meylan, 1968).

The CW stimulus is received during xylem enlargement (Timell, 1980). CW tracheids are structurally different from normal wood tracheids. In CW the S1 layer occupies a larger proportion of the secondary wall layer than in NW (Wooten et al., 1967). The S1 layer is about four times thicker compared to normal earlywood and twice as thick when compared to latewood. The S2 wall is thicker than the corresponding wall in earlywood whereas it is either of the same thickness or thinner than latewood (Timell, 1986). The S2 layer of CW has visually distinct outer and inner parts. The outer, also termed as S2(L), is very rich in lignin (Côté, 1967). The inner S2 layer in severe CW is characterised by deep fissures termed helical cavities, spiralling around the tracheid with the same inclination as the cellulose microfibrils (Timell, 1986). In mature CW microfibrils are oriented at larger angles than in NW, varying in the range of 30°-50°. In corewood the microfibril orientation is comparable in the two wood types (Donaldson, 1992). The S3 wall is absent in severe CW (Donaldson et al., 2004).

CW can be classified from mild to severe. Depending upon its severity the characteristic varies. Mild compression wood is characterised by an outer lignified S2 layer (S2(L)) but the

absence of the S3 wall and helical cavities is variable (Singh and Donaldson, 1999). MFA and tracheid length also vary with severity.

3.1.2 Measuring MFA

Donaldson (2008) reviewed different MFA measuring techniques and categorised them into two types; measurement of individual tracheids using microscopy and measurement of bulk wood samples using X-ray diffraction. He further categorised microscopic techniques into two types; one that makes use of the optical properties of crystalline cellulose such as polarised light and a second type, which visualizes directly or indirectly the orientation of microfibrils; e.g. light microscopy after biological, physical or chemical treatments, scanning electron microscopy and transmission electron microscopy.

X-ray diffraction has an edge over microscopic techniques, as it is faster, it collects information from all the cells in the path of the X-ray beam and the sample preparation is easier, whereas optical techniques are tedious and time consuming. Although X-ray diffraction is comparatively simple in data acquisition, the interpretation of the data is more complicated. There is good correlation between microscopically measured MFA and X-ray diffraction measured MFA (Huang et al., 1998; Meylan, 1967). Some authors have expressed their concerns about accuracy of using X-ray diffraction particularly in high angle material as it produces more variable results, noisier signals and curve fitting is more difficult (Kretschmann et al., 1998). However, in my study the purpose is only to compare the ranking of specimens for MFA with the more useful ranking for stiffness.

While one purpose of SilviScan has been to use X-ray diffraction in conjunction with wood density to estimate stiffness (Evans and Ilic, 2001), there has been little interest in taking the opposite approach (Huang et al., 2003). Thus, for screening hundreds of wood samples for stability and stiffness the acoustic technique is well suited. However, to check the reliability of the acoustic results some of the acoustically characterised population samples were assessed by X-ray diffraction, which gives good representation of MFAs of a large sample compared to microscopic methods which are confined to few tracheids. However, where practical outcomes are sought (as opposed to fundamental understanding) the use of acoustics to measure MFA is more direct, cheaper and faster.

3.2 X-ray Diffraction

A crystalline material displays long range order that comprises small repeating units called unit cells. The unit cell is the basic structural unit or building block of the crystal structure and defines the crystal structure by virtue of its geometry and the atom position within. The atoms in a unit cell are linked by hypothetical lattice planes. There are a number of planes in any unit cell and the interplanar distance is unique for each plane. The basic principle of X-ray crystallography is that to measure the interplanar distances by using X-rays whose wavelength is comparable to these distances. X-rays striking at a specific angle are reflected in phase (Figure 3.2a). The angle (θ) is defined by Bragg's law

$$n\lambda = 2dsin\theta \qquad 3\text{-}1$$

Where n is the multiple integer (1, 2, 3…), λ is the wavelength of the X-ray used, d is the interplanar distance and θ is Bragg's angle. All the reflected beams satisfying Bragg's law will lie on the surface of a cone of semi-angle 2θ (Figure 3.2b). Each lattice plane has its own concentric circle and the radius of which is proportional to sin2θ.

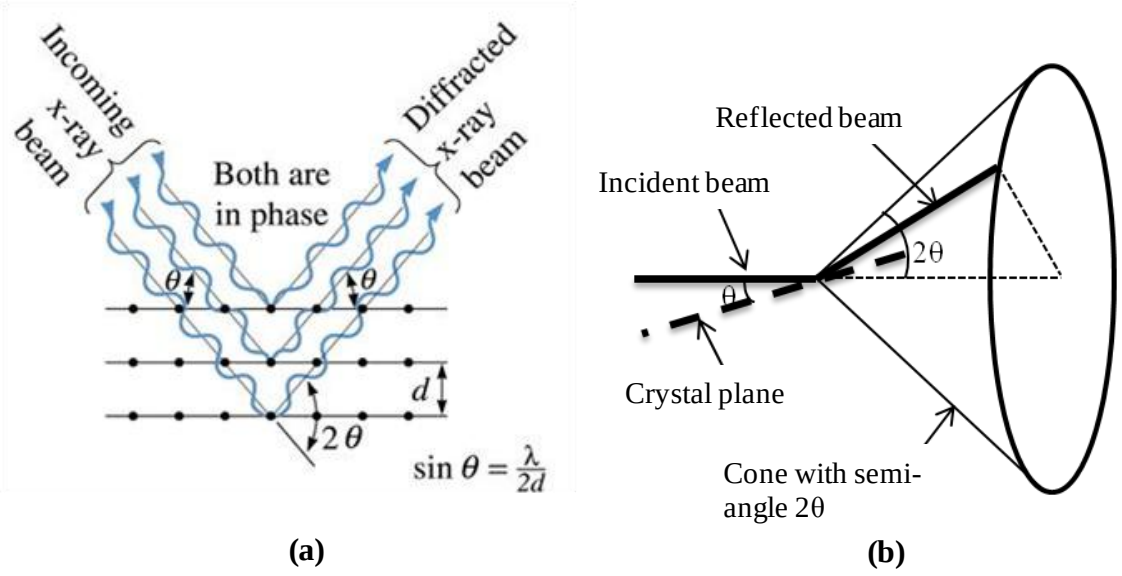

Figure 3.2 (a) Bragg's law, all the reflected beams are in phase (b) Reflected beams lie on the surface of a cone of semi-angle 2θ (Askeland et al., 2011)

3.2.1 X-ray diffraction in wood

The cross-section of each crystalline microfibril has around 20-40 cellulose molecules packed together (Fernandes et al., 2011). As observed by Newman (1998) only half the cellulose microfibrils are within the microfibril and half lie on its surface. A more appropriate definition might be that of a nanocrystalline body (in its cross-section) which will introduce line broadening due to the greater vibrational movement of the cellulose molecules lying on the surface of the microfibril. The cellulose unit cell is monoclinic (Figure 3.3a). Five different planes ((040), (021), (002), (101), and (10-1))[2] in this structure, each with a unique interplanar distance are shown in Figure 3.3b. The plane with the smallest interplanar spacing and therefore the largest Bragg's angle is for (040) plane and it can be used directly to determine the MFA distribution as the normal of this plane is parallel to longitudinal microfibril axis. However, its use is restricted by contamination from other reflections having Bragg's angles within half a degree of the (040) reflection and it is a comparatively weak diffraction (Lotfy et al., 1973). There are two sets of broad arcs lying on concentric circles corresponding to three lattice planes – the (101), (10-1), and (002). (101) and (10-1) are so close together that they merge to form one continuous arc (inner most). The normal to the (002) plane is perpendicular to the cell axis and the width of this strongest reflection can be used to determine the mean MFA (Cave, 1997). A fifth plane is the (021) which lies almost on the same concentric circle as the (002).

[2] Numbering of lattice plan e.g. (040), (002) etc is given by miller indices, which in turn are determined by taking the reciprocal of the intercept of the plane at x, y and z axis, respectively. For example the (002) plane, (taking the origin as defined in Figure 3.3(a) is not intersecting the x and y axis, and thus is taken as infinity (∞). It is intersecting the z axis at ½. The reciprocal of (∞, ∞, ½) is (002).

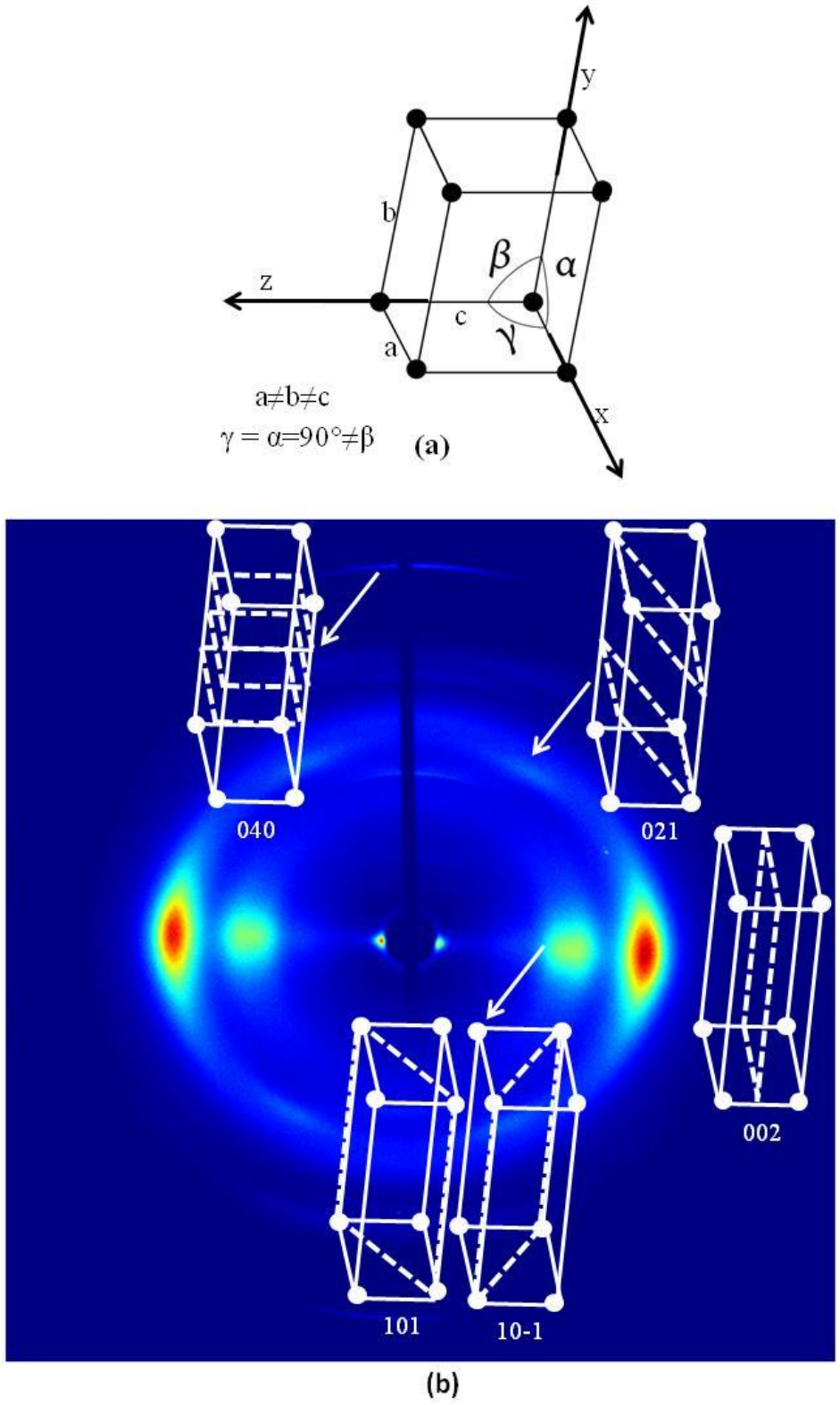

Figure 3.3 (a) Monoclinic unit cell. (b) Major cellulose crystal planes contributing to the diffraction pattern from wood. The fiber axis is vertical and is perpendicular to the X-ray beam (Evans, 1999).

3.2.2 Optical analogue

To better understand the theory behind the determination of the MFA from the (002) plane using X-ray diffraction an optical analogue was devised (Entwistle and Navaranjan, 2001). A mirror is fixed to a rod which is cut away so that the reflecting face of the mirror lies along the rod axis, and the normal of the reflecting surface is perpendicular to the rod axis. Thus the mirror represents a single (002) plane and the rod will represent a single microfibril. If a laser beam (mimicking the X-ray beam) directed perpendicular to the rod is incident on the mirror, the Bragg's diffraction condition can be achieved by rotating the rod with mirror about its vertical axis to bring the reflected beam on to the Bragg's reflection circle. For the (002) planes the interplanar distance is 0.389nm. Using copper kα radiation with 0.154nm wavelength the calculated Bragg's angle (θ) from Equation 3-1 is 11.5°. Thus when a circle of a cone of semi-angle 2θ (i.e. 23°) is drawn, with its axis coincident with the beam, then all possible Bragg's reflections from the (002) plane will lie on that circle. As the rod axis is rotated through some angle (M) in the vertical plane, the diffraction spots also rotate through angle M around the (002) circle, if the incident beam is normal to the plane in which the rod is rotated.

If a cellulose fibre were substituted for the single microfibril the X-rays would see a very large number of parallel microfibrils each with its own "reflecting mirror". Statistically there will always be a significant number of cellulose fibres in the Bragg's orientation to generate a strong spot on (002) circle. The fact that the (002) spots are rotated around the (002) circle through the same angle as the fiber is rotated is the principle used to measure the microfibril angle (M) when the X-ray beam is directed perpendicular to the set of cell walls.

When the cell is placed with its radial walls perpendicular to incident beams (Figure 3.4a), in addition to diffraction from the radial walls there will be diffraction from the orthogonal transverse/tangential walls. This condition can be achieved in the optical analogue by rotating the plane in which the rod lies through 90° and then adjusting the mirror to bring the tangential cell wall of microfibrils in the Bragg's orientation relative to the laser beam and in doing so the diffraction spots move towards the equator. Thus, the total diffraction pattern around the azimuthal angle (Chi) for the (002) is comprised of 2 sets of spots; a set for walls perpendicular to X-ray beam (radial in this case) and one for the walls parallel to X-ray beam (tangential in this case)(nearer the equator) (Figure 3.4b). The spots in X-ray diffraction lying in the (002) circle will, in the case of a real wood sample, be broadened to an extended arc (Figure 3.4c). The optical analogue represents a single microfibril. In a wood sample there

will be over 100 tracheid fibres in the beam each with over a million microfibrils. Slight differences in orientation (lamellar variation and tracheid variation within the S2 layer) about the axis direction of the fibre, lead to broadening of the spot to the arcs.

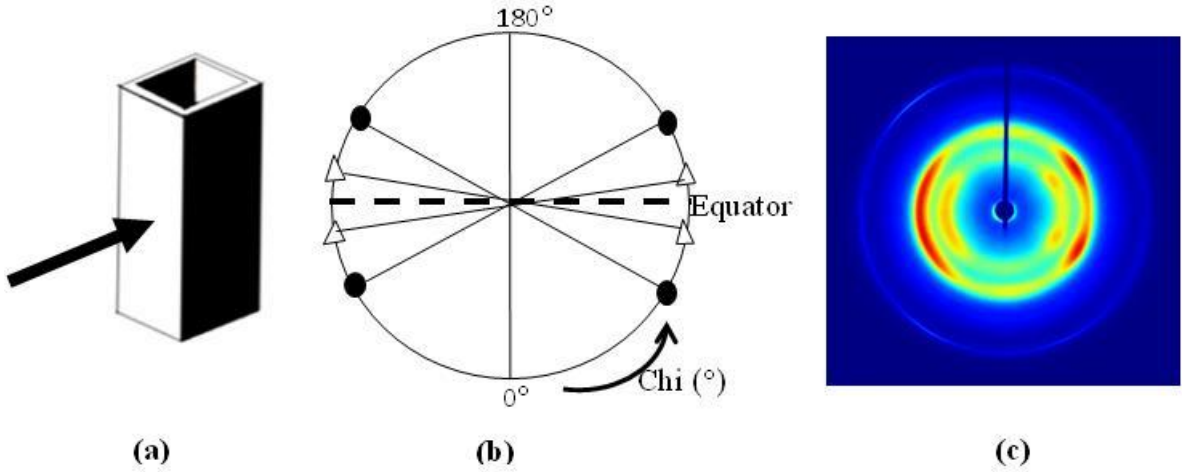

Figure 3.4 (a) Single cell; white walls representing walls perpendicular to X-rays and black walls representing walls parallel to X-rays. (b) Optical analogue for a single fiber; solid circles reflecting spots for walls perpendicular to X-rays and triangles reflections from walls parallel to X-rays (c) Diffraction pattern of wood, which shows extended arcs instead of individual spots

In the optical analogue the angle between the spots, from the walls that are perpendicular to the incident beam, is equal to twice the MFA. Hypothetically the wood sample diffraction pattern should give four peaks (each corresponding to the radial and tangential walls) which will be broadened due to slight variations in orientation. But due to overlapping of the peaks the individual peaks are not well defined. Figure 3.5 displays the hypothetical diffraction peaks of the (002) and the actual Chi diffraction profile of a wood sample obtained by integrating q between 1.57-1.66. q is related to the interplanar distance as $q=2\pi/\text{interplaner distance (Å)}$. For (002) plane q is $2\pi/3.89=1.62$

The small peak in the actual Chi diffraction profile (intensity distribution at around 0°) represents the diffraction from the S1 and S3 walls.

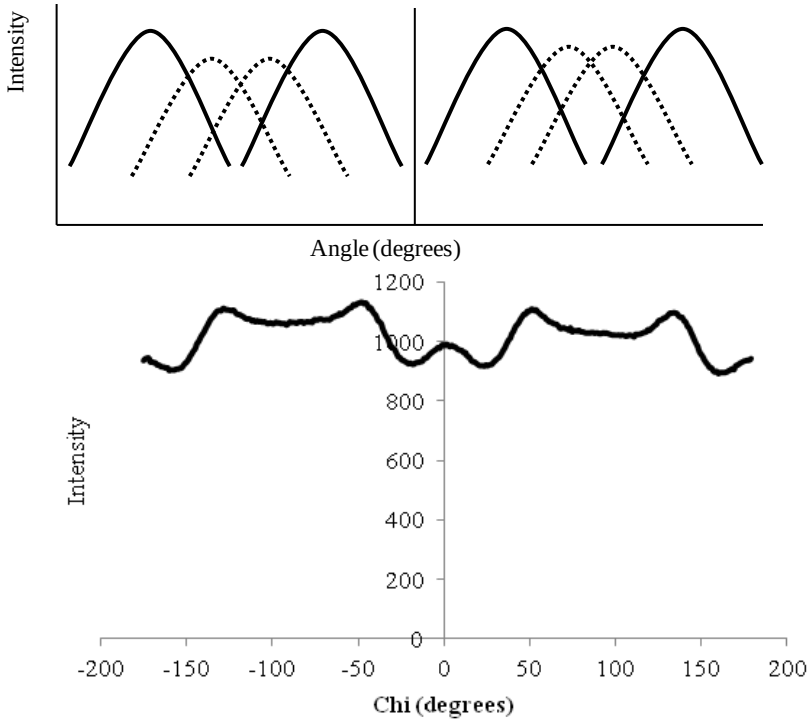

Figure 3.5 Four hypothetical independent peaks for two sets of walls, solid lines representing walls perpendicular to X-rays and dotted lines representing walls parallel to X-rays. Below is the actual integration profile for the (002) plane

Cave (1997) demonstrated that for square cells the shape of the intensity curve, due to the walls normal to the incident X-ray beam, is identical to the shape of the MFA frequency distribution[3] curve in these walls.

The outer flanks of the (002) intensity profile arises from the cell walls normal to the beam (radial walls in this case) and are unaffected by the walls parallel to the X-ray beam (transverse walls in this case). The angular distance from the equator to the point of inflexion of the intensity curve that cuts the zero intensity axis is given by the value *T* or Meylan's *T* angle (Figure 3.6). This procedure was developed by Meylan (1967) and Cave (1968).

Assuming the MFA distribution to be a simple Gaussian (Figure 3.6), Cave and Robinson (1998) suggested that *T* values can be equated to a function of mean MFA and the standard deviation (σ) of the MFA distributed in the cell walls planes normal to the beam as follows

[3] MFA frequency distribution is the plot of the number of short elements ($n\delta_L$) whose angle lie between $\theta x \pm d\theta x$.

$$T = MFA + 2\sigma$$

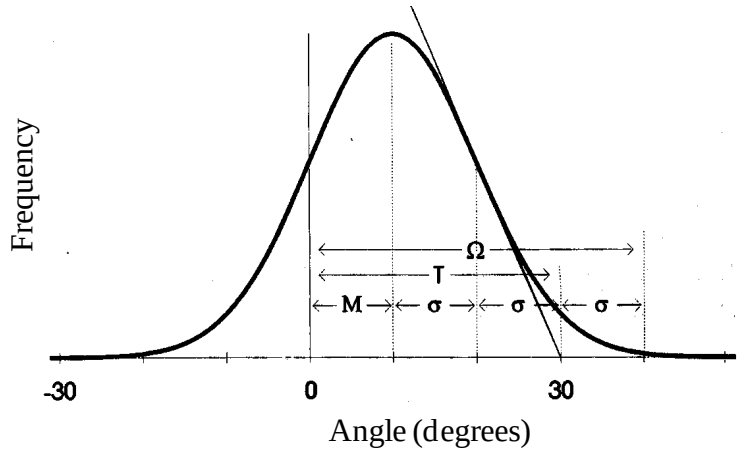

Figure 3.6 Properties of the Gaussian distribution (Cave and Robinson, 1998)

For circular cells this relationship also holds well when $M>2\sigma$. As *T* values include information about the dispersion of MFAs it may be a more useful measure than MFA alone.

The primary objectives of the work reported in this chapter are to compare *T* or MFA values in OW and CW in *Pinus radiata,* to study the variation among and within families of *Pinus radiata,* and to explore the association between MFA or *T* values and previously measured wood properties.

3.3 Material and methodology

From the 50 families in the Amberley trial, 12 families of 3 year old tilted *Pinus radiata* trees were selected that represented the full range of LS and stiffness (from the stiffest to the least stiff with others at regular intervals in between) for X-ray diffraction studies (Figure 2.19). From sawn 100mm long rectangular samples, 2mm thin (radial direction) slice was cut from side close to bark for sample preparation for further characterisation. From 2 mm thin slice samples were prepared as shown in Figure 3.7. The dimensions of sample used for X-ray diffraction was 15mm x 5mm x 1.5mm (longitudinal x tangential x radial). Two scans were taken for each sample with the X-ray beam oriented at 90° to the tangential cell wall; the second scan being 1 mm below the first to get some idea of within sample homogeneity. In total, *T* values were measured in 194 samples of opposite wood and 163 samples of compression wood.

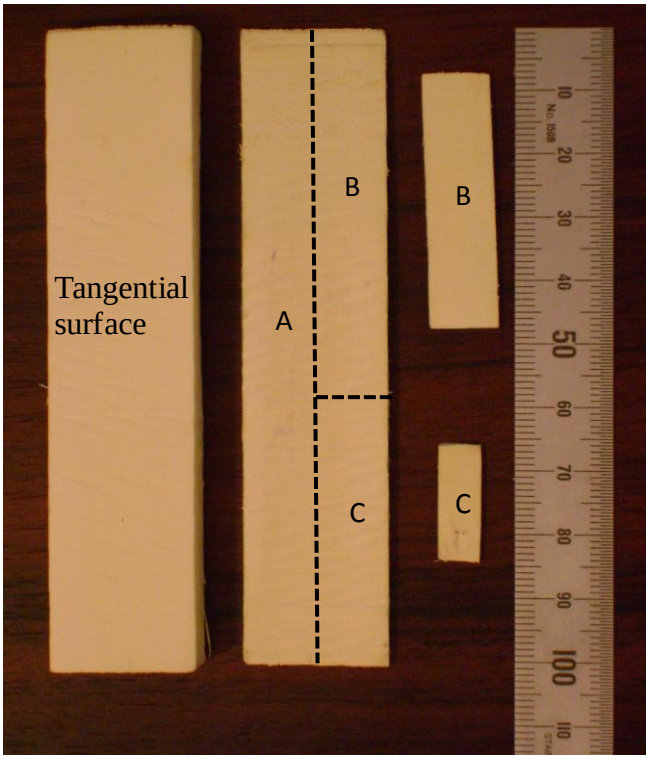

Figure 3.7 Photograph showing sampling scheme. Sample A was used for chemical analysis, sample B was used for DMA work and sample C was used for X-ray diffraction

Initial studies were undertaken with the Bruker-Nonius APEX II system using graphite monochromatised molybdenum (Mo) Kα (wavelength 0.71073 Å) as X-ray source in the Chemistry Department at the University of Canterbury. The initial data collected on Canterbury system showed unusual amount of scatter. An important source of this is scattering in the air. This can be reduced by shortening the distance between the specimen and the recording plate which further reduces the diameter of the (002) plane. But the problem with Mo radiation is that the shorter wavelength gives a low Bragg angle and therefore a small diameter (002) circle, as radius is proportional to Bragg's angle. Copper (Cu) radiation has advantage as its wavelength is twice of Mo so the diameter of the circle is approximately twice, so a shorter X-ray path length is feasible. Following damage to this instrument arising from the 2010/2011 earthquakes data were collected using the University of Auckland's Rigaku MicroMax-007 HR rotating anode instrument equipped with a Mar Research Mar345dtb detector working at 40kV and 30mA. The X-ray source was Cu so the wavelength was 1.5418Å (Cu Kα). A high MFA causes signal intensity to spread over large chi, reducing signal intensity at a given point. Since corewood has a high MFA the exposure time was 5 minutes per sample to improve the signal to noise ratio. The strong (002) equatorial reflection was used for MFA analysis. The Area Diffraction Machine Version 1

software (http://code.google.com/p/areadiffractionmachine) was used to read image files obtained from the diffractometer. The variation of diffracted intensity along chi for the (002) plane (at q between 1.57-1.66) was obtained using the same software.

The program written by Ian Cave was used to fit curves (Figure 3.8). The method is based on two assumptions. Firstly the microfibril angle distribution is a simple Gaussian and secondly the outer flanks of the diffraction profile are from the wall–pair oriented normal to the incident beam alone (Cave and Robinson, 1998). The method analysed the shape of the outer flanks of the (002) diffraction peaks. It comprised curve fitting (Figure 3.8), in which, after baseline correction (Background in Figure 3.8), the actual data curve was fitted visually by changing the numbers on the left hand side of the graph in Figure 3.8. The position, height, width and slope of the model (white peaks in Figure 3.8) can be changed reiteratively to obtain the best fit for data obtained from actual X- ray diffraction image (black peaks in Figure 3.8). The flank mean angle (MFA) is related to width of the curve whereas the flank standard deviation angle related to the standard deviation (σ) of the Gaussian intensity distribution in MFA within the wood sample. From MFA and σ, the T value was calculated using Equation 3-2. In addition to this there is correction for (021) plane (scaling factor) and the meridional peaks i.e. S1 and S3 (around 180 in Figure 3.8) can also be fitted by changing numbers on left hand side under subheading meridional peaks in Figure 3.8.

The symmetry of the peaks is dependent upon the alignment perpendicular to the beam. Care was taken to mount the sample in an exactly vertical position. Peaks were asymmetric in some samples in which case, each peak was independently fitted and the average value was taken as the final value.

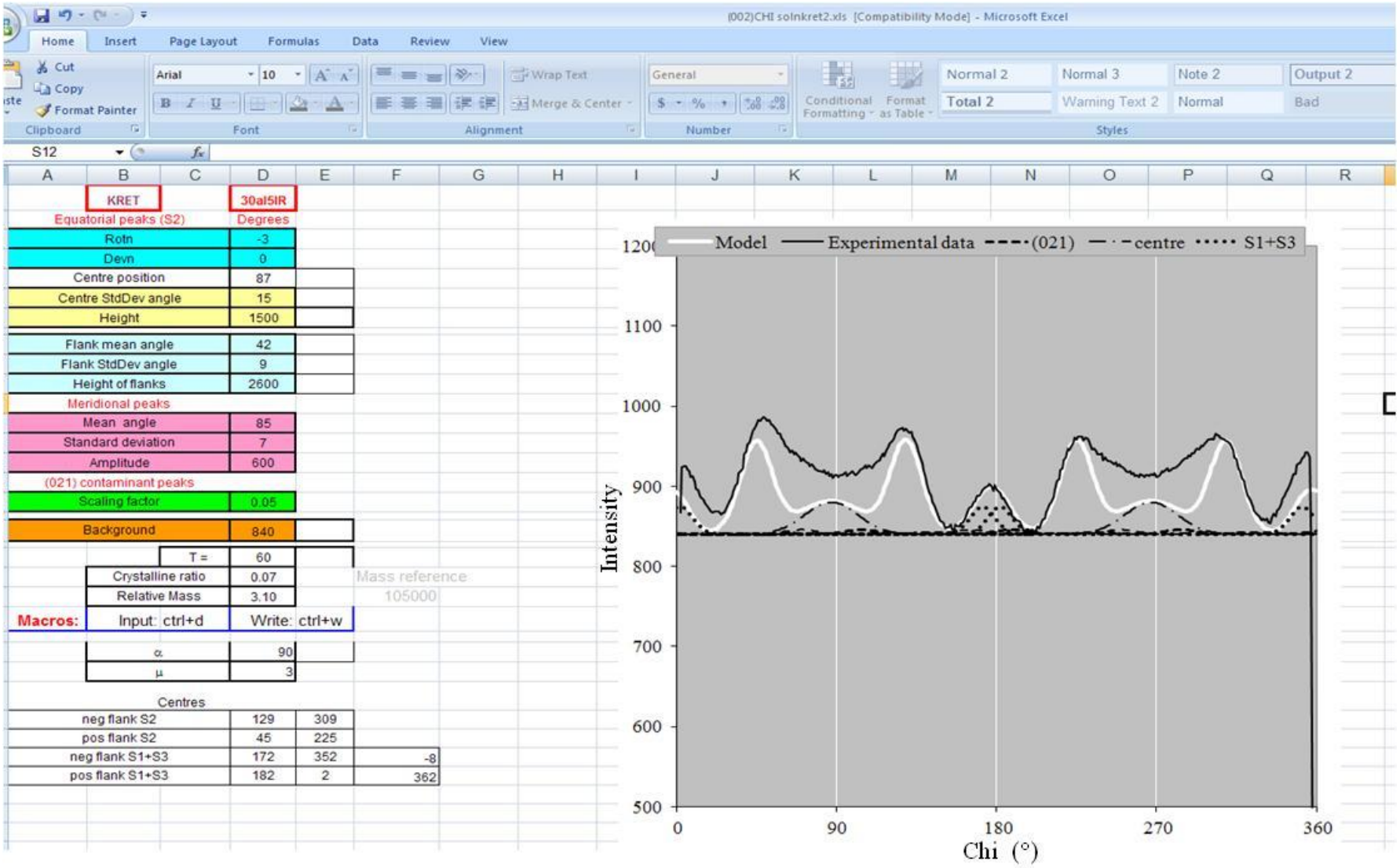

1

2 Figure 3.8 Excel sheet of Ian Cave's program showing different parameters used to fit curves to analyse data obtained from X-ray diffraction

3.3.1 Statistical analysis

The software R was used for the analysis. Summary of selected samples of 12 families were presented in terms of mean and coefficient of variation.

In order to study the effect of wood type the following model in R software was used.

$$Response = \mu + WT + R + FC + TID + e \quad \text{3-3}$$

where μ, and *WT* are the fixed effects of the overall mean (μ) and wood type (WT), *R*, *FC*, *TID*, and *e* represent the random effects of replicate, family, tree identity and residuals. The expectation of the response is *E*[*response]* = μ+*WT* and random effects have zero mean and variances σ_R^2, σ_{FC}^2, σ_{TID}^2 and σ_e^2.

Pearson correlation was also determined independently for two wood types between MFA, *T* and all other wood properties measured after subtracting the residuals (random effect and error) using model Equation 3-3. The significance level used was *p*=0.01.

Regression analysis was used to search for the most influential factors on dynamic modulus (calculated using dry density and dry velocity squared) and longitudinal shrinkage (green to 5% moisture content). MFA and basic density were used as independent variables to predict dynamic modulus and longitudinal shrinkage. The coefficients for the regression line relating response (Dynamic modulus or longitudinal shrinkage) with basic density (BD) and MFA were calculated independently for wood types using the following model, assuming that the residuals are independent, identically distributed following a normal distribution.

$$Response \sim BD + MFA + R + FC + TID + e \quad \text{3-4}$$

Variation attributed to family effect was analysed using following model independently in wood types

$$Response = \mu + R + FC + e \quad \text{3-5}$$

where μ is the fixed effects of the overall mean. *R*, *FC*, and *e* represent the random effects of replicate, family, and residuals. The expectation of the response is *E*[*response]* = μ and random effects have zero mean and variances σ_R^2, σ_{FC}^2, σ_{TID}^2 and σ_e^2.

The percent variance attributed to family effect can be calculated as

$$\sigma_{FC}^2\% = \frac{\sigma_{FC}^2}{\sigma_R^2 + \sigma_{FC}^2 + \sigma_e^2} \times 100 \qquad 3\text{-}6$$

The ranking of families in opposite wood was done in terms of indirect method i.e. dry velocity squared and direct method i.e. MFA values obtained using X-ray diffraction. Families were ranked based on the best linear unbiased predictions obtained from model Equation 3-5. Comparison of ranking in OW was done using Spearman ranking correlation test.

3.4 Results and discussion

The diffraction pattern of all the wood samples had a low noise level. Thus there was no problem in curve fitting. The summary statistics along with coefficient of variation of selected *Pinus radiata* trees is given in Table 3.1.

Table 3.1 Summary statistics of selected samples along with coefficient of variation of wood properties in young *Pinus radiata* trees

Wood type	Opposite wood		Compression wood	
No. of samples	194		163	
	Mean	CV%	Mean	CV %
Basic density (kg/m^3)	365	7.4	552	10.4
Dry acoustic velocity^2 (km/s)^2	7.12	11.9	5.70	8.2
Dynamic modulus (GPa)	2.97	15	3.44	9.9
Longitudinal shrinkage (%)	1.03	34.4	3.44	18.7
Volumetric shrinkage (%)	12.47	17	8.17	13.9
MFA (°)	39	9.4	44	6.5
T (MFA+2σ) (°)	62	6.3	62	4.6

The summary statistics of the physical and mechanical properties (details are given in chapter 2) along with *T* and MFA values after controlling the effect of replicate and family in selected samples is given in Table 3.2.

Table 3.2 Estimated means and 95% confidence intervals of physical properties and microfibril orientation in opposite wood and compression wood in young *Pinus radiata* after controlling for the effect of replicate and family

Variable	Opposite wood			Compression wood		
	Mean	Lower	Upper	Mean	Lower	Upper
Basic density (kg/m^3)	364	355	374	552	543	564
Dry acoustic velocity^2 $(km/s)^2$	7.11	6.87	7.11	5.71	5.49	5.90
Dynamic modulus (GPa)	2.96	2.84	3.09	3.42	3.28	3.53
σ(°)	11.5	11.1	11.8	8.9	8.6	9.2
MFA(°)	39	38	40	44	43	45
T (MFA+2σ) (°)	62	61	63	62	61	63
Longitudinal shrinkage (%)	1.03	0.89	1.16	3.44	3.31	3.57
Volumetric shrinkage (%)	12.44	11.98	12.83	8.11	7.68	8.53

The correlation matrices for the wood properties in young radiata pine are presented separately for opposite wood (Table 3.3) and compression wood (Table 3.4).

Table 3.3 Pearson Correlation matrix (with *p*-values in parentheses) for wood properties in opposite wood of young *Pinus radiata*

Variable	Basic density (kg/m^3)	Acoustic velocity ^{2} $(km/s)^2$	Dynamic modulus (GPa)	Longitudinal shrinkage (%)	Volumetric shrinkage (%)
T (MFA +2σ) (°)	-0.12 (0.09)	-0.64 (<0.01)	-0.56 (<0.01)	0.53 (<0.01)	0.22 (<0.01)
MFA (°)	-0.12 (0.09)	-0.68 (<0.01)	-0.53 (<0.01)	0.59 (<0.01)	0.20 (<0.01)

Table 3.4 Pearson Correlation matrix (with *p*-values in parentheses) for wood properties in compression wood of young *Pinus radiata*

Variable	Basic density (kg/m^3)	Acoustic velocity^2 $(km/s)^2$	Dynamic modulus (GPa)	Longitudinal shrinkage (%)	Volumetric shrinkage (%)
T (MFA+2σ) (°)	0.24 (<0.01)	-0.47 (<0.01)	-0.09 (0.26)	0.41 (<0.01)	0.27 (<0.01)
MFA (°)	0.26 (<0.01)	-0.50 (<0.01)	-0.10 (0.21)	0.47 (<0.01)	0.27 (<0.01)

3.4.1 Comparative study of wood types

The characteristic diffraction patterns of OW and CW are given in Figure 3.9. The first major difference was the presence of a small peak around 180° in the chi plot, which is contributed by the S1 and S3 walls. In most of the OW samples it was either very weak or missing altogether, whereas in CW it was comparatively strong. The volume of the S1 sub-layer in CW is comparatively greater than in OW (Wooten et al., 1967). Another difference is in their symmetry. OW peaks were asymmetrical and CW wood peaks were symmetrical (Figure 3.9). Symmetrical peaks in CW can be attributed to the fact that due to the circular nature of CW tracheids any error in sample placement will not affect the symmetry, whereas due to rectangular shape in OW even a small error in sample placement will result in asymmetrical peaks.

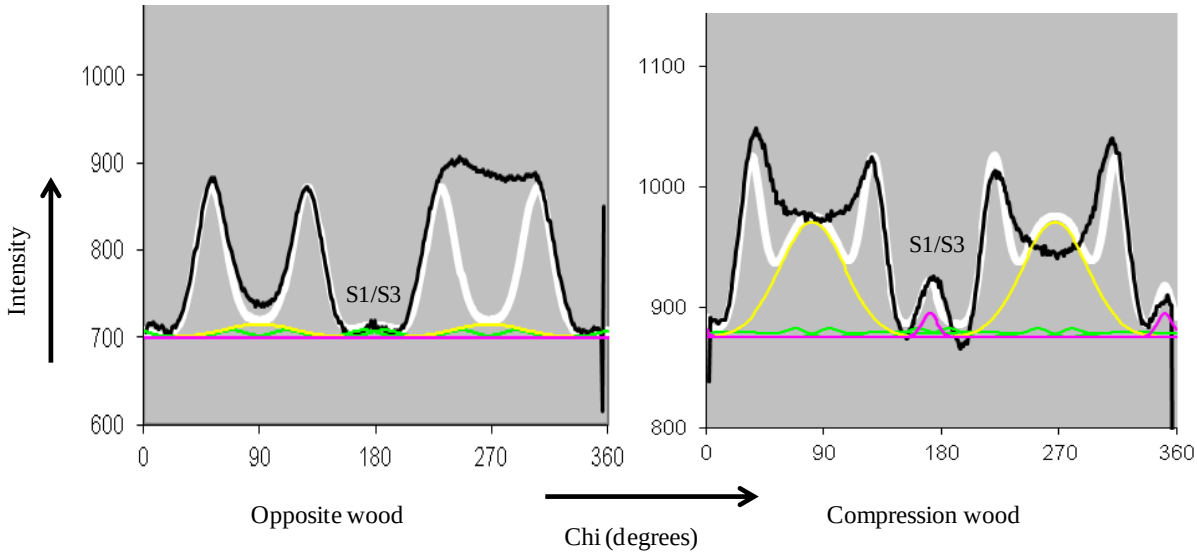

Figure 3.9 X-ray diffraction pattern in opposite wood and compression wood, where white line represent model and black lines represent actual data. In opposite wood, peaks are asymmetric thus only the left hand peak is fitted in this diagram

The flank mean angle were smaller in OW i.e. the mean MFA was smaller than in CW, whereas the flank standard deviation angle was lower in CW which implies a lower standard deviation (σ) in CW. The two wood types do not differ in T values (Table 3.2) as the mean and upper and lower limit is same for wood types. The reason could be that the MFA was low and σ was high in OW whereas there was high MFA and low σ in CW. The range in T values was higher (52°-71°) in OW than in CW (55°-69°) Figure 3.10. The MFA in OW was in the range of 28°-48°, which is consistent with results reported by Donaldson (1993) for *Pinus radiata*. The MFA and σ differ significantly for the two wood types the average difference in their MFA was ~5° and average difference in their σ was 2.6° (Figure 3.11).

Cave and Robinson (1998) suggested that at high MFA (>30°) the samples with high σ are comparatively stiffer than samples with a low σ. Thus the higher acoustic wave velocity in dry OW may be due to its comparatively low MFA and high σ. Another reason for the low acoustic velocity in dry CW could be its high density (stress wave velocity decreases with density (Nakamura and Nanami, 1993). In the present study there was a negative significant correlation between density and acoustic velocity only in CW.

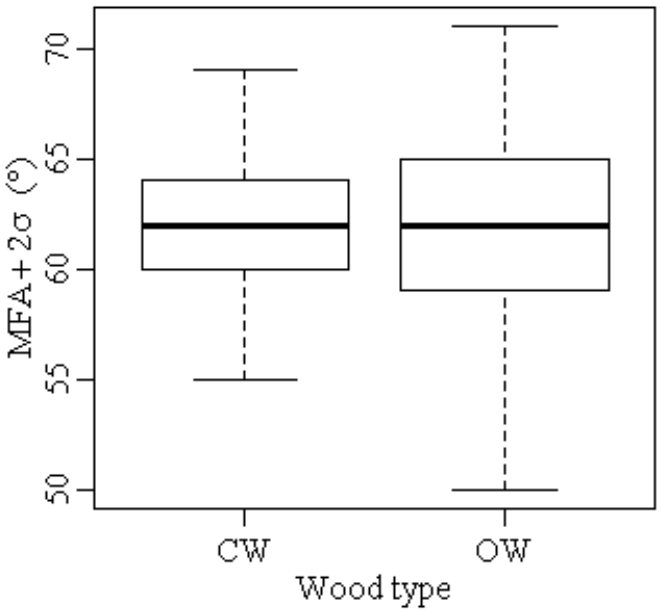

Figure 3.10 Box plot of *T* values (MFA+2σ) for compression wood and opposite wood in young *Pinus radiata*.

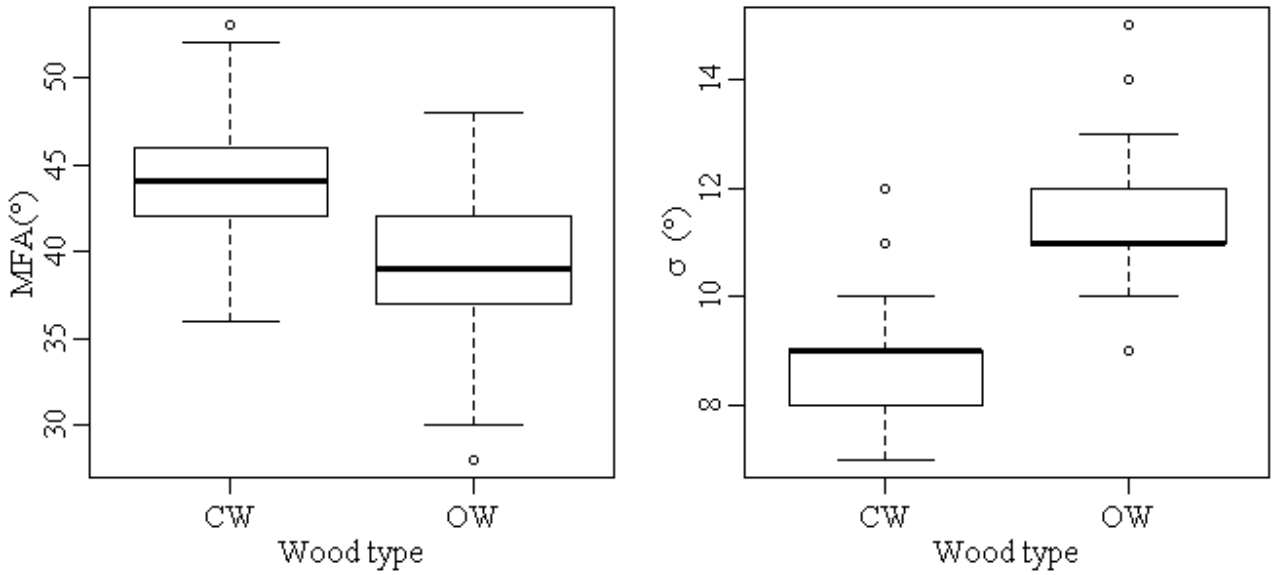

Figure 3.11 Box plot of microfibril angle (MFA) and standard deviation (σ) for compression wood and opposite wood of young *Pinus radiata*

The order of variation in wood properties was almost the same for both wood types (Table 3.1). In opposite wood the largest variation was found for LS followed by VS, dynamic

MOE, dry velocity squared, MFA and finally density. In CW the order was the same only that density was more variable than dry velocity squared and MFA.

In previous studies (Evans and Ilic, 2001; Megraw et al., 1999) the correlation between MFA and stiffness in opposite wood was high (R^2>80), as most of the studies considered a pith to bark relationship with a range between 10°-50°. In contrast, in this study the correlation between dynamic modulus and MFA values was comparatively low (R^2=0.34) as the range in MFA was comparatively small (28°-48°). The correlation between dynamic modulus and *T* values (MFA +2σ) is slightly higher than MFA alone thus it could be possible that both the MFA and its distribution within a sample effect dynamic modulus. In CW there was no significant correlation between *T* and dynamic modulus (R^2 = 0.05) but here the range is still smaller i.e. is between 36°-53° (Figure 3.12).

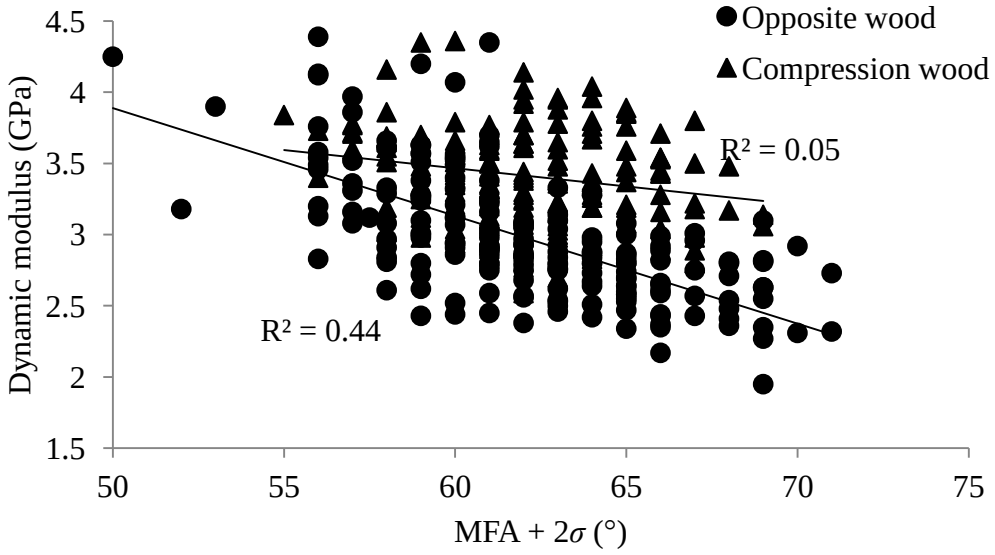

Figure 3.12 Correlation between dynamic modulus and MFA in compression wood (triangular labels) and opposite wood (circular labels) in young *Pinus radiata*

As basic density is also positively correlated to dynamic modulus in both wood types thus regression analysis was done using Equation 3-4. The intercept and (standard error) for OW was 2.96 (0.073) and for CW it was 3.41 (0.045). The regression coefficient and (standard error) for basic density in OW was 0.00977 (0.0008) and in CW it was 0.0047 (0.0003). The regression coefficient and (standard error) for MFA in OW was -0.055 (0.005) and in CW it was -0.0318 (0.005). The regression equations for the two wood types are given in Table 3.5. Basic density along with MFA explains 76% variation in dynamic modulus in OW and 70% variation in CW (Figure 3.13).

Table 3.5 Regression equations for opposite and compression wood, where DM stands for dynamic modulus, BD for basic density and MFA for microfibril angle.

Wood type	Regression equation
Compression wood	DM=3.41+0.0047*BD-0.032*MFA
Opposite wood	DM=2.96+0.0098*BD-0.055*MFA

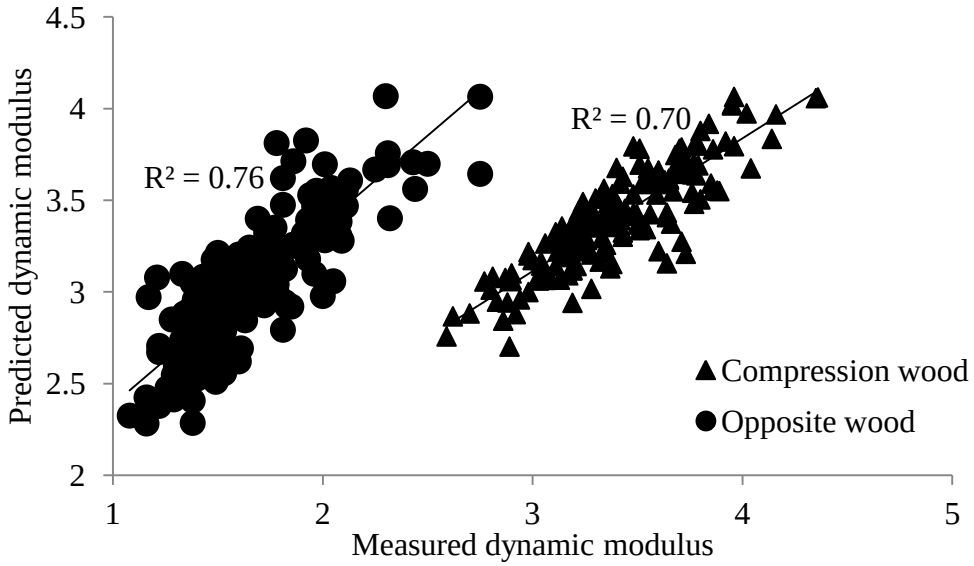

Figure 3.13 Predicted versus measured dynamic modulus in opposite and compression wood of young *Pinus radiata*

Longitudinal shrinkage was positively related to MFA. LS is minimum around 25° and increases sharply once the MFA exceeds about 35° and there is curvilinear relationship between longitudinal shrinkage and MFA (Meylan, 1968). Core wood and CW are characterised by high MFA (Donaldson, 1992) thus as expected MFA was higher than 30° in most of the samples. Megraw et al. (1998) showed that relationship between MFA and longitudinal shrinkage is very much dependent upon ring number and in loblolly pine the R^2 for ring number 5 was 0.38, it was 0.41 for ring 15 and was just 0.01 for ring number 25. In present study there was linear relationship between MFA and longitudinal shrinkage with R^2 = 0.45 in opposite wood. The comparatively high correlation in LS and MFA in OW (Figure 3.14) could be due to the fact that the range in MFA was higher in OW. Also in CW other than MFA factors like high density, high galactan content, and anatomical characteristic also

influence longitudinal shrinkage. In both wood types a wide range of longitudinal shrinkage is associated with a given MFA.

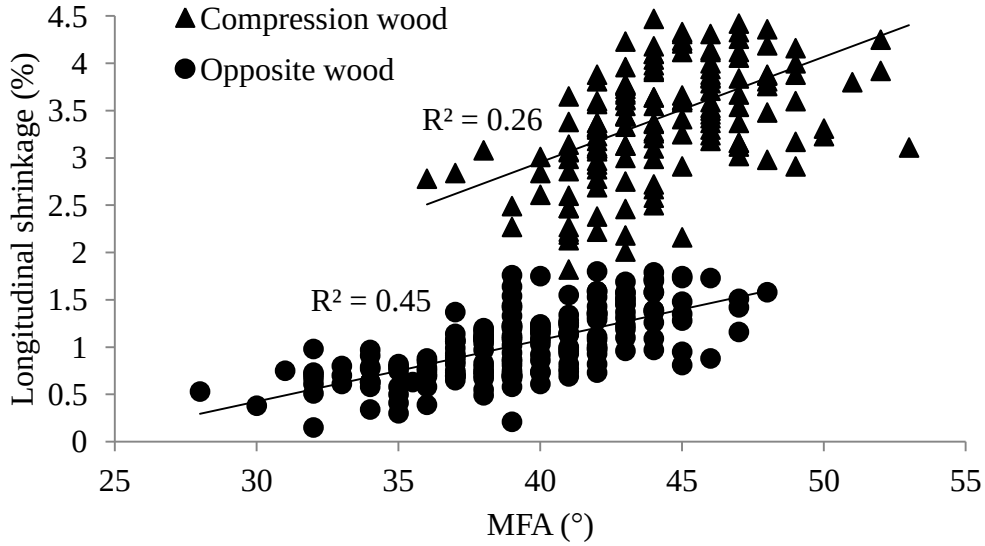

Figure 3.14 Correlation between longitudinal shrinkage and MFA in compression wood (triangular labels) and opposite wood (circular labels) in young *Pinus radiata*

In present study, other than positive relation between longitudinal shrinkage and MFA, basic density was negatively correlated to LS in OW but was positively correlated in CW. The coefficients of regression line (and their standard errors) were different for the two wood types. The intercept and (standard error) for opposite was 1.027 (0.064) and for CW it was 3.44 (0.068). The regression coefficient and (standard error) for basic density in OW was -0.0035 (0.0008) and in CW it was 0.008 (0.0005).The regression coefficient and (standard error) for MFA in OW was 0.051 (0.005) and in CW it was 0.064 (0.010). The regression equations for the two wood types are given in Table 3.6. The model explains 64% variation in opposite wood and 77% variation CW (Figure 3.15).

Table 3.6 Regression equations for opposite and compression wood where LS stands for longitudinal shrinkage, BD for basic density and MFA for microfibril angle

Wood type	Regression equation
Compression wood	LS = 3.44+0.008*BD+0.064*MFA
Opposite wood	LS = 1.027-0.0035*BD+0.051*MFA

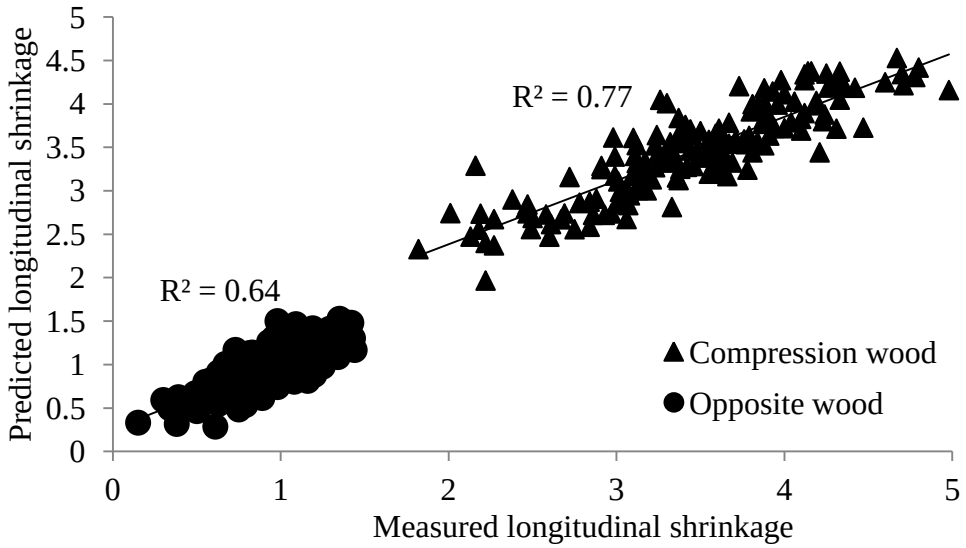

Figure 3.15 Predicted versus measured longitudinal shrinkage in opposite and compression wood of young *Pinus radiata*

Based on these results, the criteria for selection for stiffness and stability should be low MFA and high density in OW. In spite that only small sample was taken for MFA measurement there was good correlation between dry acoustic velocity squared and MFA in opposite wood (Figure 3.16). Thus dynamic MOE which reflects the density in combination with sound wave velocity (which depends upon the MFA) is obviously a better indicator of stiffness and stability of OW than considering either MFA or density alone.

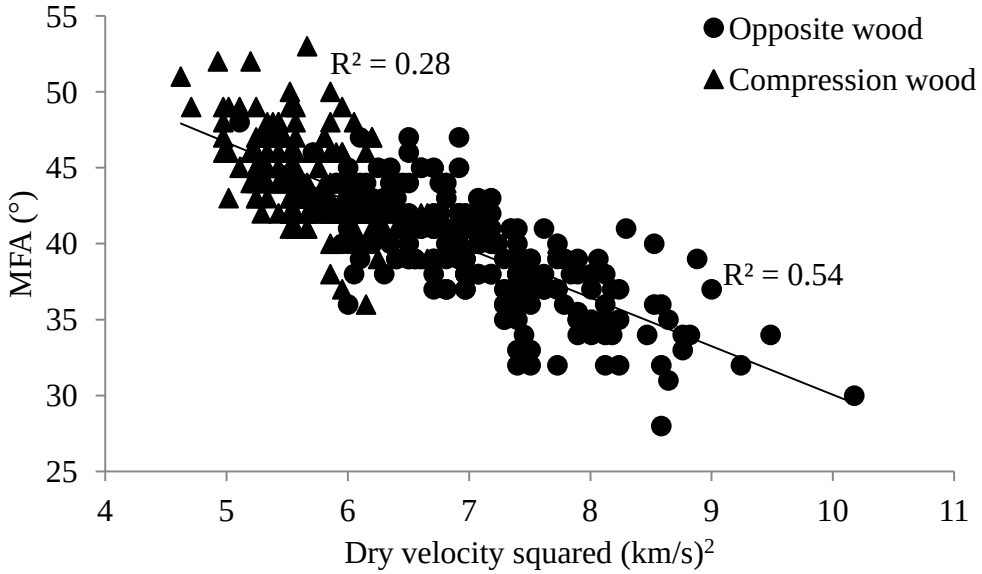

Figure 3.16 Correlation between dry velocity squared and MFA in compression wood (triangular labels) and opposite wood (circular labels) in young *Pinus radiata*

The selection criteria for selecting stable CW should be low basic density and low MFA which means that one is reducing CW stiffness in selecting low basic density.

3.4.2 Ranking of families

The properties in CW and OW behave independently; there was no correlation between MFA of OW and MFA of CW (Figure 3.17). The ranking of families was done independently in two wood types.

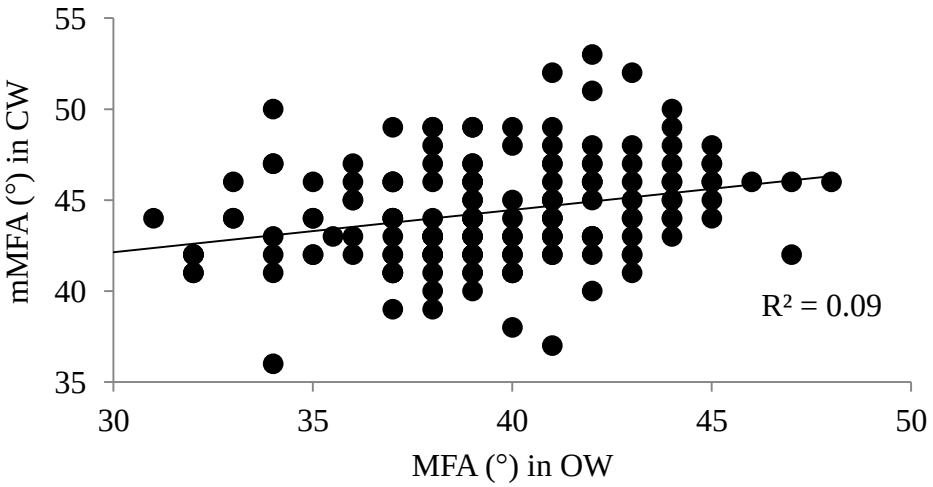

Figure 3.17 Correlation between MFA in compression wood and MFA in opposite wood in young *Pinus radiata*

3.4.2.1 Opposite wood

The mean values of measured properties in OW along with coefficient of variation for 12 families are given in Table 3.7.

Table 3.7 Mean values of wood properties and coefficients of variation in opposite wood for 12 *Pinus radiata* families

		Basic density (kg/m^3)		Dynamic modulus (GPa)		Longitudinal shrinkage (%)		Volumetric shrinkage (%)		MFA (°)	
Family code	No. of samples	Mean	CV (%)	Mean	CV (%)	Mean	CV (%)	Mean	CV (%)	Mean	CV (%)
A	20	371	5.6	3.28	12.2	0.68	26.5	10.53	11.0	37.3	8.8
B	16	384	6.9	3.34	13	0.78	34.7	11.94	11.7	38.8	8.9
C	16	377	8.6	3.29	15.4	0.82	31.6	11.95	10.6	36.8	9.9
D	20	361	6.8	3.21	12.3	0.96	26.2	13.13	22.1	36.8	9.7
E	9	370	7.1	2.97	8.8	0.87	27.5	12.23	16.7	39.1	5
F	17	359	5.1	2.94	10.4	0.84	27.6	11.48	15.5	38.7	11.6
G	18	347	7	2.85	14.6	1.02	24.3	13.19	16.9	38.1	6.9
H	15	347	6.9	2.6	14.7	1.28	21.3	12.80	10.6	40.5	6
I	11	344	7.2	2.58	7.3	1.17	23.5	12.23	13.4	40.6	9.4
J	16	371	5.7	2.74	7.1	1.26	25.9	13.28	18.7	41.1	8.1
K	19	377	8.1	2.93	17.2	1.29	31.2	13.98	12.0	42.5	6.3
L	16	361	5.3	2.74	7.6	1.39	19.5	12.76	17.8	41.7	5.3

There was large within family variation, box plots for MFA values in opposite wood for 12 families are given in Figure 3.18.

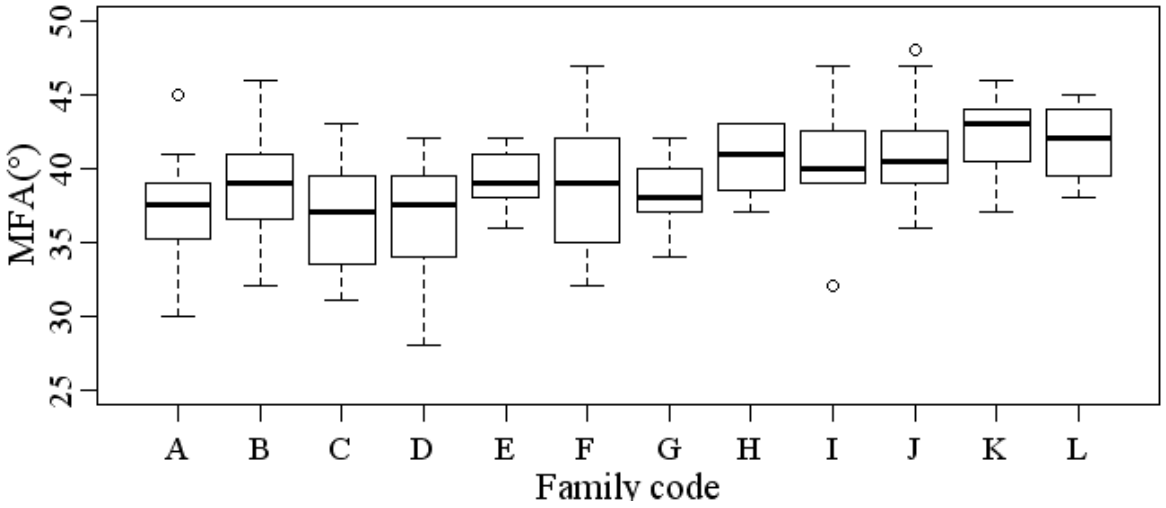

Figure 3.18 Box plots for MFA values in opposite wood for families in young *Pinus radiata*

The family (A) was stiff (3.28GPa) and low in LS (0.68%) was one of the best family in terms of MFA. The difference in average MFA between the best family (A) and the worst family (with highest average MFA (K)) was 4.8°. The small difference between families can be explained by the large variation within families. The phenotypic values of dry acoustic velocity squared and *T* values in OW of the individual trees in the best and the worst families are given in Figure 3.19. The worst individuals in the best family had comparable *T* values to the best individuals in the worst family.

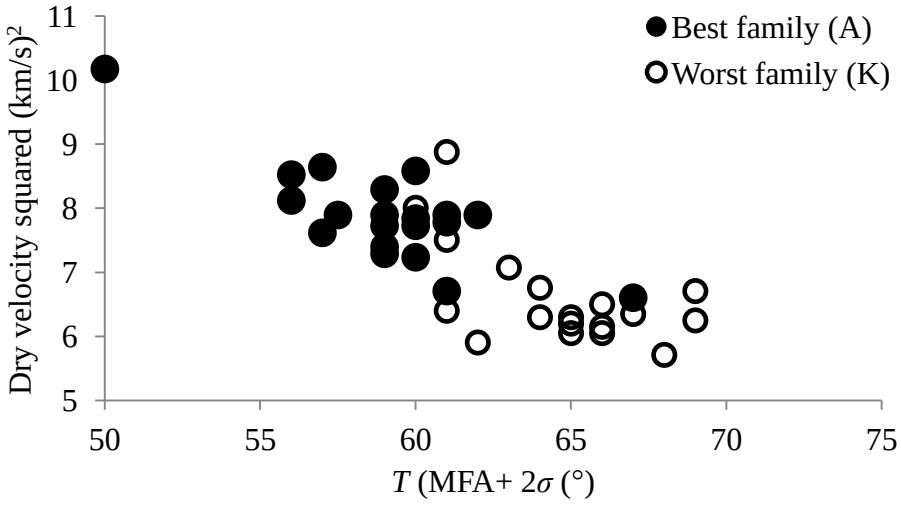

Figure 3.19 Variation in *T* (MFA+2σ) and dry velocity squared in opposite wood within the best and the worst family of young *Pinus radiata*

Result of analysis (Equation 3-5) suggests that variation in wood properties attributed to family effect was very low than variation attributed to residual effect i.e. within family variation. The variation in MFA attributed to family effect in OW was 22% (using Equation 3-6). Given in Figure 3.20 are plots for deviation in MFA from overall mean along with 95% confidence interval for families. There is clear demarcation between best three families (A, C and D with low mean MFA) and worst three families (J, K and L high mean MFA) but also there is large within family variation. Therefore it is possible to screen for MFA at age three but due to large within family variation selecting individual trees from best families will result in more genetic gains than selecting individual families.

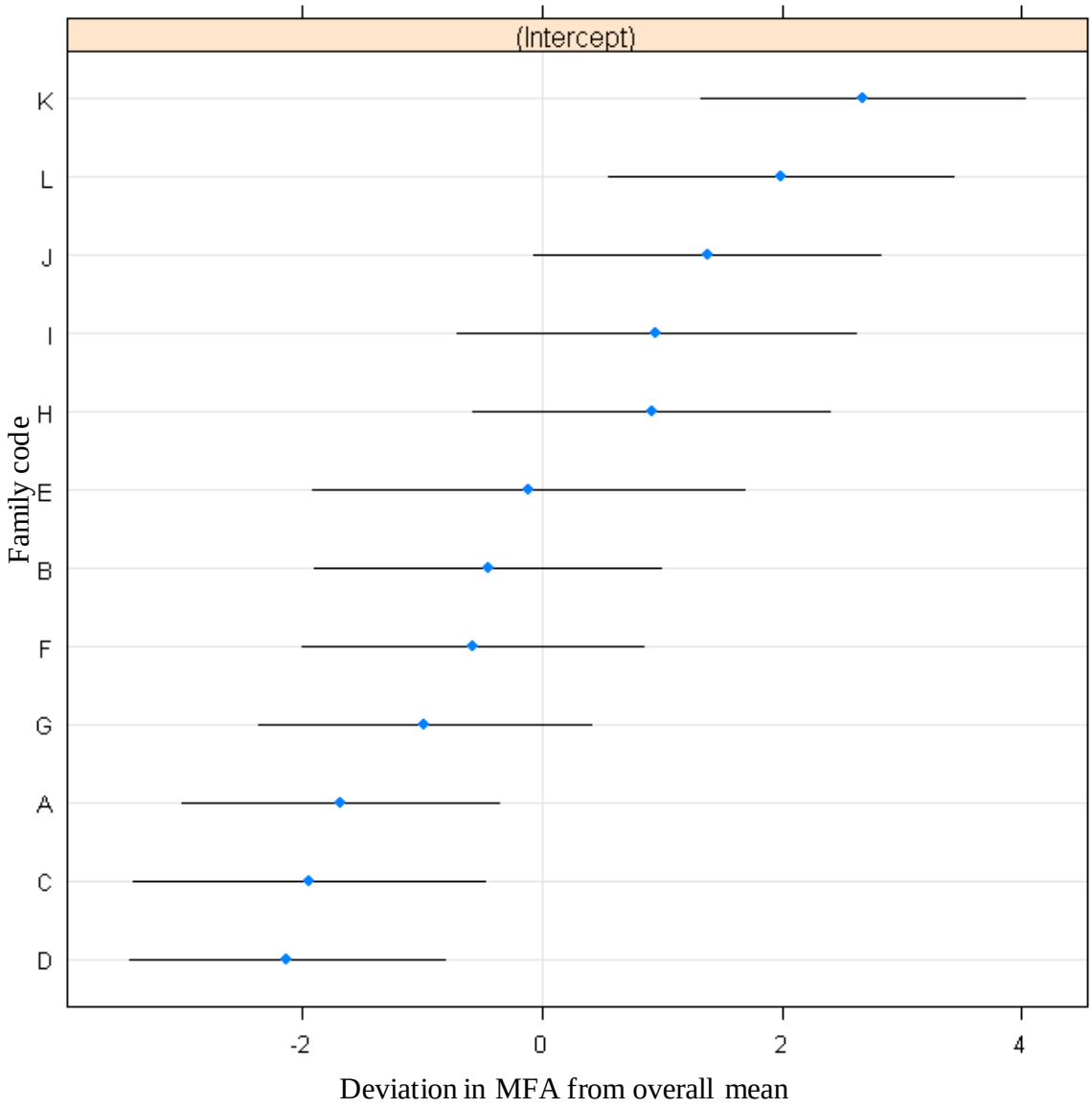

Figure 3.20 Plot representing deviation in MFA from intercept along with 95% confidence limit of families in opposite wood of young *Pinus radiata*. The intercept was 39.03°

Given in Table 3.8 are mean values and ranking of families using dry velocity squared and MFA. In spite of the fact that only small sized sample was used for X-ray diffraction the Spearman ranking coefficient (-0.80) suggests that resonance method can used effectively to screen trees with low MFA at young age.

Table 3.8 Mean values of dry acoustic velocity squared and MFA along with ranking of opposite wood for 12 families in young *Pinus radiata*

Family code	Dry velocity squared $(km/s)^2$		Microfibril angle	
	Mean	Ranking	Mean	Ranking
A	7.836154	1	37.6018	3
B	7.612349	3	38.8297	6
C	7.571513	4	37.33667	2
D	7.673917	2	37.15736	1
E	7.03713	7	39.17181	7
F	7.226179	5	38.70772	5
G	7.119557	6	38.30261	4
H	6.470563	12	40.19796	8
I	6.674276	9	40.2353	9
J	6.491909	11	40.65943	10
K	6.696309	8	41.95827	12
L	6.658144	10	41.27818	11

3.4.2.2 Compression wood

Mean values of measured properties in CW along with coefficient of variation for 12 families are given in Table 3.9.

Table 3.9 Mean values of wood properties and coefficients of variation in compression wood of 12 *Pinus radiata* families

		Basic density (kg/m^3)		Dynamic modulus (GPa)		Longitudinal shrinkage (%)		Volumetric shrinkage (%)		MFA (°)		T (MFA+2SD) (°)	
Family code	No. of samples	Mean	CV (%)	Mean	CV (%)	Mean	CV (%)	Mean	CV (%)	Mean	CV (%)	Mean	CV (%)
A	13	580	11.2	3.63	10.7	3.37	22.1	8.15	9.2	44	6.0	61	4.7
B	13	567	6.3	3.70	5.0	3.15	17.4	8.60	26.7	44	6.5	61	5.7
C	15	545	7.6	3.37	9.7	3.27	10.3	8.06	5.0	43	5.9	63	4.1
D	16	570	11.9	3.42	10.0	3.71	18.4	8.02	13.0	45	9.5	62	5.3
E	8	560	10.1	3.46	7.8	3.40	17.0	7.88	8.4	43	4.7	63	4.0
F	15	575	12.5	3.62	9.3	3.54	19.9	8.37	15.7	44	4.2	61	3.0
G	15	524	8.7	3.48	7.5	3.02	20.6	7.53	11.3	43	8.1	60	5.2
H	12	516	10.2	3.24	8.9	3.02	21.1	7.60	9.3	44	7.6	62	4.1
I	11	568	4.9	3.28	7.4	3.88	15.1	8.13	10.1	46	7.7	64	5.4
J	13	567	10.4	3.51	7.2	3.45	19.5	8.31	14.2	45	3.9	63	3.7
K	18	551	9.8	3.25	9.6	3.74	13.5	8.73	9.6	45	4.7	64	2.3
L	16	512	9.7	3.09	8.1	3.66	15.1	8.36	14.9	46	5.4	63	3.5

The main concern with CW is its high LS as this gives rise to warp when present with normal wood in a piece of timber when drying. Basic density cannot be used to rank families due to uncertainties in its values (OW bands in-between CW wood in the samples). As samples for X-ray diffraction were pure CW, it was more trust worthy to rank families using MFA in CW.

There is large within family variation in MFA in compression wood (Figure 3.21). The variance attributed to family effect was just 5% (Equation 3-6). Given in Figure 3.22 are plots for deviation in MFA from overall mean along with 95% confidence interval for families obtained using model Equation 3-5. In CW there was no clear demarcation between families as they have overlapping confidence intervals. Secondly it also suggests large within family variation. One possible reason for large within family variation in CW could be the variation in lean angle as it was not uniform in Amberley trial. Thus it could be possible that the severity of compression wood differs from tree to tree thus altering MFA.

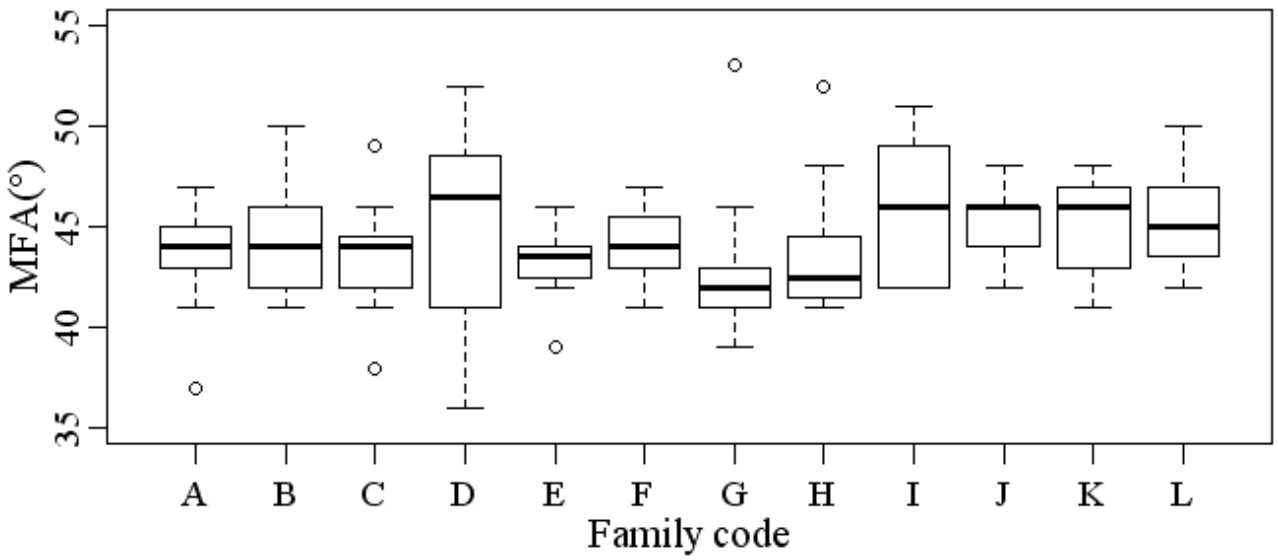

Figure 3.21 Box plots for MFA values in compression wood for families in young *Pinus radiata*

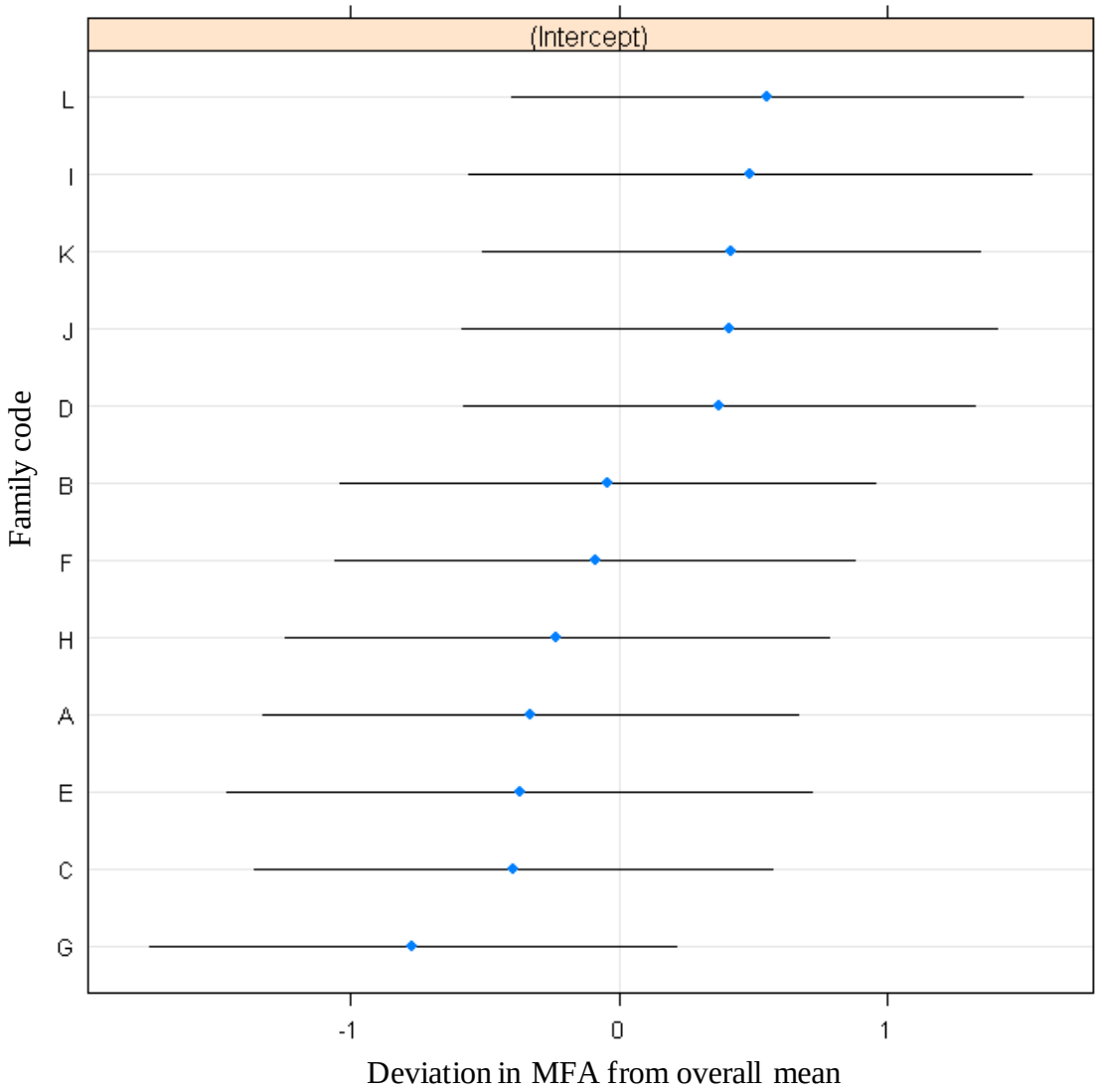

Figure 3.22 Plot representing deviation in MFA from overall mean (intercept) along with 95% confidence limit of families in compression wood of young *Pinus radiata*. The intercept was 44.33°

Despite this reservation we are looking at the worst form of CW whereas timber has CW of varying intensity (Harris, 1977; Yumoto et al., 1983) if one were to select trees on the basis of MFA in CW, the best CW family (G) (lowest MFA) displays a lower LS (21% less) than the worst family (I) (high MFA). However selection for CW in a breeding programme is not advocated.

3.5 Conclusions

- The two wood types differ significantly in their MFA. OW is characterised by lower MFA with a higher standard deviation. The MFA in OW samples was 39° compared to 44° in CW.
- No correlation was observed between MFA of OW and CW in the same tree.
- MFA along with density explain 76% variation in stiffness and 64% variation in LS in OW. In CW, MFA and density explain 70% variation in stiffness and 77 % variation in LS.
- Families vary significantly in MFA in OW but the variation between families was comparable to variation within a family.
- The strong Spearman ranking correlation between acoustic velocity squared and MFA suggests that the resonance technique can be used efficiently to screen trees for low MFA at young age.

Chapter 4. Dynamic Mechanical Analysis in Corewood

4.1 Introduction

In corewood where the MFA is high the mechanical properties are influenced by a complex interaction between the MFA and the amorphous matrix of the cell wall (Xu et al., 2011; Yamamoto et al., 2002). In addition the hemicelluloses, having a high affinity for water, control the water-dependent properties of the wood particularly its dimensional stability (Yamamoto et al., 2001). Currently the amount of hemicelluloses in wood is determined by depolymerising the polysaccharides and by quantifying the individual sugar monomers. The sugar monomer may not originate from a single polysaccharide which creates ambiguity. It is therefore desirable to develop methods able to quantify hemicellulose concentrations and their properties in the undisturbed state in the cell walls. Wood is a viscoelastic material thus studying its mechanical properties can potentially be used indirectly to gather information regarding any structural differences at molecular level among wood samples. In this chapter the chemical structure of wood is reviewed cursorily in terms of chemical composition, and the role of the amorphous cell wall matrix on the mechanical properties of wood at high and low MFA. The possibility of using dynamic mechanical analysis (DMA) to study the viscoelastic properties of wood to reveal differences amongst families and record differences between wood types. Subsequently, representative samples were analysed for wood chemistry at the University of Auckland but this work is not part of the thesis.

4.2 Stress-strain curves and viscoelasticity

The stress-strain curve gives information about such mechanical properties. The steepness of the slope is related to stiffness (MOE) and the area under the curve is related to the energy it can absorb before it breaks. The stress-strain curves for elastic, and viscoelastic states are illustrated in Figure 4.1. Brittle plastics are highly stiff (steep slope) but low in toughness. Tough plastics are tough due to the large area under curve so they absorb energy and undergo deformation before they break, and slope of the curve suggests that they are moderately stiff. Lastly elastomers are neither stiff nor tough but have high reversible elongation. Studying the transition temperature along with stress strain behaviour is very useful in defining the end use and working temperature range of polymers. Changes in mechanical properties can be used to predict structural changes at the molecular level.

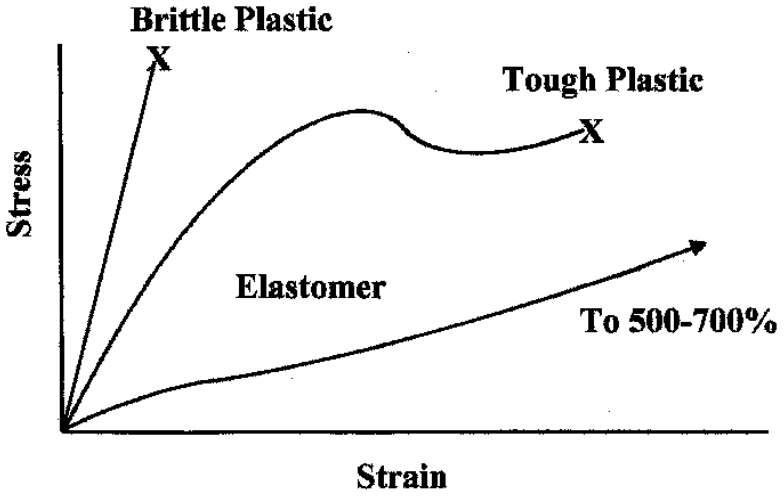

Figure 4.1 Stress-strain relationship in different materials

4.3 Dynamic mechanical analysis

DMA is a well established technique to measure thermomechanical properties of polymers. Dynamic test methods have been extensively employed to determine the relative stiffness and damping characteristics of polymeric materials. In particular, it relates the changes in the mechanical response of the material to changes at the molecular or microstructural level.

In DMA, an oscillating stress is applied to the sample and strain is measured as a function of temperature and frequency. From this, various viscoelastic properties, e.g. storage and loss moduli and damping (tanδ) can be examined. These properties are important in defining the end use and the working temperature range of polymeric materials.

Viscoelasticity is the property of materials that exhibits both viscous and elastic characteristics when undergoing deformation. DMA is used to characterise viscoelastic properties of polymers as a function of both frequency of the applied stress and temperature.

In DMA the applied stress produces a sinusoidal strain, the behaviour of which depends upon the material properties (Figure 4.2). Elastic materials strain instantaneously when stress is applied and immediately return to their original state once the stress is removed. There is no phase difference between stress and strain in perfectly elastic materials. The behaviour of elastic materials can be explained by Hook's law, which states that the resultant strain (ε) is directly proportional to the applied stress (σ) and the proportionality constant is referred to as modulus of elasticity (E) (Equation 4-1). Elastic materials store applied energy that is fully recovered after removal of the applied stress.

$$\sigma = E\varepsilon \quad \text{4-1}$$

In viscous materials the deformation depends upon the rate of change in applied stress and therefore it is the first derivative of applied stress, resulting in a phase lag of 90° between the applied stress and the resultant strain. They resist shear and strain varies linearly with time when a stress is applied. This phenomenon was explained by Newton, who proposed that the stress (σ) is proportional to the rate of strain with the proportionality constant being viscosity (η) (Equation 4-2). Viscous materials dissipate applied energy as heat and hence are unable to recover their structure on unloading.

$$\sigma = \eta \frac{d\varepsilon}{dt} \quad \text{4-2}$$

Viscoelastic materials have elements of both of these behaviours and, as such, exhibit time dependent strain, i.e. the applied stress is proportional to both the resultant strain and rate of strain. Viscoelastic materials show an intermediate behaviour as part of their behaviour is in-phase (elastic component) and a part of is out-phase (viscous component). The phase difference lies between 0°-90°, and is defined by the phase angle δ.

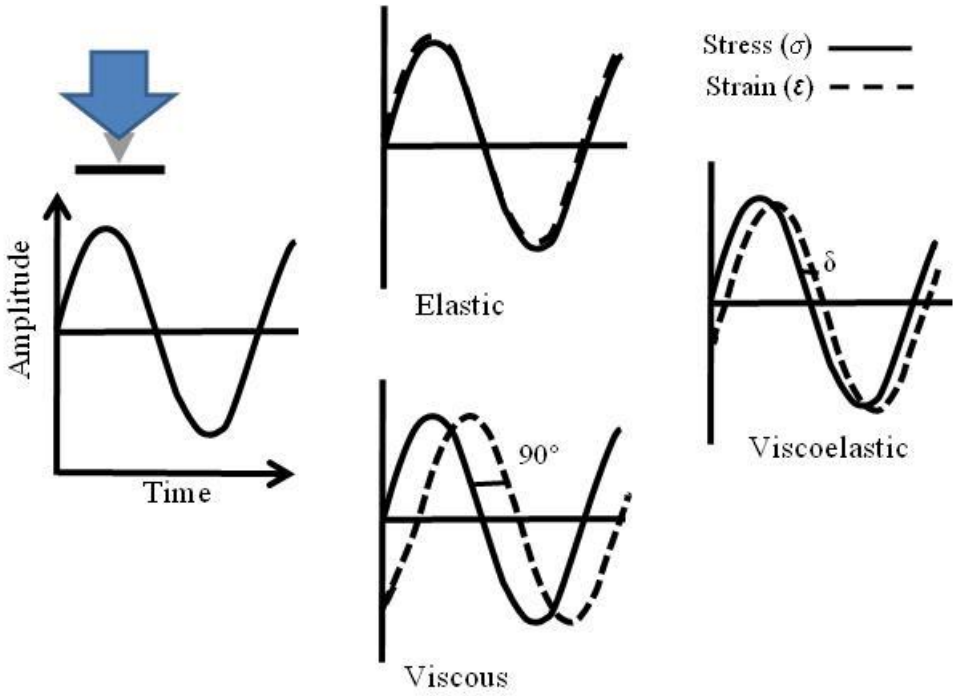

Figure 4.2 Stress-strain behaviour in elastic, viscous and viscoelastic materials

The majority of measurements of viscoelastic properties of polymeric systems are performed within a region referred to as the linear viscoelastic region. In this region, as the stress applied to the sample is increased, the relationship between the stress and the strain rate is constant, despite the variance of strain with time. Within the linear viscoelastic region stress at any time *t* is given by

$$\sigma_t = \sigma_0 sin\omega t \tag{4-3}$$

Where σ_t is the stress at time *t*, σ_0 is the maximum stress, and ω is the frequency of oscillation. For elastic materials the strain is related linearly to stress by *E* (modulus) therefore, from Equation 4-1 strain (ε_t) at any time *t* is given by

$$\varepsilon_t = \frac{\sigma_t}{E} \tag{4-4}$$

$$\varepsilon_t = \frac{\sigma_0}{E} sin\ \omega t \tag{4-5}$$

or it can be written as

$$\varepsilon_t = \varepsilon_0 sin\ \omega t \tag{4-6}$$

For viscous material stress at any time *t* is a first derivative of strain

$$\sigma_t = \eta \frac{d\varepsilon_t}{dt} \tag{4-7}$$

$$\sigma_t = \eta \frac{d}{dt} \varepsilon_0 \sin\ (\omega t) \tag{4-8}$$

$$\sigma_t = \eta\omega\varepsilon_0 \cos\ (\omega t) \tag{4-9}$$

$$\sigma_t = \sigma_0 \omega cos(\omega t)\ or \tag{4-10}$$

$$\sigma_t = \sigma_0\ \ sin(\omega t + \tfrac{\pi}{2}) \tag{4-11}$$

Thus there is a phase difference of $\pi/2$ (90°) between stress and strain in viscous materials.

Viscoelastic materials have intermediate properties and the phase difference arises because the relationship between stress and strain is an ellipse as shown in Figure 4.3 a, and it is

evident that force reaches a maximum before the strain. The area of the force displacement hysteresis loop is equal to energy lost per cycle. As there is a phase difference of angle δ between maximum stress (σ_0) and maximum strain (ε_0), the stress can be resolved into two components – in-phase stress σ' and out-phase stress σ'' (Figure 4.3 b).

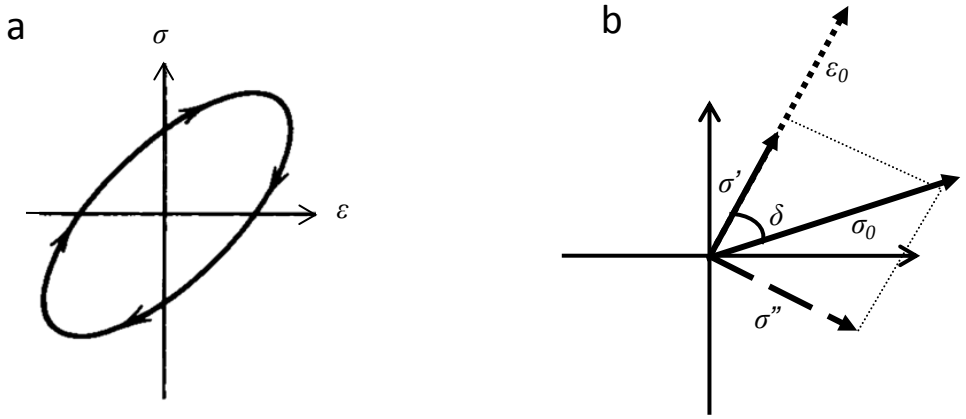

Figure 4.3 a) Force displacement curve in a viscoelastic material b) the Stress (σ_0) can be resolved into two components, in-phase (σ') and out-phase (σ'')

The relationship between the in-phase (σ') and the out of phase (σ'') components and phase lag (δ) is given by

$$\sigma' = \sigma_0 cos\delta \tag{4-12}$$

$$\sigma'' = \sigma_0 sin\delta \tag{4-13}$$

In-phase modulus (E')given by

$$E' = \frac{\sigma'}{\varepsilon_0} \tag{4-14}$$

From Equation 4-12

$$E' = \frac{\sigma_0}{\varepsilon_0} cos\delta \tag{4-15}$$

$$E' = E^* cos\delta \tag{4-16}$$

Similarly using Equation 4-13 the out-phase modulus (E'') is given by

$$E'' = E^* sin\delta \quad \text{4-17}$$

Thus in a viscoelastic material the modulus is termed as complex modulus (E^*) as it is a vector sum of loss modulus and storage modulus. The storage modulus E' is defined as the in-phase or elastic response proportional to the recoverable or stored energy; whereas the loss modulus E'' is defined as the out-phase or viscous response, and is proportional to the lost energy. The complex modulus is a vector quantity characterised by magnitude (E^*) and angle (δ) (Figure 4.4). E' and E'' represent the real and imaginary components of this vector. The ratio between the loss and storage moduli (E''/E') gives the useful quantity known as the mechanical damping factor ($\tan\delta$) which is a measure of the amount of deformational energy that is dissipated as heat during each cycle of loading.

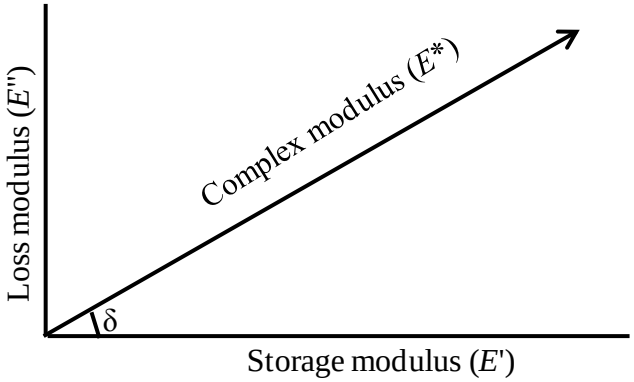

Figure 4.4 Relationship between complex, storage, and loss modulus in viscoelastic materials

Dynamic energy losses in solids commonly arise from relaxation processes. They arise when the applied stress produces atomic scale structural changes which create a time dependent strain. This process is characterised by the relaxation time τ. The loss is expressed as $\tan\delta$, and is maximum when the time period of the imposed vibration is comparable to the relaxation time. If the angular vibration frequency is $\omega=2\pi f$, then $\tan\delta$ is a maximum when $\omega\tau= 1$

$$tan\delta = \Delta E^*[\omega\tau/1 + (\omega\tau)^2] \quad \text{4-18}$$

Thus when $\omega\tau$=1, $\tan\delta$ reaches its maximum of $\Delta E/2$ where ΔE is the relaxation strength. A maximum in $\tan\delta$ can be attained either by changing the frequency or the relaxation time through its temperature dependence. The relaxation time decreases with temperature. The

tanδ is probably the most measured property in DMA because its value varies dramatically in the course of a phase transition. It is an indicator of how efficiently the material loses energy to molecular rearrangements and internal friction. A temperature scan gives information of mechanical properties which are related to changes at the molecular level. The change in storage modulus in polymers with temperature is shown in Figure 4.5. At low temperatures, only vibrational motion of atoms is possible and the polymer is hard and glassy. As the temperature is increased, loose sites in the structure, either side groups or chain segments, readjust their positions to give extra strain. These secondary relaxations (marked 5, 4 in Figure 4.5) lower the modulus by a factor of two or more. A further increase in temperature results in gradual chain movements and the material changes from a hard glassy material to a rubbery state. This is the glass transition temperature (*Tg*) at which mechanical properties change drastically (3). The amorphous portion of the polymer softens causing the modulus to drop three orders of magnitude. Beside a drop in modulus in the glass transition region, a peak in loss modulus and tanδ occur at the midpoint temperature between the glassy and rubbery state of the polymer. Further high temperatures enable large chain movements, resulting in a rubbery plateau (2) during which the polymer experiences rubbery flow. Finally the polymer can melt (1).

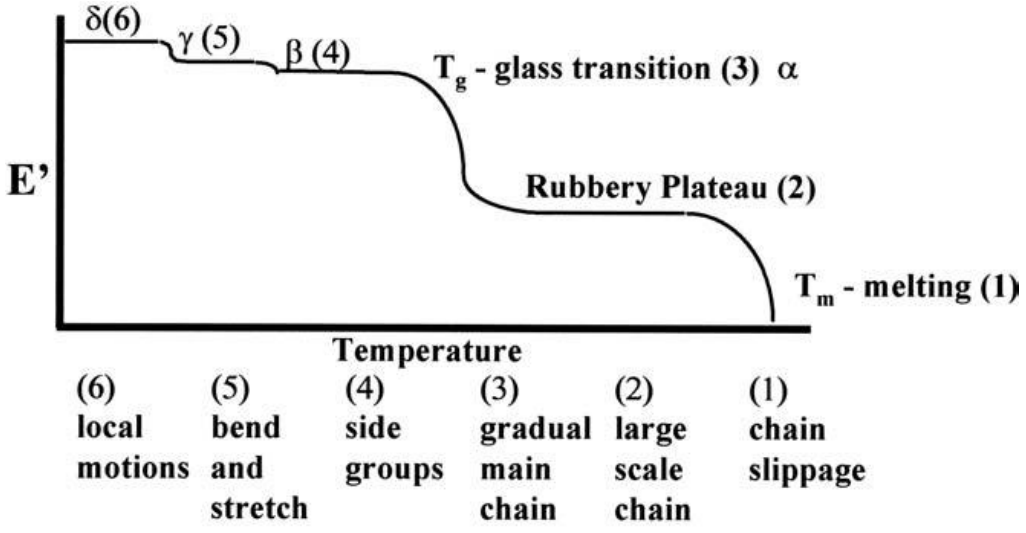

Figure 4.5 Change in storage modulus with temperature for thermo plastic materials (Menard, 2008)

Factors that influence the *Tg* are related to the structure of the polymer such as the degree of branching, the type of side groups, and backbone linkage. *Tg* is very important in defining the physical and mechanical state of polymers. Polymers with a high *Tg* are brittle at room

temperature, while materials with a *Tg* at room temperature will be leathery, and ones with a *Tg* below room temperature are viscous rubbers (elastomers) at room temperature. Each state has its characteristic mechanical properties.

4.4 Wood structure a digression – as it affects DMA analysis

The wood cell wall is composed of carbohydrates, lignin and water. The principal component is cellulose (a polymer of glucose), which is present as partly crystalline microfibrils. These microfibrils are embedded in a matrix of hemicelluloses and lignins. Hemicelluloses are hetro polymers mainly composed of five sugars namely, arabinose, xylose, glucose, mannose and galactose. The amount of hemicelluloses and the structure and composition of the individual hemicelluloses vary between genra, species, cell type and cell wall layer. In softwoods mannose is the most important monomer whereas in hardwoods xylose is the main unit. The principal hemicelluloses of softwoods are galactoglucomannans and for hardwoods are glucoronoxylans (Harris, 2006). CW of conifers contain two more polysaccharides, (1->3)-β-glucan (callose) and (1->4)-β-galactan which are either absent or present in very small amount in opposite wood. (1->4)-β-galactan is located mostly in primary wall and outer lignified secondary layer ($S2_{(L)}$) in CW (Altaner et al., 2010).

Lignin is a polymeric compound composed of substituted phenyl propane units. The three principal monomeric units are 4-hydroxy phenyl propane (H), 3-methoxy, 4-hydroxy phenyl propane (guaiacyl-propane, G) and 3,5-methoxy,4-hyroxy phenyl propane (syringyl-propane, S). The H unit is least substituted thus forms a highly branched condensed structure and is present in considerable amounts in CW (Brennan et al., 2012; Westermark, 1985). Softwood lignins consist mainly of G units which can further be distinguished into two types, branched-associated with glucomannans and linear-associated with xylans (Lawoko et al., 2005). Hardwood lignins contain both G and S units in ratios ranging from 2:4 to 2:1 (Walker, 2006).

The cellulose microfibrils are 3-4 nm in diameter. The microfibrils are in turn aggregated into large entities called macrofibrils with a diameter of 20-25 nm (Fengel, 1970). Dynamic FT-IR spectroscopic studies in spruce wood suggested that the glucomannan is closely associated with cellulose, whereas xylans are associated with lignin (Åkerholm and Salmén, 2001). The cellulose microfibrils together with glucomannan form the large macrofibrils which are surrounded by matrix (Figure 4.6) (Fahlén and Salmén, 2005). Proton diffusion studies reported distinct types of hemicelluloses associated with cellulose, and associated with lignin

(Altaner et al., 2006). The same study also reported significant distance between cellulose fibrils and lignin.

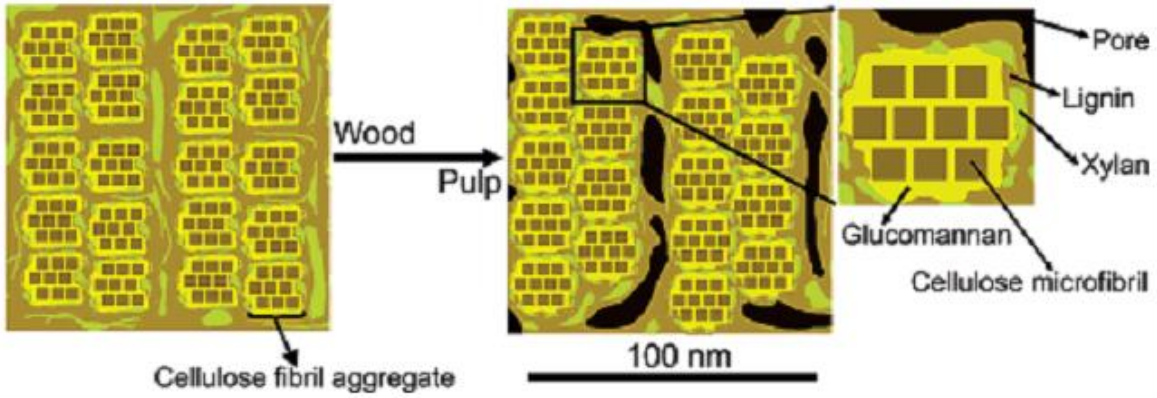

Figure 4.6 Schematic illustration of cell wall structure of S2 layer in spruce wood (Fahlén and Salmén, 2005)

The properties of the cell wall in the longitudinal direction depend upon the cellulose whereas in the transverse directions the amorphous wood polymers play a more dominant role (Salmén, 2004). MFA not only influences the mechanical properties but also shrinkage during drying (Yamamoto et al., 2002). But at high MFAs the influence of interactions of cellulose with the matrix polymers becomes more crucial for the mechanical performance and dimensional stability of the cell wall (Xu et al., 2011; Yamamoto et al., 2002). Floyd's (2005) model predicted that a large percentage of the variation in shrinkage was due to the galactose content of wood. Newman (2005) noted that galactan unlike cellulose, mannan and xylan does forms a non-linear polymer that would be harder to pack neatly within the non-crystalline matrix of the cell wall (Entwistle and Walker, 2005). Ha et al. (1997) studied dry and hydrated cell wall in onion (rich in (1->4)-β-galactan) and suggested that galactans have high affinity for water and are very mobile when hydrated. A comparatively high content of galactan in CW may be one of the reasons for its high longitudinal shrinkage.

The static stress-strain curve shows three regions (Figure 4.7) the first segment (A_1 to A_2) is almost linear and represents the elastic behaviour, and the overall modulus is attributed to behaviour of the sample without any changes at the molecular level. The second segment (A_2 to A_3) representing the irreversible deformation, results in a loss in stiffness and represents the changes in the amorphous cell wall matrix. In the third segment the tangent of the curve becomes progressively steeper, until complete failure (Navi et al., 1995). The slope of the

first segment is mostly influenced by the MFA. At small MFAs < 20°, the variation in MFA results in significant changes in modulus. But at higher MFAs >40°, the rate of variation of modulus is much smaller and is influenced by the mechanical properties of the matrix. Stress-strain curves in *Pinus taeda* show non-linear behaviour in corewood fibres up to 60% of the load carrying capacity after which the behaviour becomes linear. Outerwood fibres exhibit linear stress-strain curves up to failure (Groom et al., 2002).

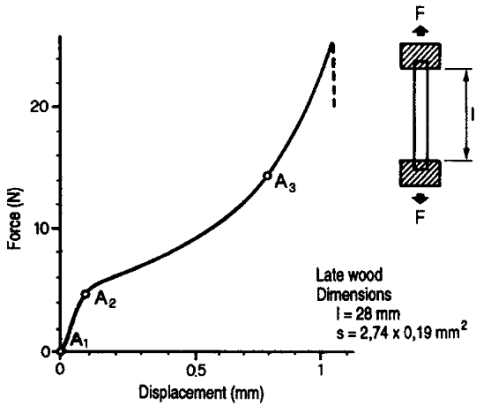

Figure 4.7 Force displacement curve for small wood specimen of *Picea sitchensis* (Navi et al., 1995)

At small MFAs the stress-strain curve of wood suggests elastic behaviour. It is related to the cellulose microfibrils. At high MFAs the stress-strain curve shows plastic deformations which are related to the amorphous mix (Figure 4.8). Low MFAs results in stiff but a rather brittle material whereas high MFA allows an increase in energy absorbing capacity but at the expense of stiffness (Reiterer et al., 2001).

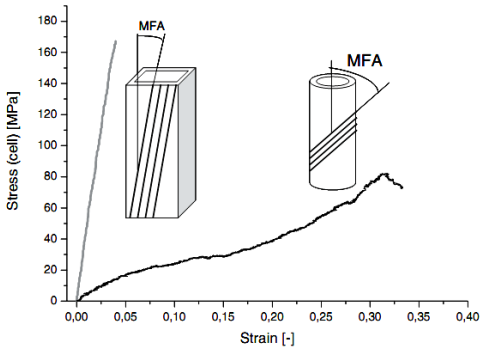

Figure 4.8Comparison of stress strain curves of an early wood (grey line) and a compression wood fibre (black line) of *Picea abies* tested in axial tension in wet condition along with schematic drawing of cell shape and cellulose MFA (Goswami et al., 2008b)

At high microfibril angles where the shear stress easily exceeds the yield stress of the cell wall material, unspecific bonds break allowing viscous flow. This corresponds to deformation beyond the yield point. When stress is released, there is no back flow but a lock-in at the new position and the unspecific bonds re-form immediately in the new positions. In individual cells, this behaviour might be mediated by the hemicelluloses attached to the celluloses (Altaner and Jarvis, 2008; Keckes et al., 2003). Goswami et al. (2008b) compared deformation behaviour of CW and enzymatically modified NW and suggested different deformation mechanisms. In CW high MFA allows gliding of cellulose fibres and the regain of stiffness after removal of load indicated that deformation is mainly mediated by the opening of hydrogen bonds in the matrix, which do not result in substantial damage. On the contrary in the enzymatically modified fiber (where xylans, glucomannans and lignin were removed) the interface between cellulose fibrils and matrix was predamaged. The observed plastic deformation without stiffness recovery was interpreted as a gliding of the cellulose fibrils after fracture events at the fibril/matrix interface. Burgert et al. (2002) reported that mechanically isolated fibres (tracheids) are stronger and stiffer than chemically isolated fibres. In both the cases stress-strain curves depend upon the S2 MFA in the usual way thus indicating the cellulose microfibrils were intact. For chemically isolated fibres the stress-strain curves are uneven, particularly at high MFA. The possible explanation for this is that the acid maceration damaged hemicelluloses attached to the celluloses which resulted in lower shear strength between the microfibrils and as a consequence resulted in a lower strength and stiffness and more uneven stress-strain curves for the entire fiber.

Also at higher moisture content the importance of the matrix in mechanical properties cannot be neglected. Hemicelluloses are the most sensitive constituents of wood to humidity because they are hygroscopic (unlike lignin) and fully accessible (unlike cellulose).

Due to the highly reinforced fiber wall structure with cellulose microfibrils embedded in a cross-linked lignin matrix, only a weak softening is expected as a result of the hemicellulose transition (Olsson and Salmén, 2004). Irvine (1984) has used differential thermal analysis to measure the glass transition temperature of hemicellulose and lignin in *Pinus radiata* and found that *Tg* lowered substantially as the water content increases. The effect of moisture content on properties reflects softening of hemicelluloses, not celluloses (Salmén, 2004). It is well known fact that decreasing moisture content increases *Tg* of amorphous matrix. Water acts as a plasticizer-a monomeric unit added to a polymer to soften it, by lowering its *Tg* and decreasing its stiffness at a given temperature. Olsson and Salmén (2004) reported that

hemicelluloses exhibit a true *Tg* at high humidity at room temperature. Olsson and Salmén (2004) have made DMA measurements on xylan coatings on inert glass braids and found that *Tg* varied from 30°C at 30% water content to 80°C at 15%. Salmén (1984) also reported a tanδ peak at about 100°C at a frequency of 1Hz for water-saturated *Picea abies* which he ascribes to lignin.

The mechanical vibrational energy losses in wood arise due to stress-induced modifications of the hydrogen bonding structure, particularly in hemicelluloses and are moisture sensitive (Entwistle, 2005). Any change in moisture content during the run will alter the structure of hemicelluloses which will be manifested as change in mechanical properties. In order to study change in mechanical properties with temperature and frequency in relation to change at molecular level in hemicelluloses, it is vital that these measurements be made under conditions where the cell wall water content does not change over the measurement temperature range. At constant moisture content such energy losses can be used to deduce the hemicelluloses mix (Entwistle, 2005)

In this chapter samples selected for X-ray diffraction were characterized for tanδ and storage modulus at constant moisture content over a range of temperatures. Our initial intention was to work between 20^{o} and 100^{o}C but the DMA facility place restrictions on both the humidities and temperatures that could be achieved. Tanδ was compared for two wood types (OW and CW) and was correlated to measured properties.

4.5 Material and methodology

From selected families used for X-ray diffraction measurements 100 samples of each wood type were selected for dynamic mechanical analysis.

A 40 x 10 x 1.5 mm (longitudinal x tangential x radial) sample was cut from each specimen for the DMA (Figure 3.7). Samples were conditioned in a humidity control box over calcium nitrate (i.e. at 50% relative humidity) which corresponds to 9% moisture content at 25°C for the wood samples. Samples were weighed before and after each DMA run to monitor any change in moisture content. Density of samples was calculated using mass and dimensions of the sample.

A DMA Q800 with a humidity control chamber from TA Instruments was used for the study. Following recommended practice mentioned in TA manual the single cantilever bending mode was used with 17.5mm distance between the clamping midpoints. Samples were

clamped on their tangential face with clamping torque of ~1Nm. A displacement of amplitude of 15µm was applied at two frequencies (1 and 10 Hz) while the temperature was gradually increased from 10° to 85°C. At the beginning of the run, the relative humidity was maintained at 50% at 10°C for 60 minutes. After that temperature was increased in 5°C steps and with every increase in temperature, humidity was increased correspondingly by 1% to maintain constant moisture content of 9% at high temperatures. Samples were left to equilibrate for 30 minutes at every step.

4.5.1 Statistical analysis

In order to study the effect of wood type the following model in R software was used.

$$Response = \mu + WT + R + FC + TID + e \quad \text{4-19}$$

where μ, and WT are the fixed effects of the overall mean (μ) and wood type (WT), R, FC, TID, and e represent the random effects of replicate, family, tree identity and residuals. The expectation of the response is $E[response] = \mu + WT$ and random effects have zero mean and variances σ_R^2, σ_{FC}^2, σ_{TID}^2 and σ_e^2.

Pearson correlation was also determined independently for two wood types between properties measured using DMA and other wood properties measured in chapter 2 (Dry velocity squared, dynamic modulus, longitudinal shrinkage and volumetric shrinkage) and chapter 3 (T and MFA values) after controlling for family and replicate effect using model Equation 4-19. The significance level used was p=0.01.

The following model with the assumption that the residuals are independent, identically distributed following a normal distribution was used to predict storage modulus using MFA values and density of DMA samples independently in OW and CW

$$SM \sim D + MFA + R + FC + TID + e \quad \text{4-20}$$

Where SM is storage modulus, D is density at 9% moisture content , MFA is microfibril angle and R, FC, TID, and e represent the random effects of replicate, family, tree identity and residuals.

4.6 Results and discussion

The change in sample weight after a DMA run was no more than 0.5%. The variation in storage modulus and tanδ with temperature and frequency for OW is given Figure 4.9.

No *Tg* was observed in temperature range between 10 and 85°C at either of the two frequencies (10 and 1Hz). This is to be expected as previous research (Salmén, 1984) has observed *Tg* in saturated wood only at higher temperatures which were ascribed to lignin. Others (Backman and Lindberg, 2001) observed *Tg* between 40-60° degrees at 33% moisture content (fibre saturation) which was ascribed to hemicelluloses.

In this study, the instrument was not able to maintain a stable humidity at temperatures above 85°C, so only the left hand shoulder of the glass transition peak was observed. Also the time required per sample was very long. This resulted in a less satisfactory outcome. Subsequently it was decided that 100 samples of each wood type should be characterized by DMA only at a single temperature and a single frequency and this information correlated with other experimental data.

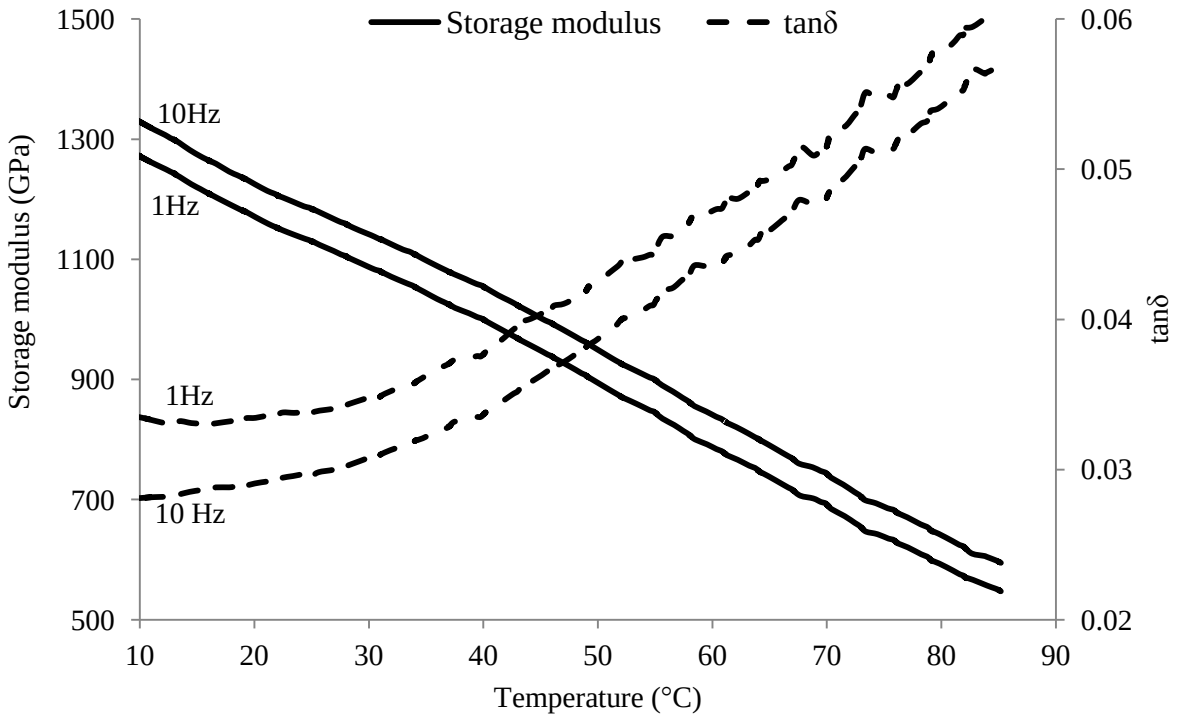

Figure 4.9 Variation in storage modulus and tanδ with temperature and frequency in young *Pinus radiata* opposite wood at 9% moisture content

Storage modulus, tanδ and density values were recorded at 25°C, 50% relative humidity (~9% moisture content) and 1 Hz. The other properties were recorded at room temperature and ~5% moisture content. The estimated means with upper and lower limit at 95% confidence interval after controlling the effect of replicate and family, of measured physical and mechanical properties for CW and OW of young *Pinus radiata* samples are shown in Table 4.1.

The correlation matrices relating all the measured properties for two wood types are presented separately for OW (Table 4.2) and CW (Table 4.3).

Table 4.1 Estimated means and 95% confidence interval of wood properties in opposite wood and compression wood after controlling for the effect of replicate and family in young *Pinus radiata.* Storage modulus and tanδ were measured at 25°C, 1Hz and 9% moisture content as was the wood density

Wood type	Opposite wood			Compression wood		
Variables	Mean	Lower	Upper	Mean	Lower	Upper
Density at 9%MC (kg/m^3)	441	427	456	606	591	620
Storage modulus (GPa)	1.96	1.86	2.06	2.04	1.95	2.16
tanδ	0.028	0.027	0.029	0.026	0.025	0.027
Dry velocity squared $(km/s)^2$	6.89	6.7	7.07	5.66	5.44	5.88
Dynamic modulus (GPa)	2.87	2.78	2.99	3.41	3.29	3.57
Longitudinal shrinkage (%)	1.13	0.98	1.26	3.41	3.28	3.56
Volumetric shrinkage (%)	12.90	12.41	13.29	8.07	7.68	8.55
T (MFA+2σ) (°)	63	62	64	62	61	63
MFA (°)	40	38	40	44	43	45

Table 4.2 Pearson correlation matrix (with *p*-values in parentheses) for wood properties in opposite wood of young *Pinus radiata*

Variable	Density at 9%MC (kg/m^3)	Dynamic modulus (GPa)	Dry velocity squared $(km/s)^2$	Longitudinal shrinkage (%)	Volumetric shrinkage (%)	*T* (MFA+2σ) (°)	MFA (°)
Storage modulus (GPa)	0.75 (<0.01)	0.74 (<0.01)	0.60 (<0.01)	-0.60 (<0.01)	-0.05 (0.62)	-0.45 (<0.01)	-0.40 (<0.01)
tanδ	-0.31 (<0.01)	-0.42 (<0.01)	-0.50 (<0.01)	0.57 (<0.01)	0.08 (0.45)	0.45 (<0.01)	0.50 (<0.01)

Table 4.3 Pearson Correlation matrix (with *p*-values in parentheses) for wood properties in compression wood of young *Pinus radiata*

Variable	Density at 9% MC (kg/m^3)	Dynamic modulus (GPa)	Dry velocity squared $(km/s)^2$	Longitudinal shrinkage (%)	Volumetric shrinkage (%)	*T* (MFA+2σ) (°)	MFA (°)
Storage modulus (GPa)	0.58 (<0.01)	0.60 (<0.01)	0.18 (0.06)	0.09 (0.40)	0.08 (0.42)	-0.21 (0.03)	-0.20 (0.04)
tanδ	0.22 (0.03)	-0.004 (0.96)	-0.24 (0.02)	0.18 (0.08)	0.15 (0.16)	0.01 (0.95)	0.10 (0.31)

Although the storage modulus for CW is some 4% greater than that for OW, when account is taken for differences in density then the normalized storage modulus for OW is roughly 30% greater than that for CW (Figure 4.10), reflecting the much higher density of CW. The same outcome is evident when comparing tanδ values (Figure 4.11). In this chapter these properties have been measured and are compared with other data (MFA, stiffness etc) that were also determined (Tables 4.1,2 &3). Underlying this gathering and comparing of data is the parallel studies at the University of Auckland that examine the wood chemistry of specimens that have been so characterised; work that will be reported elsewhere in due course.

Thus there are two lines of enquiry in wood chemistry that parallel this DMA work. The first considers the percentage and composition of lignin in both OW and CW. The percentage of lignin in CW is ~35%, where as in OW it is ~27.5% (Brennan et al., 2012). Also CW lignin contains a much higher proportion of p-hydroxylphenyl units (H-units) than OW (Brennan et al., 2012; Westermark, 1985). The more highly condensed i.e. cross-linked nature of the lignin in CW results in a more closely packed structure, and thus could lead to low energy absorption capacity. The second line of enquiry focuses on the role of the hemiclluloses and that of the galactans in particular as suggested by work of Floyd (2005) and Newman (2005). Such connections can only be drawn through the use of these UC samples.

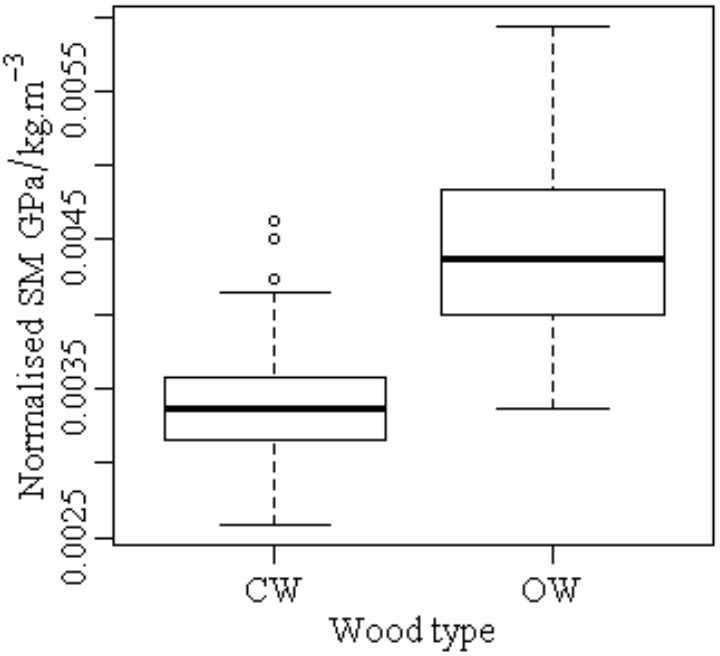

Figure 4.10 Box plot for storage modulus normalised for the density for compression wood and opposite wood of young *Pinus radiata*

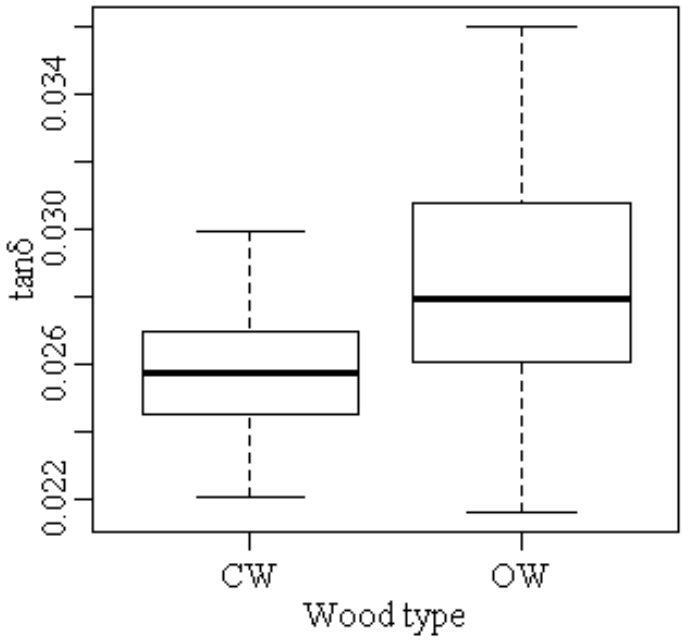

Figure 4.11 Box plot for tanδ for compression wood and opposite wood in young *Pinus radiata*

In OW acoustic velocity squared and *T* values (MFA+2σ) were related to the storage modulus (Table 4.2). In CW, the same properties were not significantly related (Table 4.3). This may be attributed to the fact that the range of MFA values in OW is greater than in CW. The range in MFA in OW was (28°-48°) whereas in CW it was (41°-53°). The correlation was significant between density and storage modulus in CW.

There was a negative correlation between the storage modulus and tanδ in OW implying that stiffer trees have comparatively low damping coefficient. This implies that the tanδ variation is affected not only by changes in chemical composition but also the MFA, which was recognized to play a role in energy absorption capacity of wood samples (Reiterer et al., 1999).

In OW, where range in MFA is comparatively large, there was a significant correlation between MFA (and *T* values) and tanδ. In CW, tanδ did not correlate with any of the measured property.

Storage modulus was slightly lower than dynamic modulus for OW and CW and this could be due partly to difference in moisture content of the samples as storage modulus was measured in the DMA at ~9% moisture content whereas the dynamic modulus was calculated

using WoodSpec at 5% moisture content (Chapter 2), but more likely due to the higher resonant frequencies used with WoodSpec, typically ca 10-20 kHz.

In spite of just a small representation of sample in DMA work the correlation between storage modulus measured by DMA and dynamic MOE measured by acoustics correlate well in OW (Figure 4.12) and thus validates the acoustic method to estimate/rank young trees for their mechanical properties in OW. The comparatively weak correlation in CW could be due to the fact that sample for DMA measurements were pure CW where as the large samples used for acoustic measurements were not homogenous due to intermixing of wood types.

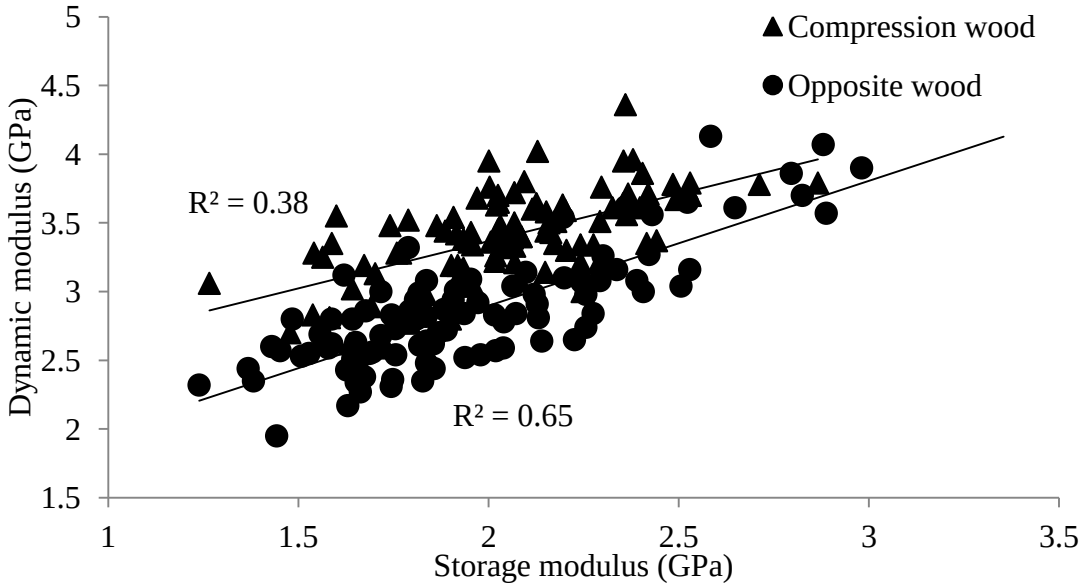

Figure 4.12 Relationship between storage modulus and dynamic modulus in compression wood and opposite wood of young *Pinus radiata*

Density was positively related to storage modulus where as MFA was negatively related to storage modulus. Model Equation 4-20 was used to predict storage modulus using MFA and density independently in CW and OW. The intercept and (standard error) for OW was 1.94 (0.056) and for CW it was 2.06 (0.037). The regression coefficient and (standard error) for density in OW was 0.006 (0.0005) and in CW it was 0.003(0.0003). The regression coefficient and (standard error) for MFA in OW was -0.04 (0.006) and in CW it was -0.032 (0.007). The regression equations for the two wood types are given in Table 4.4. The model explains 84% variation in OW (Figure 4.13) whereas just 57% variation in CW (Figure 4.14)

Table 4.4 Regression equations for opposite and compression wood, where SM stands for storage modulus, D for density at 9% moisture content and MFA stands for microfibril angle.

Wood type	Regression equation
Compression wood	SM=2.06+0.003*D-0.032*MFA
Opposite wood	SM=1.94+0.006*D-0.04*MFA

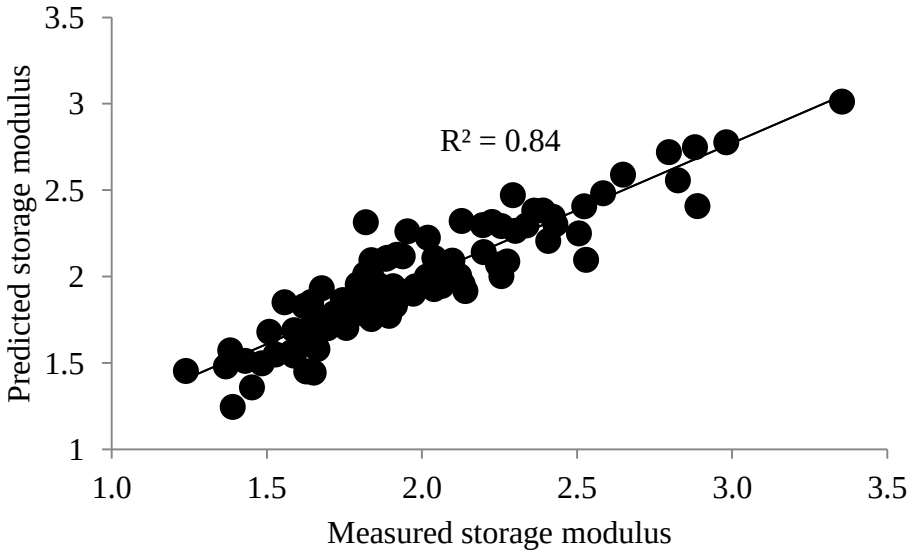

Figure 4.13 Correlation between predicted and measured storage modulus in opposite wood of young *Pinus radiata*

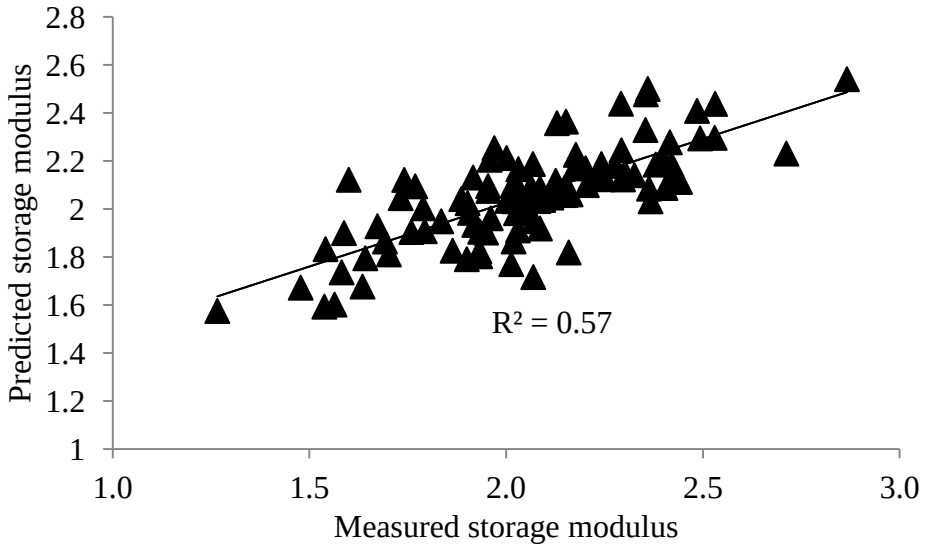

Figure 4.14 Correlation between predicted and measured storage modulus in compression wood of young *Pinus radiata*

The tanδ was significantly but weakly correlated to LS in OW but there was no correlation in CW (Figure 4.15) the reason could the large range in MFA and its influence on both LS and energy absorption capacity (tanδ) in OW.

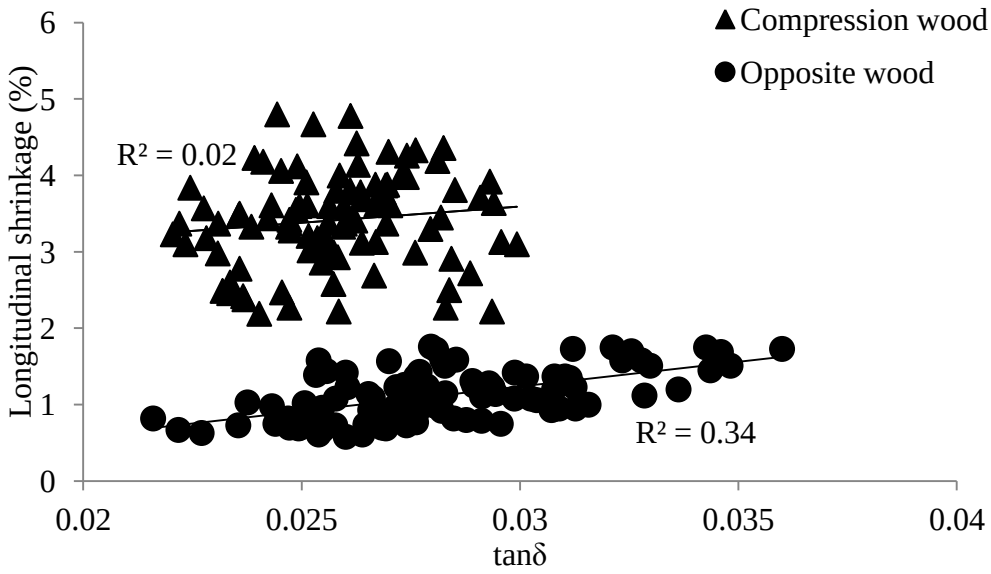

Figure 4.15 Relationship between tanδ and longitudinal shrinkage in compression wood and opposite wood of young *Pinus radiata*

The ranking of families was not done using viscoelastic properties measured using DMA. Firstly there was no additional advantage of introducing tanδ as a screening trait, secondly for few families the sample size was very small.

4.7 Conclusions

- No glass transition was observed in the temperature range 10-85°C at 1 and 10 Hz frequency at 9% moisture content.
- Comparison of data from the DMA (storage modulus and tanδ) correlated with other traditional properties (density, stiffness, MFA). Consequently, there does not appear to be any distinctive advantage in measuring DMA. However, if studies at the University of Auckland reveal a strong correlation between wood constituents (lignin, specific hemicelluloses) this might suggest merit in using the DMA to further characterize wood properties and performance.
- There is no advantage of introducing tanδ at a single temperature as a screening trait.

It is necessary to reiterate that this study used material from the Amberley trial in which the trees were only tilted after one year, and subsequent staking in very dry ground made it impossible to achieve a uniform tilt. Some trees righted themselves and some tilted at an angle to the predetermined direction of lean. Further, it became apparent as the work progressed that the control of the experimental conditions in the DMA was not ideal, therefore the experiments were inconclusive. In practice that is not critical to the broad goals of tree breeding as other tools have shown that trees can be ranked according to key wood properties.

Finally, it should be noted that the inability of the DMA equipment to maintain high humidity has meant that others at Canterbury are developing an alternative torsional system that does maintain constant humidity at high temperatures. This tool will hopefully characterize the *Tg* in wood specimens, but this work is not part of this thesis.

Chapter 5. Early Screening of Hardwood

5.1 Introduction

Worldwide, fast grown eucalypts plantations have been planted for energy and pulpwood. Recently silvicultural regimes have been adapted for solid products (Acosta et al., 2008). For sawn products hardwoods have the advantage of not forming corewood (as traditionally understood), although Panshin and De Zeeuw (1980) note "*As a general rule the low quality of corewood is more marked in conifers than in hardwoods*". Instead, the limitations that restrict their use for structural purposes are a high level of growth stress and a large amount of seemingly randomly-distributed TW. The magnitude of growth stress and its adverse effect on dimensional stability are more pronounced in hardwoods than in softwoods and seems to particularly severe in eucalypts (Dahman, 1975). TW, at least in some hardwoods (McLean et al., 2012) shrinks longitudinally 2-2.5 times more than OW, thus differential shrinkage is another reason for dimensional instability in hardwoods. The present chapter will review growth stress in hardwoods, problems associated with it, and methods to measure growth stress in trees. The purpose of this work is to demonstrate that one can screen for growth stress and other wood quality parameters in very young trees. Here, *Eucalyptus regnans* is used to study variation among trees before age two. It involves a comparative study of two wood types, OW and TW induced by leaning the stems. Correlations between growth stress and measured wood properties like basic density, green dynamic modulus, LS, and VS are also presented.

Again this chapter is not about growth stress, *per se*, it is simply concerned with new approaches to quickly characterise growth stress in very young trees with a view to screening out those individuals or families that display high values.

5.1.1 Growth stresses

By means of active dynamic tensioning of the cellulose microfibrils (Davidson et al., 2004), a tree regulates the reorientation of the stem to alter the crown position in response to environmental conditions (Nicholson, 1973). Growth stress is distinct from gravitationally induced stress and stress associated with the drying of the wood. In general, growth stresses are auto-generated internal stresses which characteristically exist within a solid body even

though no external stress producing force is acting (Kubler, 1987). The longitudinal growth stress in wood originates from a tendency of the active cambial cells to increase in cross-section while simultaneously reducing their length (Archer, 1987; Bamber, 2001; Munch, 1938). Since the contraction is restrained by older cells, the new cells experience a longitudinal tensile stress. In addition, the obstruction of the lateral expansion by adjacent cells leads to tangential compression and a matching growth stress (Kubler, 1987). The longitudinal tension force compresses the adjacent interior layer and reduces the tension in the older cells. The continuous formation of new cells with their growth stresses during tree growth results in an uneven distribution of residual stress across tree stem. The macro cumulative effect of additional wood layers laid down in tension is matched by a cumulative build up of off-setting compressive stresses around the pith. The progressive rebalancing of growth stresses produces a gradient in tensile stress with a maximum at stem periphery decreasing to zero at about one-third of the radius from the periphery, and then a progressively large counterbalancing compressive stress that increases towards the pith (Boyd, 1950b). The steepness of the longitudinal growth stress gradient depends upon the magnitude of growth stress at the periphery and on the log diameter. According to the mathematical expression given by Kubler (1959a), longitudinal strain at any point can be given by

$$\varepsilon_l = \varepsilon_{lp}(1 + 2ln\frac{r}{R}) \qquad 5\text{-}1$$

Where ε_l is the strain at a distance r from the pith, ε_{lp} is the peripheral strain and R is the stem radius. Jacob (1945) measured growth strains in some 200 *Eucalyptus delegatensis* logs and concluded that the peripheral strains remain essentially the same throughout a tree's life. Thus small diameter trees tend to have a steeper gradient of stress as compared to large diameter trees with the same peripheral stress as shown in Figure 5.1.

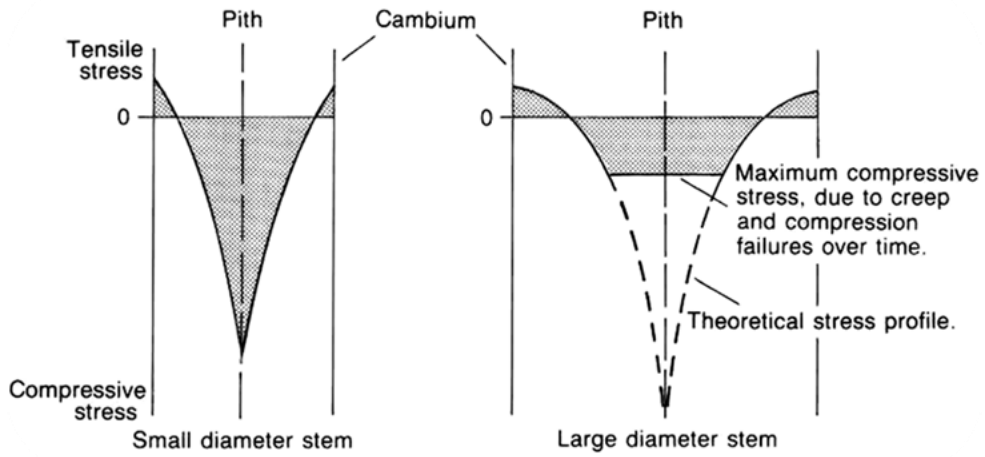

Figure 5.1 Stress distribution in small and large diameter trees (Kubler, 1987)

Initially, the origin of growth stress was explained by two alternative hypotheses "the lignin swelling hypothesis" (Boyd, 1950a) and "the cellulose tension hypothesis" (Bamber, 1979). In the first it was assumed that lignin deposition in between a network of predeposited cellulose microfibrils causes transverse expansion of spirally-wound cellulose within the cell wall and consequently a longitudinal contraction. Watanabe (1967) emphasised that in addition to lignification, the microfibril angle of the middle layer of the secondary wall also plays an important role in the generation of the longitudinal growth stresses. In the second hypothesis it was considered that the force arises from the contraction of cellulose fibrils due to crystallization (a term that was never clearly explained). Both of these hypotheses are incomplete, the first cannot explain high tensile stresses generated in TW where lignin is absent or present in low amounts. The difficulty with the second hypothesis is that crystallization would not result in an axial contraction where the microfibril angle is large. Yamamoto (1998) proposed a "unified hypothesis" in which he combined the two models "lignifications" and "contraction of cellulose microfibrils" and fitted data from *Cryptomeria japonica* using this model. According to this, growth stresses are generated by an interaction of the swelling of the matrix substance induced by a deposition of lignin between the microfibrils and the longitudinal contraction of the cellulose microfibrils during cell wall maturation. The microfibril orientation in the S2 layer (MFA) is one of the most important factor which controls the magnitude and the orientation of the growth stresses in the cell walls.

5.1.2 Growth stresses and defects

Growth stress defects fall into two categories. First, those which develop in living trees: brittleheart and heart checks. The second type develops after cutting a tree and includes end splits and warp of green lumber. The strong circumferential (tangential) compression stresses in the growing wood cause circumferential (tangential) and radial tensile stresses in the tree's inner part. These stresses get stronger and stronger as the tree grows in diameter and are the reason for defects in live trees (Kubler, 1959b). These defects become more prominent in large diameter trees and are not a big concern for trees of small diameter.

"Brittleheart" is the compressive failure parallel to the of cell walls at the centre of the tree (Byrnes and Archer, 1977). In order to counterbalance the large peripheral longitudinal tensile growth stresses during tree growth the compressive stress in the centre of the stem increases until it eventually exceeds the maximum crushing strength parallel to the grain of wood, causing numerous slip planes termed as "brittleheart" (Shield, 1995), see Figure 5.1 (RHS). The affected wood has low impact strength and can break by brash-fracture due to minute compression failures in the walls of the wood fibres. The defect has a very significant effect on the strength and therefore yield of the end product.

Heart checks usually develop in large diameter trees and start from the pith where tangential tension is greatest (Malan and de Villiers, 1976).

Growth strains are about 100 times larger than crown weight compression strains, thus the growth stresses are only slightly different in vertical standing trees and the corresponding stresses in felled trees (Jacobs, 1945). In vertical trees, tensile longitudinal stresses in the periphery are counterbalanced by compressive longitudinal stresses near the pith. When the log is cross-cut, the internal stress balance is altered, the longitudinal growth stresses at the freshly cut end are released and transform into secondary radial and tangential tensile stresses at the cut end. This results in a considerable increase in the tangential stress near the pith (Boyd, 1950c). When tangential stress exceeds the tangential tensile strength of the wood, splits develop on the log end originating from the pith. Depending upon the intensity of the growth stresses, the end splits vary in size, and in the worst cases it can split along the entire length of the log. Saw log recovery can suffer greatly from log end-splits. High growth stress trees are also difficult to process due to the gradient in longitudinal growth stress. When boards are sawn from logs, the re-distribution of residual growth stresses results in distortion (warping of boards as they are cut and the stresses are released). Quarter-sawn (radial

direction as wider face) boards spring and back-sawn (tangential direction as wider face) boards bow (Yang and Waugh, 2001). The gradient is large in small diameter trees thus the distortion is comparatively large in small diameter trees. Thus the effect is more pronounced in logs from a short rotation crop (Haslett, 1988).

Warp in lumber is fundamentally driven either by growth stresses or by differences in shrinkage within the wood as it dries. Warp in green timber occur essentially due to gradient in growth stresses level.

5.1.3 Growth stress measurements

There is no direct method to measure growth stresses in trees or logs. Stress (σ) is defined as the ratio of applied force (F) and cross-section area (A), i.e. F/A. When a force is applied to a body deformation occurs. Tensile stresses lead to an elongation whereas compressive stresses lead to a contraction. The deformation is measured in terms of strain (ε) which is the ratio of change in length (δl) and original length (l). Within the elastic limit according to Hook's law strain (ε) is proportional to stress (σ) and is given by

$$\sigma = E\varepsilon \qquad 5\text{-}2$$

where E is the proportionality constant known as modulus of elasticity (MOE).

In most of the techniques (Archer, 1978; Kikata, 1972; Nicholson, 1971) stress is measured indirectly by measuring strain resulting from the release of stress. It is derived from the strain and MOE. At the periphery (immediately under the bark) growth stresses are usually tensile so their release causes a decrease in length, and near the pith due to the release of compressive stresses there is an increase in length. Although the strain associated with growth stress can be very small, it can be measured directly by a strain gauge. Most of the techniques involve cutting the xylem and recording the longitudinal strain that is induced as the stress is relieved. Different techniques differ in the way the stress is released and the way the amount of longitudinal strain is measured. Yang et al. (2005) reviewed these techniques along with their advantages and disadvantages. The "standard" method used to measure longitudinal strain in standing trees uses strain gauges. The resistance gauges are connected to a strain meter and are glued on debarked xylem. Cuts are made at equidistance points from the gauge; one above and one below to release the stress. The strain measurements are noted from the strain meter. The strain values themselves are useful in predicting the stability of timber. Bow distortion on sawing could be predicted from the longitudinal growth strain

(LGS) measurements in 4 years old *Eucalyptus pilularis* (Muneri and Leggate, 2000). High LGS and log end-splitting were significant indicators of increased board end splitting (Okuyama et al., 2004; Valencia et al., 2011)

The strain gauges are expensive and there are delays due to the time needed for the glue to cure and bond the gauge to the stem. Therefore, they are not suitable for screening very large populations. A totally different method has been developed by Chauhan (2008) in which longitudinal growth strains are assessed when splitting small diameter trees. On splitting, the magnitude of bending in two half-rounds is a function of longitudinal growth strain, log diameter, and log length (Chauhan, 2008). Chauhan and Entwistle (2010) related the outward bending of a split semicircular beam to the surface growth strain as follows

$$Y = \frac{0.87\varepsilon L^2}{R} \qquad 5\text{-}3$$

Where Y is the deflection of split half semicircular beam from the centre, L is the length of the sample and R is the radius. The correlation (R^2) between the estimated strain from the opening as the stem is cut along the grain and the average of strain measured using strain gauges on either side of splitting was found to be 0.92 (Chauhan, 2008). This is a destructive test but is a rapid, cost-effective technique when utilised to screen large numbers of young trees.

Some authors have studied relationships between growth stresses and physical, mechanical, and chemical properties of trees to develop indirect but simpler methods to assess growth stresses. The results vary from one particular study to another and also vary between species. Boyd (1980) studied the correlations between different properties and reported significant within-tree correlations between growth strain and microfibril angle for all NW and TW tissue in straight and reorienting *Eucalyptus regnans* trees. But there was no correlation between radial growth rate and strain. He also reported a correlation between density and growth strain but only in reorienting trees. Chafe (1990) reported a correlation between density and strain in nominally vertical *Eucalyptus regnans* but there was no such relationship in *Eucalyptus nitens*. The growth strain was not related to MOE in both species. Yang and Ilic (2003) reported a significant but weak correlation between growth strain and density and no correlation between strain and MOE in *Eucalyptus globulus*. There was no correlation of strain either with wood density or MOE in *Eucalyptus cloeziana* (Muneri et al., 1999), *Eucalyptus nitens* (Chauhan and Walker, 2004), and *Eucalyptus tereticornis* (Chauhan

and Aggarwal, 2011). However, growth stress correlated positively to VS (Chauhan and Walker, 2004). High growth stresses are also related to the occurrence of TW found on the upper side of leaning trees whether with or without gelatinous fibres. Growth stress increased with decreasing MFA and with an increase in crystallinity and α-cellulose content (Okuyama et al., 1994). In terms of growth stress, a distinction cannot be made between TW and strongly stressed NW. Thus in young trees the randomly distributed TW creates uncertainties in characterising NW properties unless it is measured around the circumference of the stem.

5.1.4 Tension wood

In hardwoods, reaction wood is termed as TW and is formed on the upper side in leaning trees. However, it is not just confined to leaning trees. Young vertical and dominant trees also have large amounts of seemingly randomly distributed TW (Washusen and Ilic, 2001). TW is characterised by a reduction in frequency and size of vessels and by an increase in the proportion of fibres (Côté et al., 1969). Fibres in TW differ in structure and composition from those in NW. They are characterised by a thick cell wall, which sometimes contains a tertiary layer as a part of the secondary layer or addition to the secondary layer (Wardrop and Dadswell, 1955). It is termed as the gelatinous layer (G-layer) due to its unusual refractive appearance. There is a lot of variation among species; out of 346 Japanese hardwood species surveyed, the G-layer was found only in 137 (Onaka, 1949). Clair et al. (2006) did not detect a G-layer in 13 out of 21 rain forest species. Even within a same genra some species have a prominent G-layer e.g. *E. regnans* (Wardrop and Dadswell, 1948), while another like *E. nitens* (Qiu et al., 2008) does not have a G-layer. The G-layer consists of almost pure cellulose organized in fibril aggregates, 30-40nm in diameter and these are associated with a few percent of galactan and glucomanan (Timell, 1967). The G-layer is considered to be unlignified (Norberg and Meier, 1966; Wardrop and Dadswell, 1955), but in recent studies (Joseleau et al., 2004; Lehringer et al., 2008) traces of syringyl units of lignin have been found in the G-layer. The average MFA in the G-layer is 5° whereas in the S2 layer of normal, matching wood, it is 18° (Wardrop and Dadswell, 1955). TW without a G-layer is characterised by a low MFA, a low lignin content and increased cellulose content (Yoshida et al., 2002; Yoshizawa et al., 2000). TW is characterised by high longitudinal (Wardrop and Dadswell, 1955; 1948) and transverse shrinkage (Washusen and Ilic, 2001).

5.1.5 Variation in growth stresses

The intensity of growth stress is highly variable between species, between trees of the same species, at different location around a common circumference and at different heights in the same tree.

There is a large variation among trees. In *Eucalyptus regnans*, the highest observed growth strain value is three times the lowest observed value (Nicholson, 1973). Nicholson et al. (1975) measured strain in straight and leant 32 years old *Eucalyptus regnans* at 20 equally spaced positions around the periphery and reported a maximum coefficient of variation of 38% for straight trees whereas it was 100% for bent trees. Raymond et al. (2004) also demonstrated large variations in strain up the stem and around the circumference in individual trees of *Eucalyptus globulus*. In contrasts Nicholson (1973) studied growth stress variation in *Eucalyptus regnans* and reported that the mean level of longitudinal growth stress on the tree periphery appears to vary independently of both rate of tree growth and environmental factors such as wind exposure, stand density, site and elevation.

A recent study of 81 22-year-old *Eucalyptus nitens* trees suggested that longitudinal growth strain (LGS) is not significantly affected either by thinning treatment or tree diameter but is significantly higher in the direction of the prevailing wind (Valencia et al., 2011). Malan (1988) reported no significant effect of growth rate and crown characteristic on growth stress level in *Eucalyptus grandis* and concluded that the silvicultural practices do not appear to be an effective tool for reducing the level of growth stresses.

Growth stresses are under genetic control and heritable. There is a large variation in stress level among trees (Muneri et al., 2000; Nicholson, 1973) and so there are possibilities for breeding for low growth stress levels (Murphy et al., 2005).

5.2 Material and methodology

Eighty-seven seedlings of *Eucalyptus regnans* of unknown genetic origin were planted in September 2008 in 100 litre planter bags containing potting mix and slow release fertilized and drip irrigated. The planter bags were set out at 1meter intervals in a square array set on permeable polythene matting in an open area. This procedure insured uniformity in conditions that minimizes the effect of environmental noise on growth and wood quality. Three months after planting, the trees were tilted and tied at a 30° angle to the vertical and

were tied to garden stake to maintain the stem lean. The trees were harvested in September 2010.

All the trees were measured for height and collar diameter along and across the lean before harvesting. A 300mm bolt was taken from the base of the trees and after debarking its diameter was measured along and across the lean at the larger end (base) and along the lean the distance was measured from the pith in both the direction to measure the radius of opposite wood and tension wood. Diameter along the lean was also measured at 125mm and 250mm from the base. Acoustic velocity was also measured in 300mm bolt using WoodSpec.

KYOWA 120-ohm strain gauges with a gauge factor of 2.05 were glued, at a distance of 125mm from the larger diameter end, to the xylem surface lengthwise on either side (above and below) of the stem in the direction of lean using a cynoacrylate-based adhesive. The upper side corresponded to TW and the lower side to OW. The gauges were connected to a strain meter. After the initial measurements were made, the bolt was split in two halves along its length using a thin blade (1mm thick) band-saw. A 250 mm slit was made through the pith; beginning at the larger diameter opened an internal face that was aligned perpendicular to the direction of lean (confining TW to one half-round section and OW to the other half-round). Immediately after splitting, final strain measurements were recorded. Splitting causes an outward bending of the two semicircular halves and from this the growth strain can be predicted (Chauhan and Entwistle, 2010). The total opening (Y_0) was measured using calipers and average strain (ε_{avg}) was estimated using the following equation

$$\epsilon_{avg} = \frac{0.5\, Y_0 D_{avg}}{1.74\, L^2} \qquad 5\text{-}4$$

Where D_{avg} is the average of under bark stem diameter taken at 0mm, 125mm and 250mm from the base (large end), Y_0 is the distance between inner edges of the two semi circular half rounds (twice of Y mentioned in Equation 5-3); L is the split length as shown in Figure 5.2.

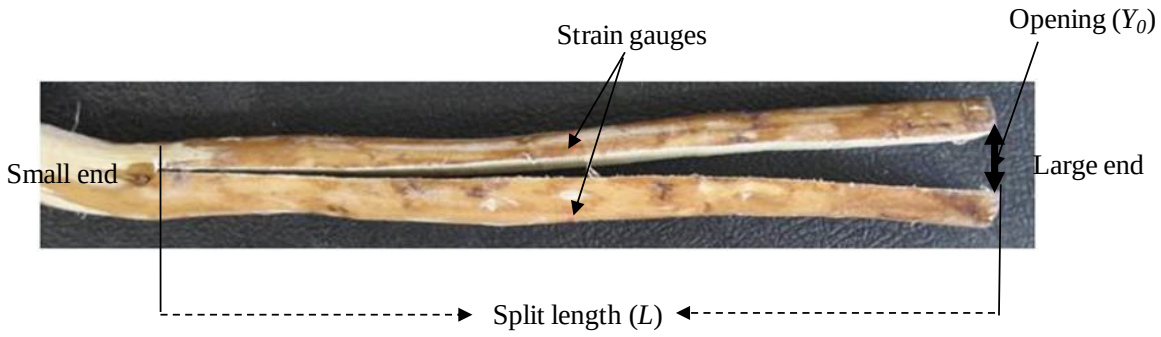

Figure 5.2 Diagram representing the different parameters used to measure strain in a spilt log

From the larger diameter end (base) of the split stem, two adjacent 100mm long samples were cut to provide replicates of OW and TW per stem. The samples were dried in an oven at 35°C until constant weight corresponded to ~5% moisture content was achieved. This was taken as "oven-dry" although that should strictly be at 0% moisture content. This drying schedule was preferred to avoid thermal degradation of the hemicelluloses at 105°C as the dried wood would be subject to chemical studies at the University of Auckland. The two wood types, TW and OW were characterised independently for green dynamic modulus, density, LS, and VS using methods described in chapter 2.

Once mechanical properties had been determined and analysed, the observed range in LS values of the opposite wood were used to select 18 samples from the population that represented that range, and from these samples specimens were taken from the opposite wood to examine in the X-ray diffractometer to see if there is a correlation between LS and MFA.

Tension wood was not examined as there was no interest is selecting wood on the basis of TW properties.

5.2.1 Statistical analysis

Statistical software R was used for data analysis. The whole stem data was presented in terms of mean, coefficient of variation along with minimum and maximum values. The significance of the effect of wood type in describing difference in the measured growth strain, acoustic velocity squared, basic density, longitudinal and volumetric shrinkage was investigated by paired t -test, using the linear model given in Equation 2-14. It was assumed that the residuals are identical and independently normally distributed with zero mean and variance σ_e^2.

$$y = \mu + WT + e \qquad 5\text{-}5$$

Where y is the wood property μ is the overall mean, WT is the effect of the wood type (opposite wood and tension wood) and e in the residual error. The Pearson correlation between wood properties and estimated strain in whole stem and correlation between wood properties and measured growth strain independently in two wood types was analysed. In addition, the Pearson correlation was also analysed between wood properties independently in opposite wood and tension wood.

5.3 Results and discussion

The summary statistics of stem characteristics are given in Table 5.1. A tree height varies from 1.3m to 2.5m with a tree mean height of 1.79m. Diametric growth also varies significantly with a nearly two-fold difference between the smallest and largest stems. The stem diameter asymmetry (eccentricity) index (DAI) is defined as the ratio of the along-lean to the across-lean diameters. Out of 87 trees, 30 trees displayed eccentricity in diametric growth with an average DAI of 0.89, ranging from 0.77 to 0.94, with along the lean diameter being smaller than that recorded transverse to the direction of stem lean. In 24 trees along lean diameter was larger, with an average DAI of 1.12, ranging from 1.05 to 1.25. The rest of the trees were almost cylindrical with average DAI of 1, ranging from 0.95 to 1.04. The pith was also eccentric with the OW radius being larger in 70 trees. The ratio of OW to TW radius is defined as pith eccentric index (PEI). The average PEI was 1.27, ranging from 0.77 to 3.

Table 5.1 Summary statistics of whole stem characteristics for 2-year-old *Eucalyptus regnans* (number of trees=87)

Variable	Mean	CV (%)	Minimum	Maximum
Height (m)	1.79	12	1.30	2.50
Along lean diameter (mm)	25.8	16	19.4	39
Across lean diameter (mm)	26.2	14	17.8	36.6
Diameter asymmetry index	0.99	10	0.77	1.24
Green acoustic velocity^2 (km/s)^2	5.85	16	3.65	7.62
Average longitudinal growth strain (με)	1136	37	423	2240
Opposite wood radius (mm)	14	23	8.64	24.9
Tension wood radius (mm)	11.2	21	0.5	16.3
Pith eccentric index	1.23	27	0.67	2.7

The average acoustic velocity squared (from WoodSpec) for the stem was 5.85(km/s)^2, corresponding to a wood stiffness of 6.38GPa (using a green density of 1100kg/m^3). The average longitudinal growth strain estimated from log splitting was 1136με. The growth strains were highly variable, with a coefficient of variation 37%. The highest estimated strain was five times higher than the lowest estimated strain.

5.3.1 Comparison of opposite wood and tension wood properties

Strain was measured using strain gauges in 48 samples during sawing. Out of 48 samples, for 40 the strains on the OW side were significantly higher compared to those on the TW side. The average TW strain was 612με while the OW strain was 1530με (Table 5.2).

Wood properties measured in small samples extracted from the upper side (TW) and the lower side (OW) of the leaning stems, are shown in Table 5.2.

The wood properties differ significantly in the two wood types. Though the difference in longitudinal shrinkage between TW and OW was significant but was very small. The difference in longitudinal shrinkage in wood types lies between 0.04 and 0.21% with the mean difference of 0.13%. Given in Figure 5.3 are the box plots for wood properties by wood type.

Table 5.2 Wood properties of opposite and tension wood in young *Eucalyptus regnans* (number of samples of each wood type=87)

Variable	Opposite wood				Tension wood			
	Mean	CV (%)	Min	Max	Mean	CV (%)	Min	Max
Green moisture content (%)	149	8.52	112	187	101	9.69	86	141
Green density (kg/m^3)	1101	3.29	967	1144	1163	2.23	1066	1210
Basic density (kg/m^3)	443	5.18	387	527	579	5.85	472	642
Green acoustic velocity $^2(km/s)^2$	2.91	24	1.08	6	8.74	15	2.68	11.28
Green dynamic modulus (GPa)	3.23	25.51	1.91	6.70	10.27	13.72	6.60	13.5
Strain* (μm)	1530	44.26	295	3385	613	75.65	-370	1504
Longitudinal shrinkage (%)	0.86	28.10	0.22	1.39	0.77	30.56	0.10	1.5
Volumetric shrinkage (%)	14.5	16.9	9.31	20.65	32.3	15.81	19.6	48.3

**for 48 samples in each wood type*

Green moisture content was nearly 50% higher in OW than in TW, whereas green density was 5% higher in TW. The green dynamic modulus of TW was three times higher than in OW. Basic density of TW side was 30% greater than that of OW. The LS was 11% higher in OW than in TW. The VS in TW was twice as high as in opposite wood.

The coefficient of variation was highest for the measured strain in both wood types. The order of variation was the same for the two wood types, strain, LS followed by MOE, then green acoustic velocity squared, VS and, finally, basic density with least variation.

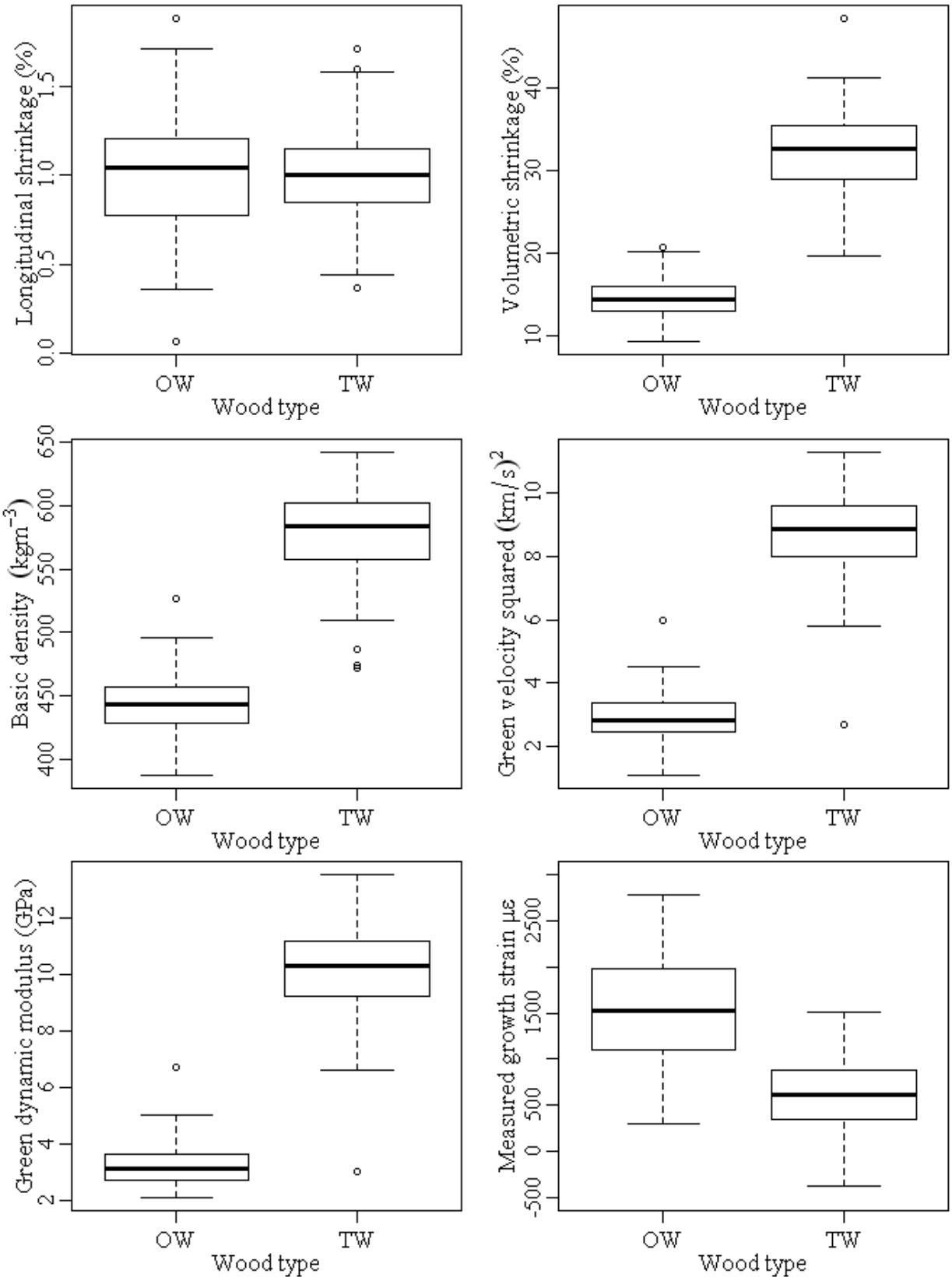

Figure 5.3 Box plots for longitudinal shrinkage, volumetric shrinkage, basic density, green acoustic velocity squared, measured growth strain, and green dynamic modulus of opposite wood and tension wood in young *Eucalyptus regnans*

5.3.2 Relationship between calculated and measured growth strain

The averaged growth strain measured using strain gauges on either side of the lean was well correlated to calculated strain derived from splitting the log (Figure 5.4). The average ratio of calculated to measured strain was 1.08 with a range of 0.78 to 1.44.

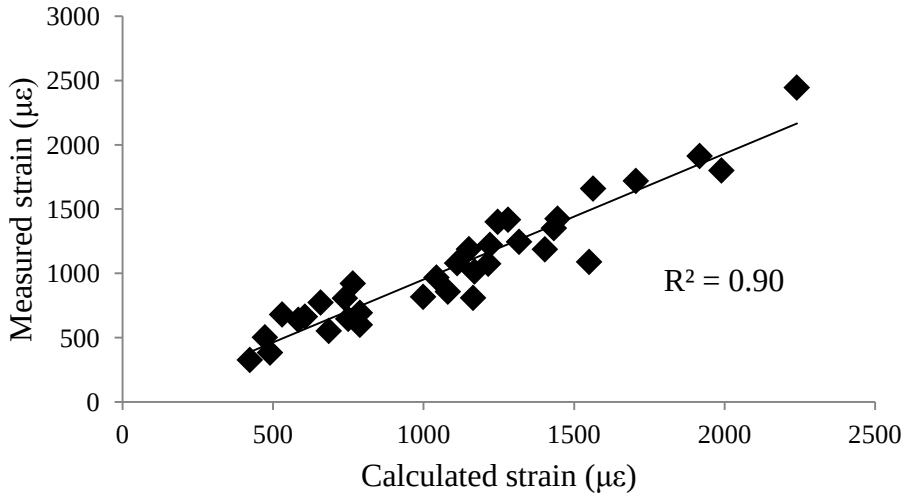

Figure 5.4 Calculated versus measured growth strain in young *Eucalyptus regnans*

Pearson correlation coefficients of growth strains with other measured whole stem traits are given in Table 5.3. DAI and acoustic velocity was positively correlated to estimated growth strain. Independently measured strain values in OW and TW side did not correlated to any of the independently measured properties in the two wood types (Table 5.4).

Table 5.3 Pearson correlation coefficients (with *p*-values in parentheses) for estimated growth strain with stem properties in young *Eucalyptus regnans* (number of stems=48)

Stem height (mm)	Collar diameter (mm)	DAI	Stem acoustic velocity^2 (km/s)^2	PEI
0.25	0.24	0.49	0.43	0.35
(0.10)	(0.11)	(<0.01)	(<0.01)	(0.02)

Table 5.4 Pearson correlation coefficients (with *p*-values in parentheses) for measured growth strain with wood properties independently in two wood types in young *Eucalyptus regnans* (48 number of samples with two gauges on either side of the stem)

	Basic density (kg/m^3)	Green acoustic velocity^2 $(km/s)^2$	Green dynamic modulus (GPa)	Longitudinal shrinkage (%)	Volumetric shrinkage (%)
Opposite wood	-0.08 (0.54)	0.04 (0.77)	0.04 (0.78)	-0.05 (0.73)	-0.36 (0.01)
Tension wood	0.11 (0.43)	0.15 (0.31)	0.13 (0.38)	-0.23 (0.11)	0.09 (0.52)

5.3.3 Interrelationship between wood properties

Pearson correlation coefficients of measured wood properties in OW and TW are given in Table 5.5 and Table 5.6.

Table 5.5 Pearson correlation coefficients (with *p*-values in parentheses) for wood properties in opposite wood of young *Eucalyptus regnans* (number of samples=87)

Variable	Green acoustic velocity^2 $(km/s)^2$	Green dynamic modulus (GPa)	Longitudinal shrinkage (%)	Volumetric shrinkage (%)
Basic density (kg/m^3)	0.51 (<0.01)	0.59 (<0.01)	-0.41 (<0.01)	0.02 (0.85)
Green acoustic velocity^2 $(km/s)^2$		0.98 (<0.01)	-0.65 (<0.01)	-0.07 (0.56)
Green dynamic modulus (GPa)			-0.66 (<0.01)	0.06 (0.58)
Longitudinal shrinkage (%)				0.05 (0.68)

In OW both basic density and green acoustic velocity squared were negatively correlated to LS. In contrast, in TW, LS exhibited a positive association with density, and no correlation with acoustic velocity. In opposite wood, VS did not correlate with any other property. In TW, VS showed a positive correlation with all the measured wood properties.

The two wood types, TW and OW, behave independently in each tree, as there was no correlation between wood properties (Table 5.7).

Table 5.6 Pearson correlation coefficients (with *p*-values in parentheses) for wood properties in tension wood of young *Eucalyptus regnans* (number of samples=87)

Variable	Green acoustic velocity^2 $(km/s)^2$	Green dynamic modulus (GPa)	Longitudinal shrinkage (%)	Volumetric shrinkage (%)
Basic density(kg/m^3)	0.51 (<0.01)	0.57 (<0.01)	0.42 (<0.01)	0.56 (<0.01)
Green acoustic velocity^2 $(km/s)^2$		0.99 (<0.01)	0.09 (0.44)	0.32 (<0.01)
Green dynamic modulus (GPa)			0.11 (0.32)	0.34 (<0.01)
Longitudinal shrinkage (%)				0.57 (<0.01)

Table 5.7 Pearson correlation coefficients (with *p*-values in parentheses) for wood properties between opposite and tension wood in young *Eucalyptus regnans* (number of samples of each wood type =87).

Variable	Basic density (kg/m^3)	Green acoustic velocity^2 (km/s)	Green dynamic modulus (GPa)	Longitudinal shrinkage (%)	Volumetric shrinkage (%)
	0.21 (0.04)	0.14 (0.26)	-0.08 (0.46)	-0.12 (0.29)	-0.04 (0.71)

Reaction wood formation in leaning trees is often associated with eccentric growth (Sinnott, 1952), with the thickening of the growth layer on the reaction wood side and reduced radial growth on the OW side (Yamashita et al., 2007). The results in this study are not in accordance with the previous statement. For 81% of the trees, the pith was towards the reaction wood side with large radial growth in opposite wood. Also, surprisingly, for 76% of the trees, the DAI, was either less or equal to unity. There was however a positive correlation found between DAI and estimated growth strain values (Table 5.3).

Calculated growth strain, from the opening on splitting along the stem in response to the cumulative effect of stress relaxation on the TW and OW sides, differed significantly among trees. It was found to vary between 423 and 2240με in stems with identical lean, suggesting a different response by individual trees to leaning. The positive correlation between acoustic velocity and estimated growth strain is in accordance with the fact that MFA has been shown to be negatively correlated to growth strain (Yoshida et al., 2002), particularly for TW with low MFAs that was associated with large growth strain.

Individual measurement on either side of the lean differed significantly, with higher strain values on the OW side in 83% of the trees and even compressive stresses on the TW side in 5 trees. The large difference in the surface strain on either side of the lean generates an internal bending moment that bends the stem to regain its vertical orientation (Yoshida et al., 2000). The results are not in accordance with previous studies, which showed that the strain was significantly greater in the upper side (TW) than underside (OW) in leaning stems. In previous studies, (Clair et al., 2003; Kuo-Huang et al., 2007) a large difference was reported but with greater tensile stress on the TW side and lower or even compressive stress, on the OW side. Large tensile growth strains are good indicator of the presence of gelatinous fibres in wood tissue taken from the immediate position, where growth strain was measured in *Eucalyptus globulus* (Washusen et al., 2003). All the previous studies were done on large trees whereas present study was done on leant 2 years old trees. Also the distribution pattern of TW changes with time as the lean angle changes through the self-righting mechanism. As shown by Coutand et al. (2007) in tilted young popular (hybrid of *Populus deltoides* and *Populus nigra*) TW sectors were produced all along the trunk on the upper side but at distal cross-sections, reaction wood was no longer produced on the upper side, but a second segment of TW was produced on the initially lower side (Figure 5.5). Although the samples were shorter in the present study as compared to above mentioned example (Figure 5.5), the systematic differences in TW distribution along the length of the sample were noted. In the present study the samples for physical and mechanical measurements were taken from the base of the 300mm, bolt but the strain was measured at the 125mm from the base. Thus it could be possible that at the point of the strain measurement has different TW distribution than at the base of the tree which was assessed in all other measurements. Possibly the observations in the present experiment were not appropriately located to highlight the major factor influencing the properties along the length on either side of the lean.

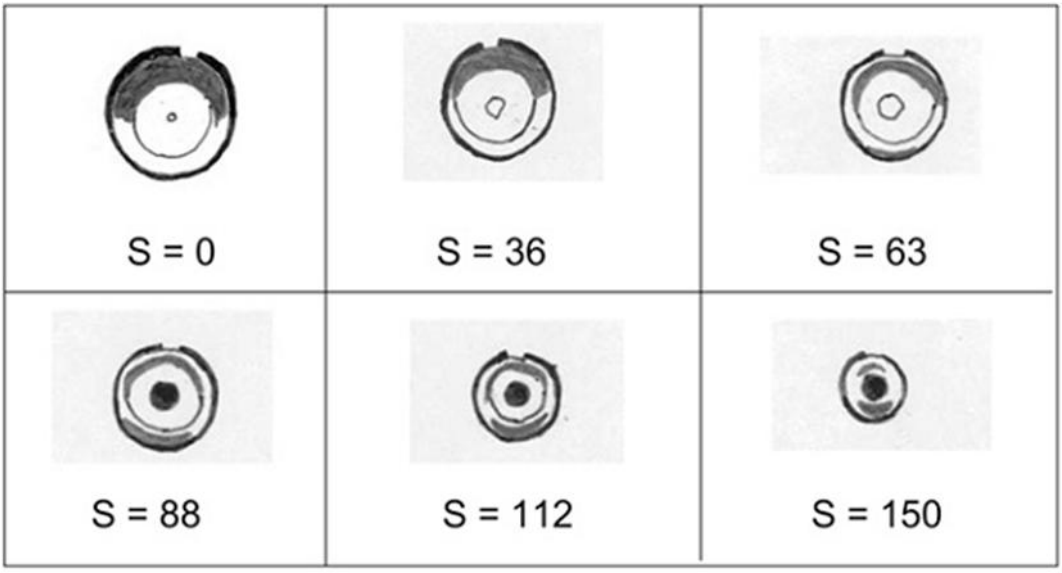

Figure 5.5 Typical cartography of tension wood sectors along a trunk 3 months after tilting. Bark and pith appear in black, tension wood sectors are in grey. The notch in the bark marks the original upper face of the trunk after the tilting. Locations of the cross sections along the stems are given on each subfigure, where number corresponds to distance from the base (S) in centimetres (Coutand et al., 2007)

The difference in basic density of OW and TW can be attributed to thickening of the cell wall fibres with a gelatinous layer (Tsoumis, 1991). The basic density is negatively correlated to vessel proportion (Ferrand, 1982), and increase in the fiber proportion implies more wall by volume in wood (Jourez et al., 2001b). TW has comparatively lower percentage of vessels and higher proportion of fibres (Jourez et al., 2001a). Thus it could be another reason for high basic density in TW.

Green acoustic velocity in TW was 74% higher than in OW. Correspondingly, the dynamic modulus of elasticity of TW was three times higher than that of OW. The results are in accordance with the fact that the MFA in *Eucalyptus regnans* in TW is as low as 5° but comparatively high in OW S2 layer (Wardrop and Dadswell, 1955), e.g. around 20-39°.

The two wood types differ significantly in LS. OW exhibited 10% higher LS than in TW. These results contrast with reported shrinkage behaviour in OW and TW. In general, TW is reported to exhibit higher LS as compared with OW (Boyd, 1977; Clair and Thibaut, 2001; Jourez et al., 2001b; Wardrop and Well, 1948). However, most of the reported results are for wood from much older trees, in which the MFA in the OW would be expected to be lower than in the ~2 year-old wood examined in this study. Comparatively high LS in OW may be

due to the juvenile nature of OW which is characterised by high MFA. The MFA was measured in 18 samples in OW (procedure as described in chapter 3). The MFA ranges from 20° to 39° in OW, with the average MFA of 29°. The MFA values were well correlated to LS in OW (Figure 5.6). Acoustic velocity squared could be used as indirect method to measure MFA as there was good correlation between MFA and acoustic velocity squared (Figure 5.7) in spite of the fact that MFA was measured only in small section of sample used for acoustic velocity measurement.

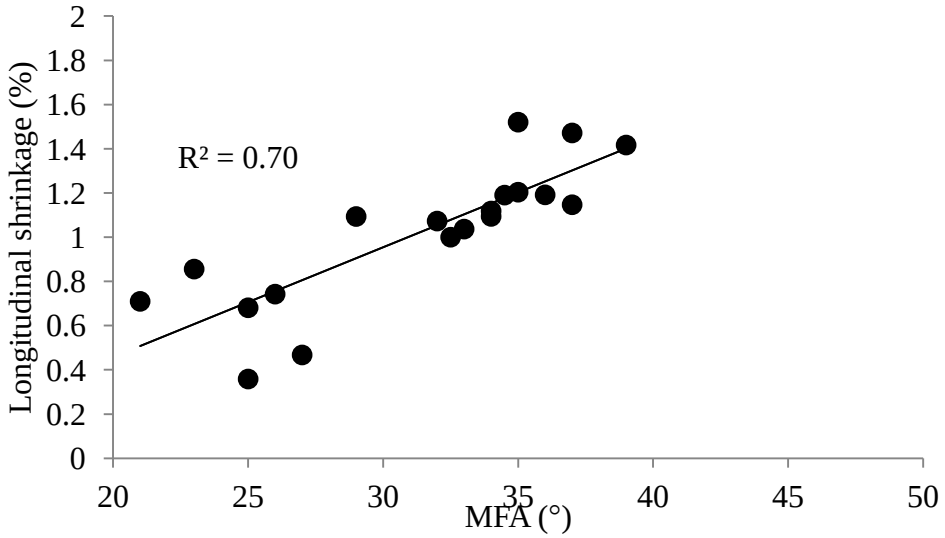

.

Figure 5.6 Correlation between longitudinal shrinkage and MFA in opposite wood of young *Eucalyptus regnans*

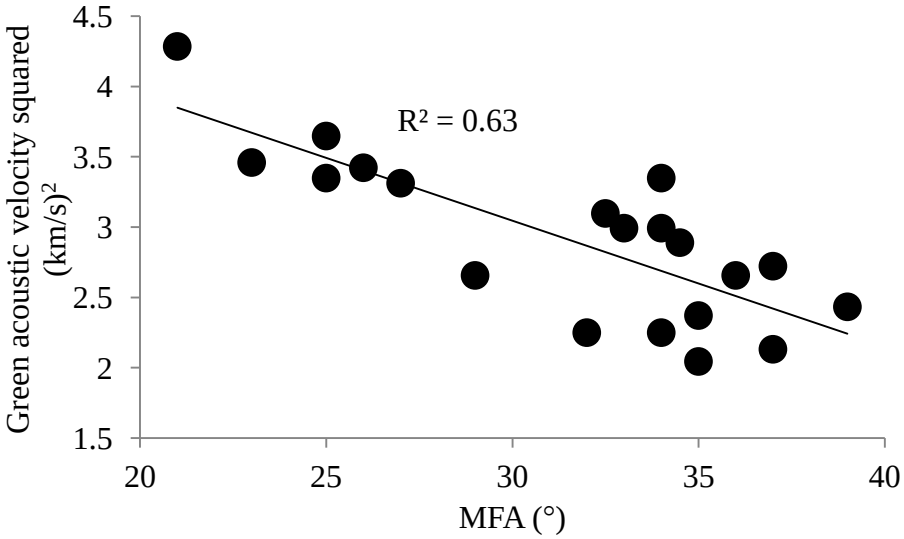

Figure 5.7 Correlation between green acoustic velocity squared and MFA in opposite wood of young *Eucalyptus regnans*

Despite of the very low MFA in the G-layer of TW, the LS with an average value of 0.78 % was practically significant. Thus in TW another factor is dominant. Different authors have diverse views regarding LS in TW. Some (Norberg and Meier, 1966) attribute it to the S1 and or S2 layer with relatively high MFA, while others (Clair and Thibaut, 2001) assume the G-layer is the main driving force for high LS in TW. Goswami et al. (2008a) proposed that the stresses developed from radial swelling of the G-layer are transformed into a longitudinal contraction of the S2 layer of the cell wall and thereby the fibre. Also the MFA in the cell wall adjacent to G-layer is comparatively high (36°) in TW. Thus, it is the interaction of the G-layer with the surrounding cell wall that produces a stiff composite structure with noticeable longitudinal contractibility (Goswami et al., 2008a). *E. regnans* has a prominent G-layer (Beckar, 2011; Chafe, 1977).

The VS in TW was high compared with that in OW. According to Wardrop and Dadswell (1955), there is high VS in TW, particularly when a thick gelatinous layer is present. Firstly due to the hygroscopic nature of the unlignified layer that undergoes large dimensional changes on drying. Manwiller (1967) also proposed that the lack of lignin in the paracrystalline sheath surrounding the microfibrils gives less obstruction for the component molecules to bond on drying. Secondly, due to the absence of the S3 layer (with high MFA), there is less restraint from the inner cell wall, and this allows the cell wall to collapse into the cell lumen.

The relationships in wood properties were different for OW and TW. However the green acoustic velocity is positively correlated to basic density in both wood types and the results are in accordance to previously reported results in straight *Eucalyptus dunnii* trees (Dickson et al., 2003). The strong negative association of LS with green acoustic velocity squared in OW (Figure 5.8) could be attributed to differences in MFA between trees. No relationship between LS and green acoustic velocity squared is observed for TW which could be due to small variation in MFA in TW.

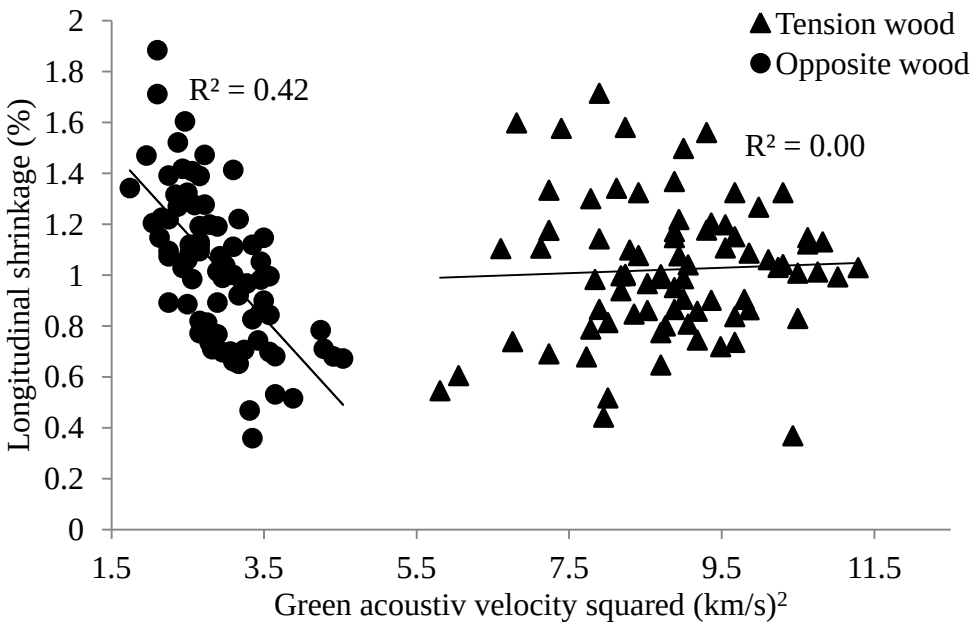

Figure 5.8 Relationship between longitudinal shrinkage and green acoustic velocity squared in young *Eucalyptus regnans*

The relationship between basic density and LS was in accordance with earlier work, where a negative correlation between basic density and LS in OW (Timell, 1986) but a positive correlation in TW (Jourez et al., 2001b) was reported. In the present study, a significant negative correlation in OW between basic density and LS, and significant positive correlation in TW was observed. In TW, basic density was positively correlated to VS, but such a relationship was missing in OW (Figure 5.9). The positive relationship in TW could be linked to the severity and proportion of TW fibres, as both density and transverse shrinkage tend to increase with severity and proportion of TW (Washusen, 2000).

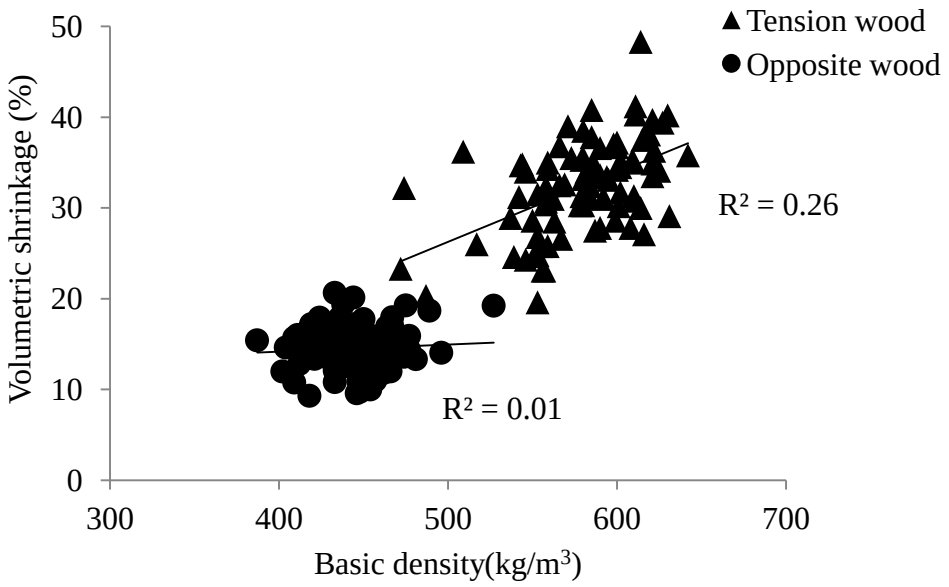

Figure 5.9 Relationship between volumetric shrinkage and basic density in young *Eucalyptus regnans*

5.4 Conclusions

The results of this study indicate that a large variation exists in average growth strain level in 2 year old trees of *Eucalyptus regnans*. The split log method is a cost efficient method to calculate average strain in young trees.

The wood types differ significantly in all the measured properties. TW has comparatively high density, high acoustic velocity and high volumetric shrinkage. The high LS in OW is due to comparatively high MFAs in young trees. The high growth strain in opposite wood in leant trees needs further investigation

The lack of correlations between growth strain and other measured properties in OW means that it ought to be possible to screen trees for growth strain without having any adverse effect on stiffness and stability. For those species that suffer from high growth stress, such as *E. regnans*, there is a straight-forward and immediate opportunity to improve wood quality by selecting low growth-strain individuals and thus increase efficiencies in subsequent processing.

While this study used seed of unknown genetic origin and so cannot quantitatively address issues such as heritability and implementing a breeding strategy, the wide range in growth

strain would suggest that a structured screening of a broad well characterised population for subsequent breeding or deployment is justified.

Just as some radiata pine breeders cavil at very early selection for wood stiffness, there will be those that would want definitive evidence of age-age correlations before entertaining such a screening programme. That is their prerogative.

Chapter 6. Summary

This study investigated variations in corewood properties and how they can be exploited through tree breeding. Until now breeding for wood quality was largely neglected and considered earliest at the age of 7-8 years. At this age samples are comparatively large and it is therefore difficult to evaluate large number of samples. In this thesis trees younger than 3 years old were screened and their properties characterised. The main problem in characterising young wood is the randomly distributed reaction wood. By leaning trees, the two wood types, opposite wood and reaction wood, can be separated and then evaluated independently without interference. The study was based on two species - *Pinus radiata* and *Eucalyptus regnans*. The two wood types, opposite wood and reaction wood, in each species were characterised for basic density, green and dry dynamic modulus, longitudinal shrinkage and volumetric shrinkage. The two wood types differ significantly in their properties. In addition, growth strain was measured in *Eucalyptus regnans*. The following conclusions can be drawn from the study.

Pinus radiata

Opposite and compression wood differ significantly in all the measured properties. Compression wood was denser than opposite wood; the mean density of compression wood at age 3 years, at ~5% moisture content was 590kg/m^3 whereas for opposite wood it was 421kg/m^3 (Chapter 2/Table 2.3). The thinner cell walls and larger lumen in opposite wood in young trees compared to compression wood can account for this difference.

Due to the young age of the trees the MFA was comparable in opposite and compression wood therefore, due to its high density; compression wood was stiffer than opposite wood. The mean dynamic modulus at age three years was 3.44GPa in compression wood and 2.98GPa in opposite wood (Chapter 2/Table 2.3). The comparable higher stiffness in compression wood highlights the necessity to lean the trees as high stiffness in straight trees might be due to randomly distributed compression wood rather than due to stiffer opposite wood. The specific stiffness (stiffness/density) was higher in opposite wood which was due to a comparably lower MFA as indicated by the high acoustic velocity squared (a surrogate measure for MFA) at ~5% moisture content in opposite wood (Chapter 2/Table 2.3). The variation in stiffness in compression wood was mainly attributed to variation in density

whereas it was related to variation in acoustic velocity (and therefore MFA) in opposite wood.

The mean longitudinal shrinkage from green to ~5% moisture content, for compression wood was three times that of opposite wood, being 3.23% and 0.99%, respectively (Chapter 2/Table 2.3) at age 3 years. The cell wall anatomy, high galactan content, high MFA, and high density are possible reasons for the high longitudinal shrinkage in the compression wood. Furthermore, longitudinal shrinkage was negatively related to acoustic velocity in both wood types. The relationship between density and longitudinal shrinkage was positive in compression wood and negative in opposite wood (Chapter 2/2.3.6/Table 2.4 and Table 2.5). High density in compression wood resulted in a stiffer but dimensionally more unstable wood. The negative correlation between basic density and longitudinal shrinkage in opposite wood suggests that it is possible to select stable wood without sacrificing basic density. The strong correlation with correlation (R= -0.69) between acoustic velocity squared and longitudinal shrinkage in opposite wood suggests that the variation in longitudinal shrinkage can be attributed to variation in MFA.

The mean volumetric shrinkage from green to 5% moisture content was 13.7% in opposite wood and 8.4% in compression wood (Chapter 2/Table 2.3). The high volumetric shrinkage in opposite wood was due to its low density, as collapse was noticed in low density samples. Compression wood despite its high density displayed low shrinkage. This can be attributed to cell wall anatomy: in the absence of the restraining influence of the S3 layer, the transverse shrinkage of the cell wall is directed towards middle lamella. This increases the lumen size without having an effect on the total tracheid volume.

The statistical variation (CV) is higher in opposite wood for all the measured properties except for basic density (Chapter 2/Table 2.2). The larger variation in basic density in compression wood can be attributed to the presence of bands of opposite wood in low density compression wood samples – it was not possible to isolate pure compression wood in every instance.

The variation between the families was comparable to variation within a family in opposite wood. Large within site variation along with genetic factors are the reasons for the large within family variation. Despite of this it was possible to distinguish between the best and the worst family. The moderate correlation between rankings at different age could be explained in terms of intermixing of two wood types in younger small-diameter 24 months' old trees

because of delayed leaning. Thus control of the environment along with leaning within 3-5 months of plantation is recommended for tree screening at early age.

For a representative set of samples, MFA was measured using X-ray diffraction; and tanδ and storage modulus were measured using a dynamic mechanical analyser (DMA). The results were correlated to previously measured properties to understand the factor(s) most influencing physical and mechanical properties in the corewood. The conclusions are as follows.

The two wood types did not differ significantly in their *T* values (MFA + 2σ). OW had a comparatively lower MFA with a mean value of 39° but with a high mean standard deviation (σ) within a sample (11.5°). CW had a higher mean MFA (44°) but with lower mean standard deviation (8.9°) within a sample. The range in MFA in opposite wood was 28° to 48° and in compression wood 36°-53°. The MFA along with density can explain 76% variation in dynamic modulus and 64% variation in longitudinal shrinkage in opposite wood (Chapter 3/Figure 3.13 and Figure 3.15). The good correlation between acoustic velocity squared and MFA with correlation coefficient of -0.68 in opposite wood suggested that the resonance technique can be employed to screen young wood for MFA. In other words while MFA is a fundamental characteristic of wood, measuring opposite wood properties using acoustics is more direct, faster and more efficient than measuring MFA.

Although the chemical composition of compression and opposite wood is vastly different, their tanδ values did not differ much (Chapter 4/Figure 4.11). The mean tanδ for opposite wood and compression wood was 0.028 and 0.026, respectively. In opposite wood a moderate correlation between MFA and tanδ suggested that the tanδ is not solely dependent on the chemical composition of the cell wall. Thus there is no additional advantage of introducing tanδ as a screening trait for quality assessment. A good correlation between dynamic modulus and storage modulus proves the reliability of the resonance technique to measure stiffness in small corewood samples.

Eucalyptus regnans

Tension wood was denser than opposite wood, the mean basic density at ~5% moisture content was 863kg/m^3 whereas for opposite wood it was 517kg/m^3 (Chapter 5/Table 5.2). The thickening of the cell wall layer with a G layer can account for the higher basic density in tension wood.

The green acoustic velocity was higher in tension wood than opposite wood thus suggesting a smaller MFA.

The green dynamic modulus was 10.27GPa in tension wood and 3.19GPa in opposite wood. The higher stiffness in tension wood can be attributed to higher density and higher velocity (smaller MFA).

The longitudinal shrinkage was 10% higher in opposite wood than in tension wood; it is 0.86% in opposite wood whereas 0.78% in tension wood. The higher MFA in opposite wood can be attributed to high longitudinal shrinkage in opposite wood. The range of MFA in opposite wood was 21° to 39°. The latter value, 39° was unexpectedly high.

The VS was higher in tension wood. The VS from green to ~5% moisture content was 32.3% in tension wood and 14.5% in opposite wood.

The negative association of longitudinal shrinkage with acoustic velocity in opposite wood suggested that its variation can be explained in terms of MFA (Chapter 5/Table 5.5). No relationship between longitudinal shrinkage and acoustic velocity was observed for tension wood which can be attributed to the fact the variation in MFA in tension wood was not as high as in opposite wood.

In contrast to reviewed literature, the growth strain was higher in opposite wood than tension wood. The mean growth strain values in opposite and tension wood were 1530μm and 612μm respectively (Chapter 5/Table 5.2). The lack of correlation between growth strain and any of the measured properties suggested that it would be possible to breed for growth strain as well as for stiffness and stability.

Strong correlation between growth strain calculated using the "slit" method and measured using "strain gauge" method suggested that slit method can be used efficiently to screen large populations for growth strain.

Recommendations and future work

This work described in this thesis was part of an active research programme which meant that many procedures and ideas were superseded over time. For example the initial intention of the Amberley trial was to grow straight trees of radiata pine on bare land and destructively test a quarter in years 1 to 4.

Today, the trees are growing in planter bags, are irrigated and tilted. The latest trial due for testing by age 2 in 2013 involves tilting the trees 5-10^{o} rather than 30-45^{o}. This will give

more uniform specimens with less sweep. This trial contains broad mix of the Radiata Pine Breeding Company's (RPBC) genetic population and consequently the results will be more relevant. Further, the retention of a whorl of branches at the groundline will permit propagation of elite individuals by cuttings.

The full value of this work lies in showing the ability to screen large populations for individuals, families and provenance that display elite wood properties. The significance of the on-going RPBC trial at Harewood lies in the disentangling of environmental and genetic effects, allowing tree breeders to characterise and select according to phenotypic and genetic parameters.

The work with *E. regnans* demonstrated that it is also possible to select elite material by age two for this species. However, the higher observed growth strain in opposite wood rather than in the tension wood poses an interesting so far unreported phenomenon. Industry, especially Forests and Wood Products Australia, indicated a preference for work on *E. nitens*. A further trial of this species was established in 2011 and its properties will be re-investigated by age 2 in 2013.

The DMA work which sought to find evidence of a glass transition of cell wall polymer below 100^{o}C proved elusive. A new system is being developed by Professor Entwistle and Dr Lengoc using a thin-walled very low damping bronze chamber. However, it is likely is primarily an intellectual challenge and the use of such a system is unlikely to be viable for the forest industry.

The X-ray diffraction work proved immensely helpful in understanding the biophysical properties of wood and in underpinning more pragmatic technologies such as acoustics. Such work will continue to be useful.

References

Abdel-Gadir AY, Krahmer RL. Estimating the age of demarcation of juvenile and mature wood in Douglas-fir. Wood and Fiber Science (1993) 25:242-249.

Abe H, Funada R. Review–The orientation of cellulose microfibrils in the cell walls of tracheids in conifers. A model based on observations by field emission-scanning electron microscopy. IAWA Journal (2005) 26:161-174.

Abe H, Funada R, Ohtani J, Fukazawa K. Changes in the arrangement of cellulose microfibrils associated with the cessation of cell expansion in tracheids. Trees-Structure and Function (1997) 11:328-332.

Abe H, Ohtani J. FE-SEM Observation on the Microfibrillar Orientation in the Secaondary wall of Tracheids. IAWA Journal (1991) 12:431-438.

Acosta MS, Concordia ER, Mastrandrea AC, Lima AJT. Wood technologies and uses of Eucalyptus from fast grown plantations for solid products In: Proceedings of the 51st International Convention of Society of Wood Science and Technology (2008) Chile.

Åkerholm M, Salmén L. Interactions between wood polymers studied by dynamic FT-IR spectroscopy. Polymer (2001) 42:963-969.

Altaner C, Apperley DC, Jarvis MC. Spatial relationships between polymers in Sitka spruce: Proton spin-diffusion studies. Holzforschung (2006) 60:665-673.

Altaner C, Hapca A, Knox J, Jarvis M. Antibody labelling of galactan in Sitka spruce (*Picea sitchensis* (Bong.) Carrière). Holzforschung (2007) 61:311-316.

Altaner CM, Jarvis MC. Modelling polymer interactions of the molecular Velcro'type in wood under mechanical stress. Journal of Theoretical Biology (2008) 253:434-445.

Altaner CM, Tokareva EN, Jarvis MC, Harris PJ. Distribution of (1→ 4)-β-galactans, arabinogalactan proteins, xylans and (1→ 3)-β-glucans in tracheid cell walls of softwoods. Tree Physiology (2010) 30:782-793.

Amarasekara H, Denne M. Effects of crown size on wood characteristics of Corsican pine in relation to definitions of juvenile wood, crown formed wood and core wood. Forestry (2002) 75:51.

Andrews M. Where are we with sonics. In: Wood Technology Reasearch Centre Workshop, Capturing the Benefits of Forestry Research (2000) University of Canterbury Christchurch New Zealand. 57-61.

Andrews M. Which acoustic speed. In: The 13th International Symposium on Nondestructive testing of wood (2004) University of California, USA. 43-52.

Apiolaza L. Very early selection for solid wood quality: screening for early winners. Annals of Forest Science (2009) 66:601-611.

Apiolaza L, Butterfield B, Chauhan S, Walker J. Characterization of mechanically perturbed young stems: can it be used for wood quality screening? Annals of Forest Science (2011) 68:407-414.

Apiolaza L, Raymond C, Yeo B. Genetic variation of physical and chemical wood properties of Eucalyptus globulus. Silvae Genetica (2005) 54:160-165.

Apiolaza L, Walker J, Nair H, Butterfield B. Very early screening of wood quality for radiata pine: pushing the envelope. In: Proceedings of the 51st International Convention of Society of Wood Science and Technology (2008) Chile. 10-16.

Apiolaza LA. Basic density of radiata pine in New Zealand: genetic and environmental factors. Tree Genetics and Genomes (2011) 8:87-96.

Archer RR. Analysis of residual stresses in orthotropic materials (1978): Technical Report, Escuela Ingeniera Civil, University of Costa Rica, San Jose, Costa Rica.

Archer RR. Growth stresses and strains in trees. (1987): Springer-Verlag.

Ashby M, Jones D. Engineering materials 2: an introduction to microstructures, processing and design, 1986 (1994): Pergamon Press, Oxford.

Askeland DR, Fulay PP, Wright WJ. The science and engineering of materials. (2011): Thomson Engineering.

Backman AC, Lindberg KAH. Differences in wood material responses for radial and tangential direction as measured by dynamic mechanical thermal analysis. Journal of Materials Science (2001) 36:3777-3783.

Bailey IW, Kerr T. The visible structure of the secondary wall and its significance in physical and chemical investigations of tracheary cells and fibers. Arnold Arboretum (1935) 16:273-300.

Baltunis B, Wu H, Powell M. Inheritance of density, microfibril angle, and modulus of elasticity in juvenile wood of *Pinus radiata* at two locations in Australia. Canadian Journal of Forest Research (2007) 37:2164-2174.

Bamber R. Origin of growth stresses. In: Proceedings IUFRO Conference Wood quality and utilization of tropical species. (1979) Philippines.

Bamber RK. A general theory for the origin of growth stresses in reaction wood: how trees stay upright. IAWA journal (2001) 22:205-212.

Bao FC, Jiang ZH, Jiang XM, Lu XX, Luo XQ, Zhang SY. Differences in wood properties between juvenile wood and mature wood in 10 species grown in China. Wood Science and Technology (2001) 35:363-375.

Barber N, Meylan B. The anisotropic shrinkage of wood. A theoretical model. Holzforschung (1964) 18:146-156.

Barnett JR, Bonham VA. Cellulose microfibril angle in the cell wall of wood fibres. Biological Reviews (2004) 79:461-472.

Barnett JR, Jeronimidis G. Wood Quality and its biological basis. (2003): Blackwell.

Beckar Vk. The presence of 1,4 -β -D - galactan in atypical reaction wood of angiosperms. In: Biology (2011): University of Hamburg.

Bendtsen B. Properties of wood from improved and intensively managed trees. Forest Products Journal (1978) 28:61-72.

Bendtsen BA, Senft J. Mechanical and anatomical properties in individual growth rings of plantation-grown eastern cottonwood and loblolly pine. Wood and Fiber Science (1986) 18:23-38.

Bertholf LD. Use of elementary stress wave theory for prediction of dynamic strain in wood (1965): Technical Extension Service, Washington State University.

Booker RE, Sell J. The nanostructure of the cell wall of softwoods and its functions in a living tree. European Journal of Wood and Wood Products (1998) 56:1-8.

Boyd J. Tree growth stresses. III. The origin of growth stresses. Australian Journal of Scientific Research (1950a) 3:294-309.

Boyd J. Relationship between fibre morphology and shrinkage of wood. Wood Science and Technology (1977) 11:3-22.

Boyd J. Relationship between fibre morphology, growth strain and physical properties of wood. Australian Journal of Scientific Research (1980) 10:337–360.

Boyd JD. Tree growth stresses. I. Growth stress evaluation. Australian Journal of Scientific Research (1950b) 3:270-293.

Boyd JD. Tree growth stresses. II. The development of shakes and other visual failures in timber. Australian Journal of Applied Science, Melbourne (1950c) 1:296-312.

Brennan M, McLean JP, Altaner CM, Ralph J, Harris PJ. Cellulose microfibril angles and cell-wall polymers in different wood types of *Pinus radiata*. Cellulose (2012) 19:1385-1404.

Burdon R. Compression wood in *Pinus radiata* clones on four different sites. New Zealand Journal of Forestry Science (1975) 5:152-164.

Burdon R, Young G. Preliminary genetic parameter estimates for wood properties from top-ranked *Pinus radiata* progenies and comparisons with controls. Proc. 11th Meet. Rep. Res. Work. Grp (1991) 1:137–140.

Burdon RD, Kibblewhite RP, Walker JCF, Megraw RA, Evans R, Cown DJ. Juvenile versus mature wood: a new concept, orthogonal to corewood versus outerwood, with special reference to *Pinus radiata* and *P. taeda*. Forest science (2004) 50:399-415.

Burgert I. Exploring the micromechanical design of plant cell walls. American journal of Botany (2006) 93:1391-1401.

Burgert I, Fratzl P. The Stick-Slip Mechanism in Wood. In: The Hemicelluloses Workshop -- Entwistle KM, Walker JCF, eds. (2005) New Zealand. 69-75.

Burgert I, Frühmann K, Keckes J, Fratzl P, Stanzl-Tschegg S. Microtensile testing of wood fibers combined with video extensometry for efficient strain detection. Holzforschung (2003) 57:661-664.

Burgert I, Gierlinger N, Zimmermann T. Properties of chemically and mechanically isolated fibres of spruce (*Picea abies* [L.] Karst.). Part 1: structural and chemical characterisation. Holzforschung (2005) 59:240-246.

Burgert I, Keckes J, Frühmann K, Fratzl P, Tschegg S. A comparison of two techniques for wood fibre isolation-evaluation by tensile tests on single fibres with different microfibril angle. Plant Biology (2002) 4:9-12.

Byrnes F, Archer R. Calculation of residual strains in log ends due to crosscutting. Wood Science (1977) 10.

Cave I. A theory of the shrinkage of wood. Wood Science and Technology (1972) 6:284-292.

Cave ID. Theory of x-ray measurement of microfibril angle in wood. Forest Product Journal (1966) 16:37-42.

Cave ID. The anisotropic elasticity of the plant cell wall. Wood Science and Technology (1968) 2:268-278.

Cave ID. The longitudinal Young's modulus of *Pinus radiata*. Wood Science and Technology (1969) 3:40-48.

Cave ID. Theory of X-ray measurement of microfibril angle in wood Part 1. Wood Science and Technology (1997) 31:225-234.

Cave ID, Robinson W. Interpretation of (002) diffraction arcs by means of a minimalist model. In: Proceedings of the IUFRO/IAWA International Workshop on the Significance of Microfibril Angle to Wood Quality--Butterfield BG, ed. (1998) New Zealand. 108-115.

Cave ID, Walker JCF. Stiffness of wood in fast-grown plantation softwoods: the influence of microfibril angle. Forest Products Journal (1994) 44:43-48.

Chafe S. Relationships among growth strain, density and strength properties in two species of Eucalyptus. Holzforschung (1990) 44:431-437.

Chafe SC. Radial dislocations in the fibre wall of Eucalyptus regnans trees of high growth stress. Wood science and technology (1977) 11:59-77.

Chauhan S, Entwistle K. Measurement of surface growth stress in *Eucalyptus nitens* Maiden by splitting a log along its axis. Holzforschung (2010) 64:267-272.

Chauhan SS. Pairing test and longitudinal growth strain: establishing the association. In: Proceedings of the 51st International Convention of Society of Wood Science and Technology (2008) Chile.

Chauhan SS, Aggarwal P. Segregation of *Eucalyptus tereticornis* Sm. clones for properties relevant to solid wood products. Annals of Forest Science (2011) 68:511-521.

Chauhan SS, Walker J. Relationships between longitudinal growth strain and some wood properties in *Eucalyptus nitens*. Australian Forestry (2004) 67:254-261.

Chauhan SS, Walker JCF. Variations in acoustic velocity and density with age, and their interrelationships in radiata pine. Forest Ecology and Management (2006) 229:388-394.

Clair B, Ruelle J, Beauchêne J, Prévost MF, Fournier M. Tension wood and opposite wood in 21 tropical rain forest species. 1. Occurence and efficiency of G-layer. IAWA journal (2006) 27:329-338.

Clair B, Ruelle J, Thibaut B. Relationship between growth stress, mechanical-physical properties and proportion of fibre with gelatinous layer in chestnut (*Castanea sativa* Mill.). Holzforschung (2003) 57:189-195.

Clair B, Thibaut B. Shrinkage of the gelatinous layer of poplar and beech tension wood. IAWA journal (2001) 22:121-132.

Côté WA. Wood ultrastructure. (1967) London: University of Washington Press.

Côté WA, Day AC, Timell TE. Studies on compression wood—part VII: Distribution of lignin in normal and compression wood of Tamarack [*Larix laricina (Du Roi) K. Koch*]. Wood Science and Technology (1968) 2:13-37.

Côté WA, Day AC, Timell TE. A contribution to the ultrastructure of tension wood fibers. Wood Science and Technology (1969) 3:257-271.

Coutand C, Fournier M, Moulia B. The gravitropic response of poplar trunks: key roles of prestressed wood regulation and the relative kinetics of cambial growth versus wood maturation. Plant Physiology (2007) 144:1166-1180.

Cowdrey DR, Preston RD. Elasticity and microfibrillar angle in the wood of Sitka spruce. Proceedings of the Royal Society of London. Series B, Biological Sciences (1966) 166:245-272.

Cown D. Variation in tracheid dimensions in the stem of a 26-year-old radiata pine tree. Appita (1975) 28:237-245.

Cown D. Juvenile wood (juvenile wood) in *Pinus radiata*: should we be concerned. New Zealand Journal of Forestry Science (1992) 22:87-95.

Cown D, Hebert J, Ball R. Modelling *Pinus radiata* lumber characteristics. Part 1: Mechanical properties of small clears. New Zealand Journal of Forestry Science (1999) 29:203-213.

Cown DJ, McKinley RB, Ball RD. Wood density variation in 10 mature *Pinus radiata* clones. New Zealand Journal of Forestry Science (2002) 32:48-69.

Dadswell H. Wood structure variations occurring during tree growth and their influence on properties. Journal of the Institute of Wood Science (1958) 1:11-33.

Dadswell HE, Wardrop AB. What is reaction wood. Australian Forestry Journal (1949) 13:22-33.

Dahman M. Eucalyptus wood and its utilization. Bulletin d'Information, Instilut National de Recherches Forestieres. Tunisia (1975) 19:24-28.

Davidson TC, Newman RH, Ryan MJ. Variations in the fibre repeat between samples of cellulose I from different sources. Carbohydrate research (2004) 339:2889-2893.

Dickson RL, Raymond CA, Joe W, Wilkinson CA. Segregation of *Eucalyptus dunnii* logs using acoustics. Forest Ecology and Management (2003) 179:243-251.

Donaldson L. Microfibril angle: measurement, variation and relationships: a review. IAWA Journal (2008) 29:387-396.

Donaldson L, Xu P. Microfibril orientation across the secondary cell wall of Radiata pine tracheids. Trees - Structure and Function (2005) 19:644-653.

Donaldson LA. S3 lignin concentration in radiata pine tracheids. Wood science and technology (1987) 21:227-234.

Donaldson LA. Within-and between-tree variation in microfibril angle in *Pinus radiata*. New Zealand Journal of Forestry Science (1992) 22:77-86.

Donaldson LA. Variation in microfibril angle among three genetic groups of *Pinus radiata* trees. New Zealand Journal of Forestry Science (1993) 23:90-100.

Donaldson LA. Between-tracheid variability of microfibril angles in radiata pine. In: Proceedings of the IUFRO/IAWA International Workshop on the Significance of Microfibril Angle to Wood Quality--Butterfield BG, ed. (1998) New Zealand. 206-224.

Donaldson LA, Grace J, Downes GM. Within-tree variation in anatomical properties of compression wood in radiata pine. IAWA Journal (2004) 25:253-272.

Dungey HS, Matheson AC, Kain D, Evans R. Genetics of wood stiffness and its component traits in *Pinus radiata*. Canadian Journal of Forest Research (2006) 36:1165-1178.

Dunning CE. Cell wall morphology of longleaf pine latewood. Wood Science, Madison (1968) 1:65-76.

Entwistle KM. The mechanosorptive effect in *Pinus radiata* D. Don. Holzforschung (2005) 59:552-558.

Entwistle KM, Kong K, MacDonald MA, Navaranjan N, Eichhorn SJ. The derivation of the microfibril angle in softwood using wide-angle synchrotron X-ray diffraction on structurally characterised specimens. Journal of materials science (2007) 42:7263-7274.

Entwistle KM, Navaranjan N. X-ray diffraction from cellulose microfibrils in the S2 layers of structurally characterised softwood specimens. Journal of Materials Science (2001) 36:3855-3863.

Entwistle KM, Walker JCF. Workshop assessment. In: The Hemicelluloses Workshop (2005) New Zealand. 179-190.

Evans R. A variance approach to the x-ray diffractometric estimation of microfibril angle in wood. Appita Journal (1999) 52:283-289,294.

Evans R, Ilic J. Rapid prediction of wood stiffness from microfibril angle and density. Forest Products Journal (2001) 51:53-57.

Evans R, Stringer S, Kibblewhite RP. Variation of microfibril angle, density and fibre orientation in twenty-nine *Eucalyptus nitens* trees. Appita Journal (2000) 53:450-457.

Fahlén J, Salmén L. Pore and matrix distribution in the fiber wall revealed by atomic force microscopy and image analysis. Biomacromolecules (2005) 6:433-438.

Fengel D. Ultrastructural behaviour of cell wall polysaccharides. Tappi (1970) 53:497-503.

Fernandes AN, et al. Nanostructure of cellulose microfibrils in spruce wood. Proceedings of the National Academy of Sciences (2011) 108:1195-1203.

Ferrand JC. Study of growth stresses 1. Measurement by mean of increment cores. Annals of Science (1982) 39:109-142.

Floyd S. Effect of hemicellulose on longitudinal shrinkage in wood. In: The Hemicelluloses Workshop (2005) New Zealand. 115–120.

Fratzl P, Burgert I, Gupta HS. On the role of interface polymers for the mechanics of natural polymeric composites. Phys. Chem. Chem. Phys. (2004) 6:5575-5579.

Gapare W, Ivkovic M, Powell M, McRae T, Wu H. Genetics of shrinkage in juvenile trees of *Pinus radiata* D. Don from two test sites in Australia. Silvae Genet (2008) 57:145-151.

Gaunt D. If you are not winning, change the rules. NZ Forest Research; Wood Process. Newsl. (Sawmilling) (1998) 23:3-4.

Gerhards CC. Longitudinal stress waves for lumber stress grading: factors affecting applications: state of the art. Forest Products Journal (1982) 32:20-25.

Gorisek Z, Torelli N, Vilhar B, Grill D, Guttenberger H. Microfibril angle in juvenile, adult and compression wood of spruce and silver fir. Plant Physiology (1999) 39:129-132.

Goswami L, et al. Stress generation in the tension wood of poplar is based on the lateral swelling power of the G-layer. The Plant Journal (2008a) 56:531-538.

Goswami L, Eder M, Gierlinger N, Burgert I. Inducing large deformation in wood cell walls by enzymatic modification. Journal of Materials Science (2008b) 43:1286-1291.

Grabianowski M, Manley B, Walker J. Acoustic measurements on standing trees, logs and green lumber. Wood Science and Technology (2006) 40:205-216.

Groom L, Mott L, Shaler S. Mechanical properties of individual southern pine fibers. Part I. Determination and variability of stress-strain curves with respect to tree height and juvenility. Wood and Fiber Science (2002) 34:14-27.

Ha M-A, Apperley DC, Jarvis MC. Molecular Rigidity in Dry and Hydrated Onion Cell Walls. Plant Physiology (1997) 115:593-598.

Harada H, Côté Jr WA. Structure of wood. (1985).

Harrington JJ. Hierarchical modelling of softwood hygro-elastic properties. In: Mechanical Engineering (2002): University of Canterbury, New Zealand.

Harris J. Wood quality of radiata pine. Appita (1981) 35:211-215.

Harris JM. Shrinkage and density of radiata pine compression wood in relation to its anatomy and mode of formation. New Zealand Journal of forestry Science (1977) 7:91-106.

Harris JM, Meylan BA. The influence of microfibril angle on longitudinal and tangential shrinkage in *Pinus radiata*. Holzforschung (1965) 19:144-153.

Harris PJ. Primary and secondary plant cell walls: a comparative overview. New Zealand Journal of Forestry Science (2006) 36:36-53.

Haslett AN. A guide to handling and grade-sawing plantation-grown eucalypts. New Zealand Ministry of Forests, Forest Research institute Bulletin 142 (1988).

Hepworth D, Vincent J. Modelling the mechanical properties of xylem tissue from tobacco plants (Nicotiana tabacum 'Samsun') by considering the importance of molecular and micromechanisms. Annals of Botany (1998) 81:761-770.

Hiller C. Variations in fibril angles in slash pine. In: Forest Products Laboratory (1954) University of Wisconsin: US Department of Agriculture, Forest Service.

http://calibre-equipment.com/.

http://www.microtec.eu/en.

Huang CL, Kutscha NP, Leaf GJ, Megraw RA. Comparison of microfibril angle measurement techniques. In: Proceedings of the IUFRO/IAWA International Workshop on the Significance of Microfibril Angle to Wood Quality--Butterfield BG, ed. (1998) New Zealand. 177-205.

Huang CL, Lindström H, Nakada R, Ralston J. Cell wall structure and wood properties determined by acoustics—a selective review. Holz als Roh-und Werkstoff (2003) 61:321-335.

Ilic J. Effects of Juvenile Corewood on Softwood Processing. Results From Recent Resource and Wood Quality Studies. Presented at the Practical Tools and New Technologies to

Improve Segregation of Logs and Lumbar for Processing, (2004) Albury, NSW, Australia.

Irvine GM. The glass transitions of lignin and hemicellulose and their measurement by differential thermal analysis. Tappi Journal (1984) 67:118-121.

Ivković M, Gapare W, Abarquez A, Ilic J, Powell M, Wu H. Prediction of wood stiffness, strength, and shrinkage in juvenile wood of radiata pine. Wood Science and Technology (2009) 43:237-257.

Ivkovic M, Gapare WJ, Abarquez A, Ilic J, Powell MB, Wu HX. Prediction of wood stiffness, strength, and shrinkage in juvenile wood of radiata pine. Wood Science and Technology (2009) 43:237-257.

Ivković M, Wu HX, McRae TA, Powell MB. Developing breeding objectives for radiata pine structural wood production. I. Bioeconomic model and economic weights. Canadian journal of forest research (2006) 36:2920-2931.

Jacobs MR. The growth stresses of woody stems. (1945): Commonwealth Forestry Bureau.

Jayawickrama KJS, Carson MJ. A breeding strategy for the New Zealand radiata pine breeding cooperative. Silvae Genetica (2000) 49:82-89.

Jayne BA. Vibrational properties of wood as indices of quality. Forest Product Journal (1959) 9:413-416.

Joseleau JP, Imai T, Kuroda K, Ruel K. Detection in situ and characterization of lignin in the G-layer of tension wood fibres of *Populus deltoides*. Planta (2004) 219:338-345.

Jourez B, Riboux A, Leclercq A. Anatomical characteristics of tension wood and opposite wood in young inclined stems of poplar (Populus euramericana cvGhoy'). IAWA Journal (2001a) 22:133-158.

Jourez B, Riboux A, Leclercq A. Comparison of basic density and longitudinal shrinkage in tension wood and opposite wood in young stems of *Populus euramericana* cv. Ghoy

when subjected to a gravitational stimulus. Canadian Journal of Forest Research (2001b) 31:1676-1683.

Kataoka Y, Saiki H, Fujita M. Arrangement and superimposition of cellulose microfibrils in the secondary walls of coniferous tracheids. Journal of the Japan Wood Research Society (1992) 38:327-335.

Keckes J, et al. Cell-wall recovery after irreversible deformation of wood. Nature Materials (2003) 2:810-813.

Kelsey KE. A critical review of the relationship between the shrinkage and structure of wood. In: Divison of Forest Products technological Papers (1963) Australia: Commonwealth Scientific and Industrial Research Organization, Australia.

Kennedy RW. Coniferous wood quality in the future: concerns and strategies. Wood Science and Technology (1995) 29:321-338.

Kibblewhite RP, Suckling ID, Evans R, Grace JC, Riddell MJC. Lignin and carbohydrate variation with earlywood, latewood, and compression wood content of bent and straight ramets of a radiata pine clone. Holzforschung (2009) 64:101-109.

Kikata Y. The effect of lean on level of growth stress in *Pinus densiflora*. Journal of the Japan Wood Research Society (1972) 18:443-449.

Kretschmann D, Bendtsen B. Ultimate tensile stress and modulus of elasticity of fast-grown plantation loblolly pine lumber. Wood and Fiber Science (1992) 24:189-203.

Kretschmann DE, Alden HA, Verrill S. Variations of microfibril angle in loblolly pine: comparison of iodine crystallization and x-ray diffraction techniques. In: Proceedings of the IUFRO/IAWA International Workshop on the Significance of Microfibril Angle to Wood Quality--Butterfield BG, ed. (1998) New Zealand. 157–176.

Kubler H. Studies on growth stresses in trees. Part II. Longitudinal stresses. Holz als Roh-und Werkstoff (1959a) 17:44-54.

Kubler H. Studies on growth stresses in trees: 1. The origin of growth stresses and the stresses in transverse direction. Holz als Roh-und Werkstoff (1959b) 17:1-9.

Kubler H. Growth stresses in trees and related wood properties (1987). 61-119.

Kumar S, Dungey H, Matheson A. Genetic parameters and strategies for genetic improvement of stiffness in radiata pine. Silvae Genetica (2006) 55:77-83.

Kumar S, Lee J. Age-age correlations and early selection for end-of-rotation wood density in radiata pine. Forest Genetics (2002) 9:323-330.

Kuo-Huang L, Chen S, Huang Y, Chen S, Hsieh Y. Growth strains and related wood structures in the learning trunks and branches of *Trochodendron aralioides*-a vessel-less dicotyledon. IAWA Journal (2007) 28:211.

Lachenbruch B, Droppelmann F, Balocchi C, Peredo M, Perez E. Stem form and compression wood formation in young *Pinus radiata* trees. Canadian Journal of Forest Research (2010) 40:26-36.

Larson PR, Kretschmann DE, Clark AI, Isebrands JG. Formation and properties of juvenile wood in southern pines. In: Forest Products Laboratory General Technical Report (2001) United States of America: United States Department of Agriculture.

Lawoko M, Henriksson G, Gellerstedt G. Structural differences between the lignin-carbohydrate complexes present in wood and in chemical pulps. Biomacromolecules (2005) 6:3467-3473.

Lehringer C, Gierlinger N, Koch G. Topochemical investigation on tension wood fibres of Acer spp., Fagus sylvatica L. and Quercus robur L. Holzforschung (2008) 62:255-263.

Lichtenegger H, Reiterer A, Stanzl-Tschegg SE, Fratzl P. Variation of Cellulose Microfibril Angles in Softwoods and Hardwoods--A Possible Strategy of Mechanical Optimization. Journal of Structural Biology (1999) 128:257-269.

Liese W. Tertiary wall and warty layer in wood cells. Journal of Polymer Science (1963) 2:213-229.

Lindström H, Harris P, Nakada R. Methods for measuring stiffness of young trees. Holz als Roh-und Werkstoff (2002) 60:165-174.

Lindström H, Harris P, Sorensson CT, Evans R. Stiffness and wood variation of 3-year old *Pinus radiata* clones. Wood Science and Technology (2004) 38:579-597.

Lotfy M, El-Osta M, Kellogg RM, Foschi RO, Butters RG. A direct X-ray technique for measuring microfibril angle. Wood and Fiber Science (1973) 5:118-128.

Malan F, de Villiers A. The effect of radial resin-infiltrated heart shakes on the yield of sawn timber from *Pinus elliottii* Engelm. sawlogs. South African Forestry Journal (1976):47-57.

Malan FS. Relationships between growth stress and some tree characteristics in South African grown *Eucalyptus grandis*. South African Forestry Journal (1988) 144:43-46.

Malan FS, Gerischer GFR. Wood property differences in South African grown *Eucalyptus grandis* trees of different growth stress intensity. Holzforschung (1987) 41:331-335.

Manwiller FG. Tension wood anatomy of silver maple. Forestry Products Journal (1967) 17:43-48.

Matheson A, Gapare W, Ilic J, Wu H. Inheritance and genetic gain in wood stiffness in radiata pine assessed acoustically in young standing trees. Silvae Genetica (2008) 57:56-64.

McLean JP, Arnould O, Beauchêne J, Clair B. The effect of the G-layer on the viscoelastic properties of tropical hardwoods. Annals of Forest Science (2012):1-10.

Megraw RA, Bremer D, Leaf G, Roers J. Stiffness in loblolly pine as a function of ring position and height, and its relationship to microfibril angle and specific gravity. In:

Proceedings of the 3rd Workshop-Connection between Silviculture and Wood Quality through Modeling Approaches, IUFRO (1999). 341-349.

Megraw RA, Leaf G, Bremer D. Longitudinal shrinkage and microfibril angle in loblolly pine. In: Proceedings of the IUFRO/IAWA International Workshop on the Significance of Microfibril Angle to Wood Quality--Butterfield BG, ed. (1998) New Zealand. 27-61.

Menard KP. Dynamic mechanical analysis: a practical introduction. (2008) Second edn.: CRC.

Meylan B. Measurement of microfibril angle by X-ray diffraction. Forest Products Journal (1967) 17:51-58.

Meylan B. Cause of high longitudinal shrinkage in wood. Forest Products Journal (1968) 18:75-78.

Moody RC. Tensile Strength of Finger Joints in Pith-Associated and Non-Pith-associated Southern Pine 2 by 6's. (1970): Defense Technical Information Center.

Moore JR. Growing Fit-For-Purpose Structural Timber: What's the Target and How Do We Get There? NZ Journal of Forestry (2012) 57.

Moreno Chan J. Moisture content in radiata pine wood: implications for wood quality and water-stress response. In: School of Forestry (2007): University of Canterbury New Zealand.

Moreno Chan J, Walker J, Raymond C. Effects of moisture content and temperature on acoustic velocity and dynamic MOE of radiata pine sapwood boards. Wood Science and Technology (2010):1-18.

Munch E. Statics and dynamics of the cell wall's spiral structure, especially in compression wood and tension wood. Flora (1938) 32:357-424.

Muneri, J.Knight, W.Leggate, G.Palmer. Relationship between surface longitudinal growth strain and tree size, wood properties and timber distortion of 4 year old plantation grown. Presented at the The future of eucalyptus for wood products, (2000) Tasmania.

Muneri A, Leggate W. Wood properties and sawn timber characteristics of fast, plantation grown 4-year-old *Eucalyptus pilularis*. In: Opportunities for the new Millennium, Australian Forest Growers Biennial Conference. (2000) Queensland, Australia.

Muneri A, Leggate W, Palmer G. Relationships between surface growth strain and some tree, wood and sawn timber characteristics of *Eucalyptus cloeziana*. Southern African Forestry Journal (1999) 186:41-49.

Murphy TN, Henson M, Vanclay JK. Growth stress in *Eucalyptus dunnii*. Australian Forestry (2005) 68:144-149.

Nakamura N, Nanami N. The sound velocities and moduli of elasticity in the moisture desorption process of sugi wood. Journal of the Japan Wood Research Society (1993) 39:1341-1348.

Navi P, Rastogi PK, Gresse V, Tolou A. Micromechanics of wood subjected to axial tension. Wood Science and Technology (1995) 29:411-429.

Newman R. How stiff is an individual cellulose microfibril? In: Proceedings of the IUFRO/IAWA International Workshop on the Significance of Microfibril Angle to Wood Quality--Butterfield BG, ed. (1998) New Zealand. 81-93.

Newman R. Solid-state NMR as a tool for studying dancing molecules. In: The Hemicelluloses Workshop (2005) New Zealand. 77-86.

Nicholson J. A rapid method for estimating longitudinal growth stresses in logs. Wood Science and Technology (1971) 5:40-48.

Nicholson JE. Growth stress differences in eucalypts. Forest Science (1973) 19:169-174.

Nicholson JE, Hillis WE, Ditchburne N. Some tree growth-wood property relationships of eucalypts. Canadian Journal of Forest Research (1975) 5:424-432.

Norberg PH, Meier H. Physical and chemical properties of the gelatinous layer in tension wood fibres of aspen (*Populus tremula* L.). Holzforschung (1966) 20:174-178.

Okuyama T, Doldán J, Yamamoto H, Ona T. Heart splitting at crosscutting of eucalypt logs. Journal of Wood Science (2004) 50:1-6.

Okuyama T, Yamamoto H, Yoshida M, Hattori Y, Archer RR. Growth stresses in tension wood: role of microfibrils and lignification. Annales des sciences forestières. (1994) 51:291-300.

Olsson AM, Salmén L. The softening behavior of hemicelluloses related to moisture. In: American Chemical Society Symposium Series (2004) Washington, DC: American Chemical Society Publications. 184-197.

Onaka F. Studies on compression and tension wood. Wood Research, Kyoto (1949) 1:1-88.

Panshin AJ, De Zeeuw C. Textbook of wood technology: structure, identification, properties, and uses of the commercial woods of the United States and Canada. (1980): McGraw-Hill New York, US.

Pearson RG, Gilmore RC. Effect of fast growth rate on the mechanical properties of loblolly pine. Forest Products Journal (1980) 30.

Pentoney R. Mechanisms affecting tangential vs. radial shrinkage. Journal Forestry Polts. Research Society (1953).

Peura M, et al. Structural studies of single wood cell walls by synchrotron X-ray microdiffraction and polarised light microscopy. Nuclear instruments and methods in physics research Section B: Beam interactions with materials and atoms (2005) 238:16-20.

Preston RD. The physical biology of plant cell walls. (1974): London.: Chapman & Hall.

Qiu D, Wilson IW, Gan S, Washusen R, Moran GF, Simon GS. Gene Expression in Eucalyptus Branch Wood with Marked Variation in Cellulose Microfibril Orientation and Lacking G-Layers. New Phytologist (2008) 179:94-103.

R Development Core Team. R: a language and environment for statistical computing (2011).

Raymond CA, Kube PD, Pinkard L, Savage L, Bradley AD. Evaluation of non-destructive methods of measuring growth stress in *Eucalyptus globulus*: relationships between strain, wood properties and stress. Forest Ecology and Management (2004) 190:187-200.

Reiterer A, Lichtenegger H, Fratzl P, Stanzl-Tschegg S. Deformation and energy absorption of wood cell walls with different nanostructure under tensile loading. Journal of Materials Science (2001) 36:4681-4686.

Reiterer A, Lichtenegger H, Tschegg S, Fratzl P. Experimental evidence for a mechanical function of the cellulose microfibril angle in wood cell walls. Philosophical Magazine A (1999) 79:2173-2184.

Ross RJ. Stress wave propagation in wood products. In: Proceedings, 5th nondestructive testng of wood symposium--Pullman WA, ed. (1985) Washington 291-318.

Ross RJ, Pellerin RF. Nondestructive testing for assessing wood members in structures. In: Forest Products Laboratory General Technical Report (1994): US Department of Agriculture, Forest Service. 1-40.

Ross RJ, Pellerin RF, Volny N, Salsig WW, Falk RH. Inspection of timber bridges using stress wave timing nondestructive evaluation tools: a guide for use and interpretation. In: Forest Products Laboratory general Technical Report (1999) US Department of Agriculture, Forest Service.

Ross RJ, et al. Comparison of several nondestructive evaluation techniques for assessing stiffness and MOE of small-diameter logs. In: Forest Products Laboratory Research Paper (2000) Madison: US, Department of Agriculture, Forest Service.

Salmén L. Viscoelastic properties ofin situ lignin under water-saturated conditions. Journal of Materials Science (1984) 19:3090-3096.

Salmén L. Micromechanical understanding of the cell-wall structure. Comptes Rendus Biologies (2004) 327:873-880.

Sandoz JL. Grading of construction timeber by ultrasound. Wood Science and Technology (1989) 23:95-108.

Schimleck L, Evans R, Ilic J. Estimation of *Eucalyptus delegatensis* wood properties by near infrared spectroscopy. Canadian Journal of Forest Research (2001) 31:1671-1675.

Shield ED. Plantation grown eucalypts: utilization for lumber and rotary veneers-primaryconversion. Seminário internacional de utilização da madeira de eucalipto para serraria (1995):133-139.

Simpson WT. Methods of reducing warp when drying. Asian Timber (1983) 2:80-81.

Singh A, Daniel G, Nilsson T. High variability in the thickness of the S3 layer in *Pinus radiata* tracheids. Holzforschung (2002) 56:111-116.

Singh A, Donaldson L. Ultrastructure of tracheid cell walls in radiata pine (*Pinus radiata*) mild compression wood. ProQuest Science Journals (1999) 77:32-40.

Sinnott EW. Reaction wood and the regulation of tree form. American journal of Botany (1952):69-78.

Skaar C. Wood-water relations. (1988): Springer-Verlag.

Sorensson CT, Cown DJ, Ridoutt BG, Tian X. The significance of wood quality in tree breeding: a case study of radiata pine in New Zealand. In: Timber management toward wood quality and end-product value (1997) Canada. 35-44.

Stamm AJ. Wood and cellulose science. (1964) New York: The Ronald Press Co.

Sutton WRJ. The need for planted forests and the example of radiata pine. New Forests (1999) 17:95-110.

Timell T. Compression wood in gymnosperms 1. (1986): Springer-Verlag, Berlin.

Timell TE. Recent progress in the chemistry of wood hemicelluloses. Wood Science and Technology (1967) 1:45-70.

Timell TE. Organization and ultrastructure of the dormant cambial zone in compression wood of *Picea abies*. Wood Science and Technology (1980) 14:161-179.

Timell TE. Recent progress in the chemistry and topochemistry of compression wood. Wood Science and Technology (1982) 16:83-122.

Tsehaye A, Buchanan AH, Beder R, Newman RH, Walker JCF. Microfibril angle: determining wood stiffness in radiata pine. In: Proceedings of the IUFRO/IAWA International Workshop on the Significance of Microfibril Angle to Wood Quality--Butterfield BG, ed. (1998) New Zealand. 323-336.

Tsehaye A, Buchanan AH, Walker JCF. Selecting trees for structural timber. European Journal of Wood and Wood Products (2000a) 58:162-167.

Tsehaye A, Buchanan AH, Walker JCF. Sorting of logs using acoustics. Wood Science and Technology (2000b) 34:337-344.

Tsoumis G. Science and technology of wood: Structure, properties, utilization. (1991): Van Nostrand Reinhold New York.

Valencia J, Harwood C, Washusen R, Morrow A, Wood M, Volker P. Longitudinal growth strain as a log and wood quality predictor for plantation-grown *Eucalyptus nitens* sawlogs. Wood Science and Technology (2011) 45:15-34.

Verrall AF. A comparative study of the structure and physical properties of compression wood and normal wood (1928): University of Minnesota.

Verrill SP, Kretschmann DE, Herian VL, Wiemann MC, Alden HA. Concerns about a variance approach to X-ray diffractometric estimation of microfibril angle in wood. Wood and fiber science (2011) 43:153-168.

Via BK, So CL, Shupe TF, Groom LH, Wikaira J. Mechanical response of longleaf pine to variation in microfibril angle, chemistry associated wavelengths, density, and radial position. Composites Part A: Applied Science and Manufacturing (2009) 40:60-66.

Walker J. Primary wood processing. (2006) Netherlands: Springer.

Walker J, Butterfield BG, Langrish TAG, Harris JM, Uprichard JM. Primary wood processing. (1993) 1st edn.: Chapman & Hall.

Walker JCF, Butterfield BG. The importance of microfibril angle for the processing industries. New Zealand Forestry (1996) 40:34-40.

Walker JCF, Nakada R. Understanding corewood in some softwood: a selective review on stiffness and acoustics. International Forestry Review (1999) 1:251-259.

Wang E, Chen T, Karalus A, Sutherland J, Pang S. Stability properties and performance of Douglas-fir and comparison with radiata pine (2009): Department of Chemical and Process Engineering, University of Canterbury Christchurch New Zealand.

Wang X, Ross RJ, Carter P. Acoustic evaluation of standing trees: recent research development. In: International Symposium on Nondestructive Testing of Wood (2005) Eberswalde, Germany, University of Applied Sciences. 455-465.

Wardrop A, Dadswell H. The nature of reaction wood. I. The structure and properties of tension wood fibres. Australian Journal of Scientific Research (1948) 1:1-16.

Wardrop A, Dadswell H. The nature of reaction wood. IV. Variations in cell wall organization of tension wood fibres. Australian Journal of Botany (1955) 3:177-189.

Wardrop A, Well HED. The nature of reaction wood. Australian Journal of Biological Sciences (1948) 1:3-16.

Wardrop AB, Harada H. The formation and structure of the cell wall in fibres and tracheids. Journal of Experimental Botany (1965) 16:356.

Washusen R. The occurrence and characteristics of tension wood and associated wood properties in *Eucalyptus globulus* Labill. In: Department of Forestry (2000): University of Melbourne Australia.

Washusen R, Ilic J. Relationship between transverse shrinkage and tension wood from three provenances of *Eucalyptus globulus Labill*. European Journal of Wood and Wood Products (2001) 59:85-93.

Washusen R, Ilic J, Waugh G. The relationship between longitudinal growth strain and the occurrence of gelatinous fibers in 10 and 11-year-old Eucalyptus globulus Labill. European Journal of Wood and Wood Products (2003) 61:299-303.

Watanabe H. A study of the origin of longitudinal growth stresses in tree stems. In: Meeting of IUFRO (1967). 169-176.

Westermark U. The occurrence of p-hydroxyphenylpropane units in the middle-lamella lignin of spruce (*Picea abies*). Wood Science and Technology (1985) 19:223-232.

Wilson BF, Archer RR. Reaction wood: induction and mechanical action. Annual Review of Plant Physiology (1977) 28:23-43.

Wooten TE, Barefoot AC, Nicholas DD. The longitudinal shrinkage of compression wood. Holzforschung (1967) 21:168-171.

Wu HX, Powell MB, Yang JL, Ivkovic M, McRae TA. Efficiency of early selection for rotation-aged wood quality traits in radiata pine. Annals of Forestry Science (2007) 64:1-9.

Xu P. The mechanical properties and stability of radiata pine structural timber. In: School of Forestry (2000): University of Canterbury, New Zealand

Xu P, Liu H, Donaldson L, Zhang Y. Mechanical performance and cellulose microfibrils in wood with high S2 microfibril angles. Journal of Materials Science (2011) 46:534-540.

Xu P, Liu H, Evans R, Donaldson LA. Longitudinal shrinkage behaviour of compression wood in radiata pine. Wood Science and Technology (2009) 43:423-439.

Xu P, Walker J. Stiffness gradients in radiata pine trees. Wood Science and Technology (2004) 38:1-9.

Yamamoto H. Generation mechanism of growth stresses in wood cell walls: roles of lignin deposition and cellulose microfibril during cell wall maturation. Wood Science and Technology (1998) 32:171-182.

Yamamoto H, Kojima Y. Properties of cell wall constituents in relation to longitudinal elasticity of wood. Wood Science and Technology (2002) 36:55-74.

Yamamoto H, Kojima Y, Okuyama T, Abasolo WP, Gril J. Origin of the Biomechanical properties of wood related to the fine structure of the multi-layered cell wall. Journal of Biomechanical Engineering (2002) 124:432.

Yamamoto H, Sassus F, Ninomiya M, Gril J. A model of anisotropic swelling and shrinking process of wood. Wood Science and Technology (2001) 35:167-181.

Yamashita S, Yoshida M, Takayama S, Okuyama T. Stem-righting mechanism in gymnosperm trees deduced from limitations in compression wood development. Annals of Botany (2007) 99:487-493.

Yang JL, Bailleres H, Okuyama T, Muneri A, Downes G. Measurement methods for longitudinal surface strain in trees: a review. Australian Forestry (2005) 68:34-43.

Yang JL, Ilic J. A new method of determining growth stress and relationships between associated wood properties of Eucalyptus globulus Labill. Australian Forestry (2003) 66:153-157.

Yang JL, Waugh G. Growth stress, its measurement and effects. Australian Forestry (2001) 64:127-135.

Yeh TF, Goldfarb B, Chang H, Peszlen I, Braun JL, Kadla JF. Comparison of morphological and chemical properties between juvenile wood and compression wood of loblolly pine. Holzforschung (2005) 59:669-674.

Ying L, Kretschmann DE, Bendtsen BA. Longitudinal shrinkage in fast-grown loblolly pine plantation wood. Forest (1993) 53705.

Yoshida M, Ohta H, Yamamoto H, Okuyama T. Tensile growth stress and lignin distribution in the cell walls of yellow poplar, *Liriodendron tulipifera*. Trees - Structure and Function (2002) 16:457-464.

Yoshida M, Okuda T, Okuyama T. Tension wood and growth stress induced by artificial inclination in *Liriodendron tulipifera* Linn. and *Prunus spachiana* Kitamura f. *ascendens* Kitamura. Annals of Forest Science (2000) 57:739-746.

Yoshizawa N, Inami A, Miyake S, Ishiguri F, Yokota S. Anatomy and lignin distribution of reaction wood in two Magnolia species. Wood Science and Technology (2000) 34:183-196.

Youming X, Han L, Chunyun X. Genetic and geographical variation in microfibril angle of loblolly pine in 31 provenances. In: Proceedings of the IUFRO/IAWA International Workshop on the Significance of Microfibril Angle to Wood Quality--Butterfield BG, ed. (1998) New Zealand. 388-396.

Yumoto M, Ishida S, Fukazawa K. Studies on the Formation and Structure of the Compression Wood Cells Induced by Artificial Inclination in Young Trees of *Picea glauca*: . Gradation of the Severity of Compression Wood Tracheids. Research Bulletins of the College Experiment Forests Hokkaido University (1983) 40:409-454.

Zobel BJ. Imbalance in the world's conifer timber supply. Tappi (1980) 63:95-98.

Zobel BJ, van Buijtenen JP. Wood variation its cause and control. (1989): Springer, Berlin Heidelberg New York.